Y3.N21/5:16/4080
BUSINESS, SCIENCE & TECH. DEPT
HARTFORD PUBLIC LIBRARY
HARTFORD, CONN.
GOVT. DOC.

NATIONAL ADVISORY COMMITTEE FOR AERONAUTICS

TECHNICAL NOTE 4080

SOME EFFECTS OF VANES AND OF TURBULENCE IN TWO-DIMENSIONAL WIDE-ANGLE SUBSONIC DIFFUSERS

By Carl A. Moore, Jr., and Stephen J. Kline

Stanford University

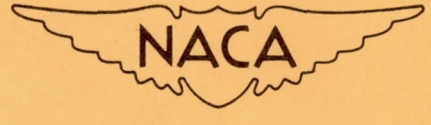

Washington

June 1958

JUN 2 6 1958

TABLE OF CONTENTS

	Page
SUMMARY	1
INTRODUCTION	2
SYMBOLS	4
DIFFUSER GEOMETRY AND ENTRANCE VELOCITY AND PRESSURE PROFILES	8
DIFFUSER GEOMETRY	8
FLUX PLOTS	9
ENTRANCE VELOCITY AND PRESSURE PROFILES	9
Wall Curvature	9
Potential-Flow Velocity Profiles	11
PARAMETERS INVOLVED IN PROBLEM	11
MATHEMATICAL SOLUTIONS	11
DISCUSSION OF PARAMETERS	12
WATER-TABLE TESTS	13
GENERAL DESCRIPTION	14
Water Table	14
Placement of Bluing Jets	14
Water-Table Diffusers	15
Aspect Ratio	15
Boundary-Layer Trip	16
Secondary Flow	16
Turbulence of Entering Flow	17
Dynamic-Similarity Considerations	18
Method of Procedure in Photographic Studies	19
WATER-TABLE DIFFUSERS WITHOUT VANES	19
Large Water-Table Diffuser	19
General description	19
Separations resulting from increasing angle in vaneless diffusers	21
Effect of changes in Reynolds number on separation	25
Variation of angles of separation with change in L/W_1	26
Effect of turbulence	26
Small Water-Table Diffuser	28
Reasons for building small diffuser	28
Small-diffuser tests at small angles	28
Small diffuser at very large angles	29
Superimposed Plots of Large- and Small-Diffuser Results	30

Page

INSERTION OF VANES IN LARGE WATER-TABLE DIFFUSER 30
Tests With Vane Having an Airfoil Profile 31
Tests With Flat-Plate Vanes 31
Vanes used 31
Short vanes at an L/W_1 ratio of 8 32
Rationalization of findings on optimum vane placement . . . 33
Long vanes at an L/W_1 ratio of 8 36
Vanes at different L/W_1 ratios 38
General Conclusions From Tests With Vanes Inserted 38
INSERTION OF RODS IN LARGE WATER-TABLE DIFFUSER 39
First Experiences With Rod Insertions 39
Sizes and Placement of Rods Used in Present Work 40
Rod diameters 40
Placement 40
Results and Discussion of Tests With Rod Insertion 41
Upstream rods 41
Downstream rods 44
Comparison of rods with vanes 45

A I R - D I F F U S E R T E S T S 45
APPARATUS 46
OBSERVATIONAL TECHNIQUES AND COMPUTATION OF PARAMETERS 46
Location of Separations 46
Visualization of flow using smoke 46
Visualization of flow using tufts 47
Determination of Recovery and Efficiency 47
Location of static-pressure orifices 47
Measuring and recording static pressure 48
Static pressure during different flow regimes 48
Computation of recovery and efficiency 48
AIR DIFFUSER WITHOUT VANES 50
General Description 50
Experimental procedure 50
Variation of turbulence 50
Boundary-layer trip 50
Separation Behavior 51
Types of separation encountered 51
Separations at 7° and 10° 52
Separation at 12° 52
Separation at 15° 52
Separation at 20° 53
Separation at 22.5° 53
Separation at 30° 53
Separation at 45° 54
Comparison with water-table results 54

Page

Results and Discussion of Recovery and Efficiency 56
Tabulated recovery and efficiency data 56
Crossplotting 56
Comparison with Reid's data 56
Position of maximums with respect to first separation angle 56
Interpretation of recovery and efficiency graphs 57
AIR DIFFUSER WITH VANES AND RODS 58
Vanes 58
Vanes used 58
Diffuser angles investigated 59
Improvement of separation conditions 59
Improvement of performance parameters 59
Rods 60
Two cases of rod insertion 60
Air-diffuser rod indications 61

CONCLUSIONS 61

APPENDIX A - DEFINITION AND DERIVATION OF ENERGY PARAMETERS AND THEIR COMPARISON WITH PRESSURE PARAMETERS 65
ENERGY RECOVERY FACTOR 65
ENERGY EFFICIENCY 69
COMPARISON OF ENERGY WITH PRESSURE PARAMETERS 70

APPENDIX B - EFFECT OF EXIT-VELOCITY-PROFILE SQUARENESS ON PRESSURE RECOVERY AND PRESSURE EFFECTIVENESS 72

APPENDIX C - ACCURACY 77
BRIEF DISCUSSION OF PROCEDURE 77
ACCURACY OF PRESENT DATA 79

REFERENCES 81

TABLES 84

FIGURES 98

NATIONAL ADVISORY COMMITTEE FOR AERONAUTICS

TECHNICAL NOTE 4080

SOME EFFECTS OF VANES AND OF TURBULENCE IN TWO-DIMENSIONAL WIDE-ANGLE SUBSONIC DIFFUSERS

By Carl A. Moore, Jr., and Stephen J. Kline

SUMMARY

Tests on two aspects of the behavior of wide-angle, plane-walled, two-dimensional diffusers with essentially incompressible flow have been conducted in the Mechanical Engineering Laboratory at Stanford University. First, a thorough study of the flow mechanism has been made using dye injection in a water table. The four regimes of flow found are delineated on graphs in terms of the three important parameters. Test data from a large water-table unit and a small water-table unit are given. Second, data are presented which demonstrate means for producing efficient diffusers for total included angles up to at least 45° by use of simple, short, flat vanes.

In the absence of vanes, or other means of boundary-layer control, all of the following parameters are important in determining the behavior of the flow: (a) Divergence angle, (b) ratio of throat width to wall length, and (c) free-stream turbulence; divergence angle alone is definitely insufficient. Variations in Reynolds number and aspect ratio seem to have little effect on the flow regime for the range of aspect ratios normally encountered and for all Reynolds numbers in excess of a few thousand. Inlet-boundary-layer shape and thickness probably also have an effect on performance but have not been investigated in the present tests.

Starting from very low divergence angles and maintaining other conditions constant, the following four entirely different regimes of flow are found as the divergence angle is increased from zero: (a) Unstalled flow, (b) transient, three-dimensional stalls, (c) steady, two-dimensional stalls, and (d) jet flow separated from both walls. With the turbulence level held constant, increasing the ratio of wall length to throat width from 4 to 20 decreases the angles at which both three-dimensional transient and two-dimensional steady stall occur by a factor of the order of 2 or 3 to 1. Increasing turbulence level, with the ratio of wall length to throat width held constant, increases the angle at which transition occurs from three-dimensional transient separation to two-dimensional

steady separation by roughly $1\frac{1}{2}$ to 1 but has little effect on the angle at which three-dimensional separation begins. Any type of turbulence-promoting device inserted in the flow has about the same effect as an increase in the free-stream turbulence.

Overall pressure recovery and efficiency are high in the unstalled regime and drop only a small amount through the three-dimensional-stall zone, but they drop to very low values as soon as two-dimensional steady separation begins.

The use of multiple, short, straight vanes placed just downstream from the throat can eliminate all separation up to angles as high as 45° as well as provide a means for controlling the exit velocity profile and for smoothing the flow. Water-table results on both vanes and flow regimes are confirmed by preliminary data from the air apparatus.

INTRODUCTION

The present report is a condensed and revised version of the Ph. D. dissertation of Dr. C. A. Moore (ref. 1). Reference 1 includes additional details concerning apparatus and procedures.

In internal flows of fluids in ducts, among which are included those of centrifugal compressors and turbines, jet engines, air-conditioning equipment, pumps, and many other machines, it frequently becomes necessary to decrease the fluid velocity and, simultaneously, to increase the static pressure. "Diffusion" denotes the process of simultaneously decreasing the velocity and kinetic energy and increasing the pressure and flow work of the fluid.

The process of diffusion is usually an inefficient one because of the effect of the positive pressure gradient on the boundary layer of the flow. In particular, attempts to decrease the length and weight of diffusers by increasing the divergence angle results in very large losses and poor performance unless some means of boundary-layer control is employed. In fact, the earliest systematic investigation by Gibson (refs. 2 and 3) showed that the losses can exceed those of a sudden enlargement for certain particularly bad, wide-angle geometries.

Many other workers have investigated the performance of subsonic diffusers including Jones and Binder (ref. 4), Tults (ref. 5), Patterson (ref. 6), and Reid (ref. 7). The combined papers of Tults, Patterson, and Reid provide an excellent summary of the literature, and it is consequently unnecessary to repeat that information here. Some of their

data, together with those of Vedernikoff (ref. 8), Nikuradse (ref. 9), Demontis (ref. 10), and Polzin (ref. 11), are given in table I for convenient reference.

A great deal of attention has been given by previous investigators to the problem of the divergence angle yielding optimum performance. The most comprehensive summary and the most careful data on optimum performance are given by Reid (ref. 7). Reid noted that the angle for optimum efficiency was decidedly different from that for optimum recovery. In addition, the data of different observers are in very poor agreement concerning the optimum angle.

The present study had two main objectives: First, to study more systematically and in more detail the flow models in subsonic diffusers, and, second, to investigate the use of vanes in the flow as a means for producing efficient wide-angle diffusers. The first objective has been largely accomplished. Using dye injection in a water table to visualize the flow, as described below, four regimes of flow were found. The boundaries of these regimes are determined by three parameters which are discussed in detail. Quantitative graphs delineating these regimes of flow are given. These results have been verified by use of two different water-table units and an air apparatus.

While the water table provides an excellent and simple means for studying flow mechanism and while it also provides quantitative data concerning the effects of the controlling parameters on the flow mechanism, it does not provide any data on overall recovery or efficiency. It is to provide these data that the air apparatus was constructed. Since the taking of data in the air apparatus is a long and tedious process, the water-table results are also being used to guide the air-apparatus tests.

Unlike the water-table tests, the air-apparatus tests are still in progress, and final results have not been obtained. However, included in this report are enough preliminary data from the air unit to: (1) Verify the effect of the governing parameters on the flow models as found in the water table; (2) demonstrate that the water-table flow-model studies do provide the proper indications concerning regions of high and low performance; and (3) indicate that the vane configurations developed in the water table show very considerable promise.

Since the air-apparatus tests are only preliminary, and since the water-table studies provide very useful information by themselves, the present report deals primarily with the results of the water-table units and includes only a brief section on the air-apparatus results.

This investigation was conducted at Stanford University under the sponsorship and with the financial assistance of the National Advisory Committee for Aeronautics.

SYMBOLS

A	cross-sectional area of diffuser
a	distance along x axis from origin to center of vortex
a-a	line indicating points of transition to first stall (see figs.)
b-b	line indicating points of transition from three-dimensional to two-dimensional separation (see figs.)
c	width of core, core being region of flow having uniform velocity
c-c	line indicating points of transition from two dimensionally separated flow to jet flow (see figs.)
C_{ER}	energy recovery factor
C_{PR}	pressure recovery factor
d-d	line indicating points of transition from jet flow to two dimensionally separated flow (see figs.)
f^*	arbitrary function of velocity u
$G/2$	depth of water above horizontal glass bottom in water table
$(G/2)_{cl}$	depth of water measured above glass plate on center line of diffuser at throat, in.
G	distance between parallel Plexiglas walls of air diffuser
H	height of lip of outlet gate or weir above glass plate, in.
h	z-direction width of fluid flowing; replaced G and $G/2$ in derivation of appendix B
I_d	integral in denominator of equation (A9)

Ik	integral representing rate of flux of kinetic energy into diffuser
I_n	integral in numerator of equation (A9)
Io	integral used for mathematical manipulations
Iw	integral representing flow work
Iw_{2a}	integral defined by equation (A5)
J	height of bluing jets above glass bottom of water table
J = A	all jets 3 inches above glass plate
J = B	five jets ahead of throat at 3-inch height, downstream jets 1/4 inch above glass plate
J = C	five jets ahead of throat 1/16 inch above glass plate, downstream jets at 1/4-inch height
k	coefficient, a function of entering profiles and diffuser geometry
L	diffuser length, distance from throat to diffuser outlet measured along center line of diffuser
L_v	vane length
M	length of flat-plate portion of diverging walls of diffuser
m	number of vanes used
N	distance from throat to diffuser exit measured along diverging wall, $N = M + r_s\theta$
n	normal to streamline
p	static pressure
p_o	total or "reservoir" pressure
Q	volume flow rate or water flow rate, lb/sec
q	dynamic pressure, $\rho V_1^2/2$

R	area ratio, A_2/A_1
R_d	rod-diameter Reynolds number
R_L	Reynolds number based on diffuser length L and bulk average throat velocity V_1
R_r	Reynolds number based on u_{max} and coordinate r at point of stall
R_W	Reynolds number based on throat width W_1 and bulk average throat velocity V_1
r	radius in general
r	radial coordinate in polar coordinates
r_s	radius of entrance-section semicylinders
S	uncertainty in a variable
S_β	uncertainty in a result
s	coordinate along a streamline
T	temperature of flowing water, ^oF
U	velocity of core, constant at a cross section
u	variable x-direction (or r-direction) velocity
u',v',w'	components of turbulence
V	one-dimensional mass flow velocity or bulk average velocity
v	variable y-direction (or θ-direction) velocity
v_w	velocity of a potential flow at wall of throat
v_{cl}	velocity at center line of throat
W	diffuser channel width
W_1	throat width

W_v	spacing of vanes at their leading edge
w	variable z-direction velocity
X	complex potential function
x,y,z	Cartesian coordinates
x_n	variables
y	in boundary-layer analysis, distance from a diverging diffuser wall
z	vector on complex plane, $x + iy$
β	result (used in appendix C)
γ	constant used in development of flow between cylinders
δ	boundary-layer thickness
δ^*	displacement boundary-layer thickness, $\int_0^\infty \left(1 - \frac{u}{U}\right) dy$
η_E	diffuser energy efficiency, $C_{ER}/C_{ER_{ideal}}$
η_p	diffuser pressure effectiveness, $C_{PR}/C_{PR_{ideal}}$
θ	polar coordinate
$2\theta_v$	vane angle, total included angle between two vanes or between a vane and a diverging wall
2θ	diffuser angle, total included angle between straight, diverging walls of diffuser
λ	Lagrange multiplier, a constant parameter
μ	viscosity
ϕ	velocity potential
ψ	stream function

ρ mass density of fluid

Subscripts:

o stagnation or "reservoir" conditions

1 diffuser throat

2 diffuser outlet

w diffuser wall condition

c center line

In the photographs, small black arrows indicate location of dye-injection points downstream of throat. In all cases where dye is shown, flow is from left to right.

DIFFUSER GEOMETRY AND ENTRANCE VELOCITY AND PRESSURE PROFILES

DIFFUSER GEOMETRY

All the diffusers used in this investigation had entrance sections and diverging walls of the form shown in figure 1. The flow entered from the left through the curved-wall entrance section and was diffused as it passed to the right out through the plane-wall section. These ski-shaped surfaces were formed by rolling the end of a metal plate into a half cylinder, although the juncture between plane and cylinder was relieved slightly by grinding and polishing so that the boundary layer would not be subjected to a sudden change in curvature.

The ski-shaped walls were pivoted about the centers of curvature of the half cylinders so that the angle of divergence 2θ could be varied at will, and the distance between the pivots was adjustable so that the throat width W_1 also could be changed. Variation in the length-to-width ratio L/W_1 was obtained by adjusting W_1 rather than by changing the plate length M. Thus, the apparatus gave great flexibility with no need for cutting or modifying diffuser elements to obtain the required changes in configuration.

FLUX PLOTS

In light of the work of Rouse and Hassan (ref. 12), it was feared that using a cylindrical entrance section only $4\frac{1}{4}$ inches in radius might result in the creation of localized positive pressure gradients ahead of the throat, thereby making separation possible at the wall even before the flow reached the diffuser proper. Therefore, a number of flux plots using Teledeltos conducting paper were made in order to investigate the pressure gradients generated at the wall of the entrance section. No positive pressure gradient was found to exist until the throat width was increased to 9 inches where a slight positive pressure gradient was found at a position $1\frac{1}{2}$ inches upstream from the throat as measured along the curved wall of the diffuser. Since all tests were run at throat widths of 6 inches or less, it was concluded that the cylindrical entrance shape would not cause prethroat separation. Indeed, no separations were observed ahead of the throat in any of the actual tests conducted.

ENTRANCE VELOCITY AND PRESSURE PROFILES

Wall Curvature

In any diffuser, regardless of whether the flow transition is from a straight duct flow or from a large quiescent region as in the present case, the necessary increase in cross-sectional area requires that the diverging diffuser wall be curved at least at the juncture of the diverging walls and the entrance section. The corresponding curvature of the streamlines just outside the boundary layer is accompanied by a local lowering of the static pressure near the walls, as is quickly demonstrated by Euler's dynamical equation taken normal to the streamlines, the development of which is given, for example, by Shapiro (ref. 13, p. 281):

$$\partial p/\partial n = \rho v^2/r$$

where n, the normal to the streamline, is directed away from the center of curvature. Thus, as the boundary layer leaves this localized zone of low pressure near the curved walls, the positive pressure gradient it encounters is intensified, although the gradient in advance of the turn is more favorable.

Furthermore, since the flow comes from a region of constant total pressure upstream, and since Bernoulli's equation applies along each streamline outside a thin boundary layer, the variation in pressure across the throat implies, necessarily, a variation in velocity across the throat. This is true in all diffusers, but the amount of nonuniformity in velocity will vary from unit to unit depending on the inlet geometry. This raises the question whether the results of tests with one inlet geometry can be used to predict performance in other units.

In addition, in the present unit, W_1 is varied to achieve a change in L/W_1. Consequently, the price paid for flexibility is a small change in inlet velocity profile from one geometry to another. This, again, raises a question concerning comparison of data obtained with different inlet velocity profiles.

Johnston (ref. 14) found that a change in inlet velocity profile caused an appreciable change in performance. However, the changed velocity profiles in Johnston's work were far from the potential flow patterns for the entrance geometry involved, their nonuniformity having been generated by uneven distribution of gauzes on screens ahead of the inlet.

On the other hand, Robertson and Ross (on pp. 5 and 6 of the discussion of their paper (ref. 15)) mention tests in water in which variation in the shape of the inlet had no serious effect on a diffuser. Copp (ref. 16) systematically varied the radius of curvature at the juncture in a conical diffuser from near zero to as high as 40 inches and found the static-pressure performance was entirely independent of the inlet wall shape, although, as the radius of curvature of the inlet junction was increased, the mass flow rate increased slightly. Furthermore, modifying the contour of the diffuser inlet ahead of the section of minimum area produced no systematic trend in exit profile shape.

The tests discussed in the preceding paragraph were all conducted at small divergence angles and area ratios which, in themselves, avoided separation; consequently it has not been positively demonstrated that a nonuniform entrance profile will not affect separation characteristics. The evidence points toward the conclusion that, excluding sharp-edged junctures, no significant separation or change in performance will result so long as the nonuniform profile approximates that of a potential flow for the geometry of the inlet in question. However, it is admitted that the problem needs further study.

In the above reasoning it is not implied that performance will be unchanged if alterations in the entrance section change the boundary-layer characteristics materially, for, as shown by Robertson and Ross (ref. 15), Copp (ref. 16), Copp and Klevatt (ref. 17), and Peters (ref. 18),

the effect of thickening the entrance boundary layer is to decrease the pressure effectiveness of a diffuser. In Peters' study, however, variable amounts of spiral flow were tolerated, and it is possible that this condition, together with the possibility for variable turbulence intensities, seriously compromises the value of his data. In fact, in all of the four references listed above, the variation of boundary-layer thickness was obtained by inserting a straight length of pipe ahead of the diffuser entrance. It should be noted that, while thickening the boundary layer, this length of pipe might also change the intensity of the free-stream turbulence either up or down. As shown later in this report, changing the turbulence level has an important effect on diffuser performance.

Potential-Flow Velocity Profiles

Because a function which would map a potential net onto the exact form of the present diffuser was not known, estimates of the velocities which existed at the throat were made in two ways.

First, an estimate of the maximum nonuniformity was made by investigating the potential solution for flow between cylinders as shown in figure 2. An expression for the velocity profile at the throat is derived in appendix A of reference 1, and the resulting profiles are presented in figure 3 for a range of throat widths great enough to cover the values of W_1 employed in this work. Values for the ratio of velocity at the cylinder wall to velocity at the center line of the throat v_w/v_{c1} together with the ratios of the dynamic pressure q_w/q_{c1} are given in table II.

Second, these velocity ratios were estimated by measuring them on the flux plots previously mentioned. As expected, it was found that the profiles were more nearly uniform at low diffuser angles while at very large angles the ratios approached those for flow between cylinders. The flux-plot values for v_w/v_{c1} and q_w/q_{c1} for $2\theta = 7^\circ$ and 30° with $W_1 = 3$ inches are compared in table III with the values obtained in flow between cylinders.

PARAMETERS INVOLVED IN PROBLEM

MATHEMATICAL SOLUTIONS

The only available analytical solutions for flow in a diffusing passage with an increasing pressure are those for laminar flow as given

by Hamel (ref. 19) and Goldstein (ref. 20). These solutions are of little utility since the flow is almost always turbulent in the diffuser boundary layer. Consequently, the only available theoretical resort is a dimensional analysis.

DISCUSSION OF PARAMETERS

Normalization of the Navier-Stokes equations, as given in appendix D of reference 1, provides a means for determination of the governing nondimensional parameters although the method becomes particularly complicated in this case. It was therefore taken together with a study of the available data of earlier workers (see above) to determine as much as possible about the parameters of importance. The results show that the overall performance is a function of the following variables: Geometry, Reynolds number, Mach number, wall roughness, and state of the inlet boundary layer. As explained above, inlet velocity profile is omitted. The experiments described below show that free-stream turbulence is also an important independent variable. Geometry is itself a function of three variables, namely, divergence angle, aspect ratio, and ratio of wall length to throat width. In the present study, Mach number was eliminated by the use of essentially incompressible flows, and inlet boundary layer has been held essentially constant by control of the inlet conditions. The other variables have been studied, and the results are given below.

The overall dependent performance parameters of most concern are pressure recovery C_{PR}, pressure effectiveness η_p (often called pressure efficiency), energy recovery C_{ER}, and energy efficiency η_E. The first two are defined in the usual way as follows:

$$C_{PR} = \frac{(p_2 - p_1)}{q_1} = \frac{(p_2 - p_1)}{\frac{1}{2}\rho V_1^2}$$

and

$$\eta_p = \frac{C_{PR}}{C_{PR_{ideal}}} = \frac{C_{PR}}{\left[1 - (1/R^2)\right]}$$

Thus, as usual, C_{PR} is the actual pressure regain divided by the inlet dynamic pressure for incompressible flow, and η_p is the actual pressure recovery divided by the pressure recovery that would occur in an ideal, that is, frictionless, diffuser with one-dimensional, incompressible flow.

These parameters lose significance when the inlet flow is not one dimensional. For this reason the energy parameters have been defined. The energy recovery is taken to be the mean increase in flow work per pound of flow divided by the mean kinetic energy entering at the throat per pound of flow. The energy efficiency is defined as the actual energy recovery divided by the energy recovery that would occur if the flow in the diffuser from the throat onward occurred without any dissipation of energy. Using the control volume of figure 4(a), derivations are given in appendix A from which evaluation of the energy parameters can be made for any entrance velocity profile. (Other control volumes are given in figs. 4(b) and 4(c).) It should be noted that insertion of the conditions of incompressible flow, with a uniform inlet velocity and uniform outlet pressure, reduces the energy recovery to the conventional pressure recovery and the energy efficiency to the conventional pressure effectiveness.

It should also be noted that deviations of the order of 5 percent of inlet velocity from a one-dimensional profile can easily cause deviations of 10 percent between the actual recovery and efficiency and the values indicated from a wall static-pressure measurement at the throat. Since, as previously noted, pressure and velocity variations at the throat of some magnitude must occur in all diffusers, considerable care is necessary in computing recovery and efficiency.

Simple approximate means for computing the energy parameters are derived in appendix A. Appendix B contains a discussion of the very important effect of exit velocity profile on recovery and efficiency. It is shown in appendix B that any deviation at the exit from the square velocity profile of one-dimensional flow will seriously and adversely affect the performance of the unit.

A discussion of the relation between the more general nondimensional Euler number used in boundary-layer calculations and the pressure recovery is given in reference 1, where it is indicated that the pressure recovery is a special form of the Euler number.

WATER-TABLE TESTS

Since the still photographs contained in this paper cannot show the transient flow phenomena of the water table entirely adequately, a motion picture covering the phenomena discussed in this section has been prepared

and is available on loan. A request card form and a description of the film will be found at the back of this paper on the page immediately preceding the abstract and index pages.

GENERAL DESCRIPTION

Water Table

The water table used in these tests is described in detail in appendix G of reference 1. It consists of a horizontal glass plate over which water flows. A calming chamber precedes the test section.

Figures 5(a) to 5(g) show the water table. In these photographs the large and small diffusers, the ink distribution system, and the last upstream screen can also be seen.

At the downstream edge of the water-table glass, an adjustable-height weir was used to fix the water depth at any value up to 5 inches above the glass plate, thereby controlling the throat aspect ratio. Flow rate was controlled by an upstream valve and was measured by weighing the outflow. The throat width was set with gage blocks and the exit width with a machinist's scale.

The glass plate had 1-inch squares ruled on its under side and was illuminated from beneath, so that conditions were ideal for observing streamlines and trajectories made apparent by injecting bluing into the water and photographing it against a grid background.

Placement of Bluing Jets

Five bluing streamlines were introduced upstream of the throat. Two of these were released in the boundary layer by means of jets in contact with the walls of the entrance section 4 to 6 inches in advance of the throat. The other three were introduced so that they quartered the main stream.

There were four downstream jets the placement of which was varied in order to achieve the best effect in each case, although the two of these which were placed in contact with the walls were usually placed 10 inches inside the outlet of the diffuser. All of these downstream jets injected bluing vertically downward; hence the observer needed to watch only the direction of movement of the bluing in order to determine when a stall had been encountered. Thus, in the photographic studies, when bluing was seen upstream of one of these jets (or forming a motionless

blob directly beneath it) rather than moving downstream toward the outlet, the existence of backflow (or a stall) was established.

The vertical position of all the bluing-injection jets could be varied so that bluing could be released and streamlines delineated at any height between the surface of the water and the glass bottom. In the first tests, pictures were made while varying this height at 1/2-inch intervals through the depth of the water. These tests indicated that, with water depth at approximately 4.5 inches, it was sufficient to limit jet heights to three conditions as follows:

(1) J = A: All bluing injected 3 inches above the glass plate.

(2) J = B: Five jets ahead of the throat located at the 3-inch height; jets downstream of the throat located at the 1/4-inch height.

(3) J = C: Five jets ahead of the throat located at the 1/16-inch height; downstream jets, if any, located at the 1/4-inch height.

When tests were run at decreased depths in order to vary the aspect ratio, the 3-inch height was decreased proportionally.

Water-Table Diffusers

The general geometric form of the diffusers employed has already been discussed at the beginning of this report and only dimensions peculiar to the water-table diffusers are added here. The large water-table diffuser, which was of nearly the same size and shape as the air diffuser tested later, had a straight wall length M, shown in figure 1, of 24.375 inches and an r_s of 4.55 inches, but the small diffuser, which was geometrically similar in profile but only about one-third scale, had M = 7.65 inches and r_s = 1.55 inches. In the z-direction, the diffusers were 4.8 inches high, but the maximum practical water height G/2 was only about 4.5 inches. Actually G/2 varied with velocity in different parts of the water table; but the velocities employed were so low that the small changes in G/2 could not be measured accurately, and this variable could be considered constant. This, in fact, is the reason why quantitative recovery data were not obtained in the water-table tests.

Aspect Ratio

For purposes of comparison with the air diffuser to be tested later, the water-table-diffuser dimension G was taken equal to twice the depth of the water, whereas in the air diffuser G was the entire z-direction dimension of the flowing air. This was done, of course, because the upper

surface of the water was free; therefore, the water-table diffuser had only one horizontal glass wall offering frictional retardation of the flow while there were the two parallel Plexiglas walls in the air diffuser.

The aspect ratio for the water-table diffuser, then, was defined as $2h/W_1$ as compared with h/W_1 for the air diffuser. Aspect ratios in the large water-table diffuser were much smaller than those in the air diffuser, but the small water-table diffuser and the air diffuser had approximately the same aspect ratio.

Boundary-Layer Trip

Because diffusers usually are operated with a turbulent wall boundary layer at the entrance, a boundary-layer trip of 0.020-inch-diameter wire was attached to each lacquer-smooth entrance section of the large diffuser at a point 2.75 inches upstream of the juncture between the flat plate and cylinder. These trips were seen to generate tiny Helmholtz waves which, however, did not usually grow so long as the boundary layer remained in the region of strongly accelerated flow.

Trips were omitted from the small-water-diffuser entrance section because this diffuser was less carefully made than the large diffuser, and slight waviness of the rolled entrance sections offered sufficient roughness to accomplish the same result as a trip.

Care was exercised in both the small diffuser and the large diffuser to make sure that the boundary layer was turbulent, as indicated by dye dispersion, at the throat. Thus, in all cases where data were recorded, there was no possibility of laminar separation.

Secondary Flow

As a result of the low heads of water at the edges of the throat (caused by curvature of the streamlines near the cylindrical walls), an appreciable secondary flow was generated. The direction of this flow, as observed at cross sections both before and after the throat, is shown by the heavy arrows in figure 6, which is a full-scale cross-sectional sketch of the throat of the water-table apparatus set at $W_1 = 3$ inches with the observer looking downstream.

The secondary flow was strongest near the bottom of the channel. In fact, the strong secondary flows occasionally seen at the surface of the water appeared to be merely the result of capillary spreading of any bluing which happened to reach the surface. Sometimes, also, the density

of the bluing mixture was appreciably greater than that of the water, and this density difference also caused secondary-flow disturbances as the colored streamers tended to incline downward through the diffusers. In most cases this effect was slight, however.

Turbulence of Entering Flow

In the first tests conducted in the water table with the large diffuser, the screens used to even the inlet flow and to damp entrance turbulence in the upstream section of the water table were not selected properly. The result was the introduction of turbulence which was evident at the diffuser entrance in the tortuous shape of the entering streamlines. Fortunately, a full series of separation-angle determinations was made before this high-turbulence condition was corrected, and a good set of data for comparison with low-turbulence performance was obtained.

To reduce the turbulence, five 16-mesh screens were added which operated at a Reynolds number (based on the 0.0113-inch wire diameter and free-area velocity) varying from 0.3 to 1.6 depending on the flow rate used. These dampers resulted in an extremely low turbulence level as evidenced by the absence of all streamline irregularities other than those imposed by the previously discussed secondary flow. A second complete series of separation-angle determinations was made under the new low-turbulence conditions.

The wide difference in the turbulence in the entrance caused by the addition of screens is illustrated by the photographs of figure 7.

At constant temperature and water depth $G/2$, the flow rate is directly proportional to the diffuser-throat Reynolds number as shown by the defining equations

$$R_W = \frac{W_1 \rho V_1}{\mu} = \frac{2(Q\rho)}{G\mu}$$

where $Q = W_1 V_1 (G/2)$.

The Reynolds number of the damping screens also was directly proportional to the flow rate; therefore, they operated at constant Reynolds number when the throat Reynolds number was constant, regardless of the variation in throat width and accompanying change in L/W_1. Since the turbulence ahead of the damping screens remained constant at constant flow rate, and since the damping capability of a screen system is determined by its geometry and its Reynolds number, it is believed that the

turbulence level in the water just ahead of the entrance section is nearly constant when throat Reynolds number is held constant. There may, however, be a small variation of relative turbulence u'/V_1 at the throat when L/W_1 is changed owing to the variation of the amount of contraction with changes of W_1.

Even with changes in throat Reynolds number, the turbulence level must have changed only slightly, for at no flow setting were small scale wiggles observable in the entering streamlines so long as the five additional damping screens were installed. This result arose, no doubt, from the damping screens having a large, nearly constant, damping coefficient because their Reynolds number, based on wire diameter, remained of the order of magnitude of unity.

It must be emphasized that the claim of negligible change of upstream turbulence with flow rate does not apply to the high-turbulence tests in which the five additional screens were not used. In those tests an increase in flow rate caused an increase in the turbulence level. At constant flow rate, however, turbulence in the headwaters ahead of the contraction still showed little or no variation.

The reader is referred to the work of Dryden and Schubauer (ref. 21), Schubauer and Spangenberg (ref. 22), and Eckert and Pflüger (ref. 23) for information on selection of screens and sources of the opinions formed above.

Dynamic-Similarity Considerations

The flows used in the water-table diffuser fixed the throat Reynolds number R_W at values varying between 2,000 and 12,000. These values were too low to afford complete dynamic similarity between the water-table diffuser and the air apparatus to be tested later which operated at values of R_W greater than 100,000. Increasing the Reynolds number by enlarging the water table was not feasible because a size factor of about 20 was involved. Furthermore, increasing the flow rate in the water table would have resulted in rapid (shooting) flow at the throat showing that, analogously speaking, sonic velocity had been reached, whereas the air-flow apparatus was designed to operate at Mach 0.2 or less at the throat. However, in spite of the difference in Reynolds number in water and air flow, remarkable success was enjoyed in extrapolating from one system to another. It is believed that this success rests on two factors: (1) The Reynolds number being large enough so that further increases do not shift the flow from one regime to another, and (2) the care taken to insure a turbulent boundary layer at the throat.

Method of Procedure in Photographic Studies

The general procedure followed was first to set the throat width W_1, thereby establishing L/W_1 and N/W_1 and fixing M/W_1. Next the flow rate was adjusted to give the desired throat Reynolds number. With the above two settings held constant, the diffuser was varied through the spectrum of angles, first in order of increasing and then in that of decreasing magnitude, so that any hysteresis effects would not be overlooked. The variation of angles was then repeated with vanes inserted and, still later at a value of L/W_1 of approximately 8, with turbulence-inducing rods. After each angular setting was made, no photographic data were recorded until 5 or more minutes had elapsed because the act of changing the angle itself usually created turbulent disturbances in the flow which required time to die out.

Flow configurations for the large water-table diffuser were studied photographically at L/W_1 ratios of approximately 4, 8, 16, and 24, plus, in the high-turbulence runs only, one series of $L/W_1 = 6$. At each L/W_1 setting, the angle of divergence 2θ of the large diffuser was varied from well below the angle where a stall was first observed to the maximum angle of 40° to 45°. Photographs were taken at angular intervals of as little as 1° in regions of greatest interest.

Pictures of angles larger than those possible using the large diffuser were obtained by substituting the one-third-scale diffuser in the water table and operating it at M/W_1 ratios in the range between 4 and 20. In these cases the angular interval was no less than 5°, and the angular settings were extended to angles of 90° for $M/W_1 = 4$ and 8 and to 180° for $M/W_1 = 16$. All of the small-diffuser tests were run under the low-turbulence conditions.

All of the above tests were repeated for different throat Reynolds numbers. A total of some 1,300 frames of 35-millimeter film were exposed. Typical photographs are reproduced in the figures (see, e.g., fig. 7).

WATER-TABLE DIFFUSERS WITHOUT VANES

Large Water-Table Diffuser

General description.- More time was spent and more photographic data compiled with a diffuser with a 3-inch throat $\left(L/W_1 \text{ of about } 8\right)$ than with any other, although sufficient work was done at other settings to determine, as a function of L/W_1, the variation of angle at which

separation occurred. Consequently, the diffuser behavior in zones of transition to separated flow is described in detail with reference to an L/W_1 ratio of approximately 8, and comparative behavior at other settings is presented more briefly.

In the explanations below a distinction will be made repeatedly between a two-dimensional separation and a three-dimensional one. Figure 8(a) and the line 1-1 in figure 8(b) define the two-dimensional separation. Thus, a flow which takes place down one diverging wall and has virtually the same flow pattern at all depths is two dimensional. If, instead, the separation is confined mainly to one corner as shown by line 2-2 in figure 8(c) or varies markedly in pattern at different heights above the glass wall of the water table, the flow is three dimensional. More simply, the three-dimensional flow shows marked variation in the z-direction, and the two-dimensional flow does not.

In investigating the occurrence of first stall, a jet height of either $J = B$ or $J = C$ was used in order to have the two downstream wall jets deep in the corners of the diffuser where the first stall was always found to occur in the range of throat Reynolds numbers and L/W_1 ratios of the flows depicted. However, a few flows, notably some at high flow rates and at L/W_1 ratios greater than 24, were observed in which first stall occurred near the surface of the water, far removed from any diffuser corner. A first stall at this position would correspond to stall near the center of a diverging wall of the air diffuser. Pictures of these noncorner first stalls are not reproduced herein because the high flow rates involved caused gravity waves large enough to cast doubt on the validity of the analogy to closed-duct flow of any real fluid.

In the entire discussion which follows, the parameter of the ratio of diffuser length to throat width L/W_1 will play a very important role. Although this parameter is a simple geometric description, two more significant physical meanings may be noted.

First, L/W_1 is the ratio of length Reynolds number to throat Reynolds number. Now, the boundary layer on the wall depends on a Reynolds number based on the length measured down the wall. The length Reynolds number R_L, therefore, has significance with respect to the condition of the boundary layer at the outlet. Since R_L is related to R_W by L/W_1, which is a constant for a given diffuser, R_W can be used equally well in connection with discussions of the boundary layer at the outlet.

Second, L/W_1 is of use in connection with the diffuser angle 2θ in specifying the area ratio R. As indicated earlier and as derived in

appendices C, D, and E of reference 1, both the ideal pressure recovery factor and the ideal Euler number are functions of R only. Reid (ref. 7) has discussed in detail the important connection between R and the pressure recovery of a diffuser, and his data are presented as functions of R and N/W_1. In the present investigation 2θ and L/W_1 were chosen as the geometrical parameters. Their relationship to the area ratio can be appreciated through the simple approximation

$$R = \left(\frac{W_2}{W_1}\right) = 1 + 2\left(\frac{L}{W_1}\right)\tan\left(\frac{2\theta}{2}\right)$$

If the angle is held constant, the effect of L/W_1 on R and, consequently, its influence on the recovery and the Euler number become obvious.

Separations resulting from increasing angle in vaneless diffusers.- Figure 9 shows the changes which took place in the flow configuration as 2θ was changed from an angle of 10° where no separation took place to an angle of 17° where the flow was diverted by a stable asymmetric separation of two-dimensional form.[1]

Figure 9(a), which used J = B (defined earlier as five upstream jets at 3 inches, four downstream jets at 1/4 inch, above the glass plate), shows flow at 10°. Comparison with figure 7(a) points out the marked change in flow configuration which took place as a result of the increase in angle. The smooth incoming streamlines developed waviness which degenerated into an apparently random turbulence at about 3L/4. The diverging-wall boundary layer thickened markedly as shown by the slower-moving fluid in the areas near the walls where the bluing of the two wall streamlines was being dispersed by turbulence. The boundary layers in figure 9(a) appeared to have coalesced by the time the diffuser exit was reached, but this was not definite because turbulent mixing in the core now tended to destroy the contrast in color between boundary layer and core, and some other cases were noted in which the central core definitely was intact at the diffuser exit. One must not confuse the widening zone of the turbulent boundary layer with separation, which will be encountered later. Adjacent to all walls, even in the corners, there was always a forward motion in the same direction as the main flow, and no stall or backflow existed.

---

[1]In figure 9 and subsequent photographs, the location of the downstream dye-injection points are marked by very small black arrows. Since the flows are all from left to right, the presence or absence of stalls can be seen by noting the direction of dye movement from the arrows.

Figure 9(b) shows that the same general conditions existed at $2\theta = 11^{\circ}$. However, at 12° (fig. 9(c)), the downstream jet on the upper wall in the picture indicated a lack of motion and even a slight backing which announced the first stall. Unfortunately, this condition is made apparent to the reader only by the stagnant and spreading blob of bluing beneath the jet owing to the difficulty of depicting a very slight backflow in a still photograph. However, the condition was easily discernible by an observer on the scene who could see the vertically injected, downstream jets bend back toward the throat rather than bend in the expected downstream direction. The determination of the angle of first stall by the method described gave definite quantitative results which were reproducible to within $2\theta = 1^{\circ}$.

At this point it must be acknowledged that the vertical tubes used for introducing the bluing downstream of the throat might have influenced the results; nevertheless, it is believed that their effect is small since tilting the tubes and injecting bluing from a number of different directions produced no change in the results. It would have been better to introduce the coloring matter through holes in the wall, but this solution would have been inconvenient and would have complicated the apparatus.

In most of the tests the downstream wall jets were fixed at one location, and it might be argued that this would cause the observer to miss some stalls at other points along the wall. However, a stall at one point was seen to move along the length of the wall and cause stalls to exist momentarily at other points on the same wall. In addition, the bluing released served as an indicator for other points as it moved away from the point of release.

The data obtained in figure 9(c) were interpreted to mean only that stall can occur at angles as low as that observed, for it cannot be said that some vagary of the flow will not produce a momentary flicker of a stall at some still smaller angle if the time of observation is extended indefinitely. At higher turbulence levels it is especially important to consider the time element. In this investigation, if no stalls were observed over a 5-minute period after steady flow had been established, it was assumed that the angle in question was free from separations. Therefore, the conclusion in this case was that, with a diffuser with $L/W_1 = 8.22$, $R_W = 10{,}380$, and $G/W_1 = 2.93$, the first backflow would appear at $2\theta = 12^{\circ}$ in the corner of the diffuser cross section, but, at an angle 1° smaller, that there would be no separation. The larger angle was used in plotting the data. Furthermore, the separation observed was an intermittent one which did not always occur in the same corner, but appeared and disappeared in both corners in an erratic fashion.

The beginning of separations marked the beginning also of an unsteady flow regime which is best illustrated by figure 9(d) at $2\theta = 15^{\circ}$. Here

the main flow was seen to wander aimlessly around in the diffuser with separations and backflow appearing repeatedly on both walls, though not necessarily alternately. The separations were three-dimensional in form. At 16° with jets now all at the 3-inch height (J = A) the three-dimensional separation and unsteadiness continued, but the flow showed a definite preference for the right wall. In some instances it chose the left wall instead, the choice seeming to depend more on which wall the stronger intermittent stall happened to be when the diffuser angle was widened than on any nonsymmetry in the geometry of the diffuser itself.

In descriptions of the three-dimensional separations above, they have frequently been referred to as transient three-dimensional separations in contrast with the so-called steady two-dimensional stalls. This has been purposely done, and it is to be noted that not only are the three-dimensional separations always of a transitory nature but also the two regimes of stall, two-dimensional and three-dimensional, are entirely different in their flow patterns, in the appearance and steadiness of the flow, and in the resultant overall performance of the unit.

The two-dimensional separation corresponds with the classical picture of stall appearing in most of the textbooks. The three-dimensional separation, on the other hand, does not seem to have been well described, and the results would at least suggest that it is a very common regime.

As just noted, three-dimensional separation is not only transient, but also transitory. The stall appears for a moment in one position only to be washed downstream and to reappear again in the same or some other location a moment later. The size of these local transitory stalls varies greatly as does the duration of their survival. When the angle is first increased into the three-dimensional-stall zone, very small stalls appear, and they persist for a very short time. As the angle is increased both the size and duration of the stalls grow until finally they become so large that a transition to the steady two-dimensional separation pattern occurs. It is believed noteworthy that the smallest observable stalls were associated with the highest frequencies of motion, and, conversely, the largest with the lowest frequencies. This is probably due to the inertia of the dead water or stall region. It is interesting to speculate concerning whether still smaller stalls, occurring at frequencies too high to observe with a dye technique, actually do occur in the region which has been called unstalled. The manometer fluctuations described below for the air-diffuser flow suggest that this might be the case. However, no investigations on this point have yet been made.

Another speculation, of even more general interest, concerns whether transitory stalls of the nature of those observed in these tests are also found in other situations such as the positive-pressure-gradient zones of an airfoil. In the authors' opinion it is possible that they are.

Furthermore, the frequencies of motion may well be high enough so that most conventional instruments would not reveal them. If such transient stalls do occur, it would certainly explain, among other things, the reason for the failure of mathematical boundary-layer theory to predict separation accurately inasmuch as such calculations are normally based on a steady two-dimensional physical model.

At $2\theta = 17^\circ$, figure 9(e), the flow stabilized in two-dimensional form along the lower wall in the photograph. The flow was much steadier, and a large wedge of stagnant water along the upper wall began to darken as larger quantities of bluing from the jet on the separated wall began to concentrate there. This configuration was a stable one which remained for as long as the flow continued, although it could be forced to change walls by introducing a vane or even by deflecting the flow by hand. After being deflected it would be stable in its new position hugging the upper wall, leaving the lower wall in a separated condition. The main flow in figure 9(e) was very little wider at any point in the diffuser than it was at the diffuser throat, showing that little or no diffusion had taken place.

Runs were also made at angles up to 50°, the maximum possible setting of the large water-table diffuser, and photographs illustrating some of these flows are discussed in the section on vanes. The larger angles exhibited no significant changes in flow pattern except for the development of a stronger affinity for remaining separated along one diverging wall. In all cases where two-dimensional separation occurred the same inability of the main stream to expand its cross-sectional area was observed. This was not true with a three-dimensional separation, where only a part of the flow failed to decelerate.

It is noteworthy that all flows which oscillated from side to side in the diffuser were confined to the lower half of the 12° to 16° three-dimensional flow zone. Above 15°, and especially after the complete establishment of the two-dimensional flow regime, the flow no longer wandered about, although waves and fluctuations developed along the outer boundary of the main flow. The action at this outer boundary appeared to be a continual tug of war between the kinetic energy of the high-speed stream and the inertia of the fluid in the dead-water region.

The determination of the exact two-dimensional-stall angle was less objective than the determination of the first stall angle because the opinion of the observer as to steadiness and two-dimensionality entered. However, this difficulty was resolved simply by extending the tolerance or uncertainty in 2θ. Thus, the conclusion in this case was that in a diffuser with $L/W_1 = 8.25$, $R_W = 11{,}150$, and $G/W_1 = 3.0$ a two-dimensional separation with steady flow existed at 17°, whereas an unsteady flow with a three-dimensional separation existed at 15°. For plotting purposes the larger value was again used.

The detailed description given above is typical of the relative sequence of events as angle is increased and of the models observed for all the series of runs made. However, as will be seen below, the numerical values of the angles involved at first stall and at two-dimensional separation vary over a surprisingly large range depending on the value of the governing parameters, L/W_1 and free-stream turbulence.

Effect of changes in Reynolds number on separation.- Figure 10 shows the effect of lowering the throat Reynolds number to about 6,000 by diminishing the flow rate. This change resulted in an increase of the angle of first stall as shown by the change from the flow of figure 10(a), where no stalls existed, to that of figure 10(b) in which the downstream jet on the upper wall in the picture indicated stall in the corner.

Figure 10(a), incidentally, is the first photograph shown thus far in which all jets are near the glass bottom (J = C). The flow near the throat indicates the effect discussed earlier of the low heads near the curved walls in producing secondary flow.

The transition from a wandering three-dimensional flow to a stable asymmetric one is illustrated by figure 10(c). Thus, the angle at which the flow became two dimensional was decreased by 1° to 16°.

The evidence discussed above was not at first considered conclusive because the 1° changes in angle were but slightly greater than the uncertainty involved in fixing the angle of separation. However, in changes of Reynolds numbers at four different L/W_1 ratios (fig. 11), only one curve, that of first stall at $L/W_1 = 4$, showed a trend that did not match that of the others.

Thus, it would appear that, in this range of operation, increasing throat Reynolds number tends to decrease the angle of first stall and increase the angle of complete two-dimensional separation. Therefore, the extent of the unstable flow regime tends to increase at higher Reynolds numbers. The rate at which these changes occur with changing Reynolds number, however, is very small.

It would have been desirable to extend the water table to cover a wider range of Reynolds numbers. Unfortunately, this was not feasible. Flows giving higher Reynolds numbers caused gravity waves in the throat which affected the results. Flows at lower Reynolds numbers necessitated impossibly long waits for the decay of turbulence which was introduced whenever the water was disturbed by changing the diffuser angle or making other adjustments. Failure to provide this stilling time would have allowed a high relative turbulence in the throat, and, as shown later, the increased turbulence intensity would have affected the results markedly.

Variation of angles of separation with change in L/W_1.- Figure 11 indicates that changes in geometrical configuration, as manifested by variation in L/W_1, cause very large changes in the values of the separation angles when throat Reynolds number and free-stream turbulence are held constant. For example, doubling L/W_1 to a value of approximately 16 lowered the first separation angle to 8° as shown in figures 12(a) and 12(b) in which the jet on the upper wall in the photograph gave evidence of considerable backflow. Figures 12(c) and 12(d) show the transition to stable two-dimensional separation.

Figure 13 presents the data of figure 11 (see also tables IV) on a logarithmic plot of separation angle versus the L/W_1 ratio. The throat Reynolds numbers R_W are indicated by the figures beside the data circles. In figure 13 the solid lines are curves for constant throat Reynolds number and a nearly constant depth of water. The dashed lines are for constant depth, constant length Reynolds number, and, since L was held constant in all tests, for constant bulk average throat velocity V_1. Curves a-a show the variation of first stall angle with a change in L/W_1. The outstanding feature of the solid a-a curve is its linearity.

Tests also were run in which the L/W_1 ratio was changed while holding aspect ratio constant at $G/W_1 = 1.01$. There was no significant change in the two-dimensional separation curve. In the first-stall curve there was only a slight change which, at values of L/W_1 greater than 8, resulted in approximately bisecting the area between the constant R_W and the constant R_L curves.

From figure 13 and the information in the paragraphs above it may be concluded that at approximately constant turbulence conditions the Reynolds number, the aspect ratio, and small variations in entrance velocity cause only minor changes in the separation angles compared with those produced by simple variation of the L/W_1 ratio.

Effect of turbulence.- As mentioned earlier, a set of data was obtained when the turbulence was at high intensity before the five additional damping screens were installed. Photographs of the diffuser flows with high-turbulence entrance conditions are presented in figures 14(a) to 14(d) for $L/W_1 \approx 8$ and in figures 14(e) to 14(h) for $L/W_1 \approx 16$. The reader is referred again to figure 7(b) for a larger scale illustration of the variability of the entering flow.

Figures 14(a) and 14(b) where $J = C$ (all jets near the glass wall) show the transition to first-stall condition at $2\theta = 12^\circ$. The upper wall

jet in figure 14(b) shows a bad stall. Actually, a corner stall was also found at 11°, but it was a slight one and the 12° photograph is substituted for purposes of illustration. Figure 14(c) shows a three-dimensional, unsteady separation at 25° which settled down to a uniform, though turbulent, two-dimensional separation at 26°.

Figures 14(e) and 14(f) show, for $L/W_1 \approx 16$, the first-stall condition which began at 9°. A bad backflow then suddenly developed in the right-hand corner. The transition to two-dimensional separation is illustrated in figures 14(g) and 14(h) at 19° and 20°, respectively. Figures 14(a) and 14(b) and figures 14(e) and 14(f), where the entering streamlines are at the bottom of the channel (J = C), again show the effects of secondary flow at the throat.

The stall and separation angles from these and other photographs are presented in tables V and in the logarithmic plot of figure 15, where the curves are again for constant throat Reynolds number (R_W = 6,000). The solid lines are the high-turbulence curves, and the dashed curves, which were transferred from figure 13 for purposes of comparison, are for low-turbulence entrance conditions.

In the case of first stall (curves a-a) the effect of increased turbulence was to raise the separation angle slightly for values of L/W_1 greater than 13 and to decrease it slightly for values of L/W_1 less than 13. However, the scatter in the data, particularly at high turbulence levels, is almost as much as the changes noted. In the case of the transition from three- to two-dimensional separation (curves b-b) a much larger and easily discernible effect was found. Increasing turbulence markedly increases the angle of transition at all values of L/W_1. As indicated by the upward shift of curve b-b in figure 15, this increase varies from 6.5° at an L/W_1 of about 24° to 16° at an L/W_1 of about 4.

This last finding undoubtedly is one of the important products of the present investigation. The effect of a change in turbulence intensity is shown to be large enough in itself to account for the current uncertainties in specification of diffuser performance; moreover, it appears that attempts to duplicate diffuser performance will meet with failure unless the turbulence, probably both as concerns scale and intensity, is controlled.

Thus, figure 15 and the discussion in the foregoing sections point up two important conclusions about prediction of diffuser performance, neither of which have been clearly understood previously:

(1) It is meaningless to discuss or attempt to measure one single "best angle" which represents optimum performance for all diffusers. There are at least three factors that will inevitably frustrate any such

attempt. These are: Optimum efficiency and optimum recovery occur at considerably different angles; variations in free stream turbulence strongly affect the flow patterns; and, most important, probably, simple variation in geometry can change separation angles by a factor of at least two. It would appear unfortunate indeed that so much of the litera ture has been devoted to the question of a unique "best angle."

(2) Since turbulence level does play an important role in performanc considerable judgment must be exercised in utilizing, for design purposes diffuser data in which no measure of turbulence is recorded. This is par ticularly true in adapting laboratory test data, where turbulence is usually low, to diffusers for pumps and compressors, where the disturb-ances are usually exceptionally large.

Small Water-Table Diffuser

Reasons for building small diffuser.- There were two principal reason for constructing and testing a geometrically similar, but smaller scale, water-table diffuser.

First, it was mentioned earlier that the water table had an adjust-able weir or gate at the downstream extremity of the glass plate. In the tests with the large water-table diffuser, the diffuser outlet was within $1\frac{1}{2}$ inches of the blank wall formed by the weir; consequently, it was feared that this proximity was responsible for failure to observe the oscillating separations at large angles of divergence which were reported by other authors and, perhaps, had affected other results as well. The small water-table diffuser, on the other hand, had a space greater than the length of the diffuser between its outlet and the gate of the water table; therefore the waters outside the outlet more nearly approximated a plenum.

Second, the largest angle possible with the large water-table dif-fuser was too small to enable determination of whether or not the two-dimensional type of separation would break away into a jet type of flow at larger angles. Accordingly, the small diffuser was proportioned so that its angle 2θ could be diverged to beyond 180°.

The small diffuser also offered the possibility of checking some of the results of the large diffuser in a device of different size and pro-vided more readily a very wide range of aspect ratio.

Small-diffuser tests at small angles.- First tests of the small dif-fuser showed immediately that the end gate or weir was not the cause of the stable asymmetric separations, for the behavior of the small diffuser was qualitatively the same as that of the large one at all flow rates;

that is, the diffuser first stalled and formed transient three-dimensional separations which became stable, asymmetric, two-dimensional separations as the divergence angle 2θ was increased.

Moreover, it was found that the angle at which two-dimensional separation began agreed to within 1° with that found in the large diffuser so long as the throat Reynolds number was kept below 5,000. At higher throat Reynolds numbers, which are synonymous with higher velocities, the separation angle increased markedly, just as it did when higher turbulence was introduced at the entrance of the large diffuser. It is believed that this increase in angle was caused by a much higher relative roughness of the entrance section and consequent creation of increased turbulence in the flow. The higher relative roughness was caused by careless bending of the small-diffuser entrance section during its manufacture.

It was not possible to check the curve of first stall because the tubes used in introducing bluing were too large relative to the size of the diffuser and downstream streamlines could not be introduced without markedly disturbing the flow.

Small diffuser at very large angles.- The behavior of the small water-table diffuser at very large angles is illustrated by figure 16 for one throat width and a single flow rate.

In the flow of figure 16(a) where $2\theta = 65^\circ$ and in that of figure 16(b) with $2\theta = 80^\circ$, a two-dimensional stall existed. Again the flow was seen to travel down one wall while a large stagnant wedge lay against the other wall. The water in all of the plenum was darkened by the mixing of bluing of the streamlines. The two-dimensional-stall condition existed continuously as the angle was increased to 85° by 5° steps.

When the angle was increased to 90° the flow, as depicted in figures 16(c), 16(d), and 16(e), slowly fought its way out from its wall position until finally it reached and maintained the central jet position shown in figure 16(e). It took from 3 to 5 minutes for the energy of the incoming flow to rearrange the motions in the plenum symmetrically and arrive at this central jet position. At angles of 85° and lower, configurations similar to those of the first two pictures (figs. 16(a) and 16(b)) were allowed to run for as much as 15 minutes at a time with no indication of any tendency for a similar transition.

After the jet was fully established, the angle was decreased progressively as shown in figures 16(f), 16(g), and 16(h). Using intervals of 5°, it was possible to reduce the angle 2θ to as low as 65° (fig. 16(g)) with no apparent effect on the jet. When the angle was reduced another 5° to 60°, however, the jet immediately snapped to the wall position. Unlike

the increasing-angle transition at 90° when the change took place slowly, the movement to the wall position now was so rapid that the observer was unable, with manual operation of a still camera, to photograph intermediate positions of the jet during the transition. This snap action furnished ample evidence that the wall position was the stable and the preferred one in the lower part of the hysteresis zone.

This hysteresis phenomenon was investigated further at two other throat widths. The data obtained are presented in tables VI and in figure 17, in which the angle of change from two-dimensional separation to jet flow, and vice versa, is plotted against the ratio N/W_1, where N is the length of the diverging wall. This graph shows that the regions of jet and of two-dimensional operation are separated by a hysteresis zone.

Superimposed Plots of Large- and Small-Diffuser Results

In figure 18, data from experiments with the large water-table diffuser and those obtained with the small diffuser are presented on the same logarithmic plot of 2θ against N/W_1 and the performance zones are indicated.

The data from the small diffuser, curves c-c and d-d, are plotted from data taken at $R_W = 3{,}700$, while those from the large diffuser, curves a-a and b-b, are for $R_W = 6{,}000$. These values were used simply because more data were available at these particular Reynolds numbers. In view of the small dependence on Reynolds number as shown in figures 13 and 18, the difference in Reynolds number should cause no difficulty.

INSERTION OF VANES IN LARGE WATER-TABLE DIFFUSER

The initial idea in the tests with vanes inserted in the large water-table diffusers was to use the vanes to deflect energy of the main-stream flow into the boundary layer in order to replace the boundary-layer energy ordinarily lost to friction, thereby preventing boundary-layer stall and consequent separation.

Many water-table vane tests were run with high turbulence as well as with low turbulence in the entering flow. The photographs reproduced in this report, however, are only of tests with low turbulence, and the discussion is centered around these low-turbulence cases. However, at the higher turbulence levels, vanes were even more efficacious in eliminating bad separations because the effects of the vanes and the turbulence were additive.

Tests With Vane Having an Airfoil Profile

It was felt at first that a high-lift airfoil with a high stall angle would prove to be most efficient in accomplishing the desired flow deflection; accordingly an airfoil with an NACA 4418 wing-section profile was fabricated.

Preliminary experiments had shown that it would be necessary to place the vanes near the throat where the highest speed flow occurred; otherwise, the vane was likely to find itself in a dead-water region caused by a separation, where there was no kinetic energy to deflect. The narrowness of the throat region dictated a small airfoil thickness which, in view of the decision to use a 4418 section, required a small chord. A chord length of 1 inch was used.

It was noted that these airfoils, even when kept at angles of attack near 0°, were always in a stalled condition whenever they were placed in a region of decelerating flow. Hence the original intention of operating the airfoils at large angles of attack and high lift conditions was precluded by the presence of the decelerating diffuser flow at least for this airfoil shape.

In the paragraphs which follow, the successful application of flat-plate vanes is described. However, the lengths of the successful vanes were, except in the 15° case, at least three times the 1-inch chord length of the airfoil mentioned above. Perhaps the failure of the airfoil was just that it was too short, and this matter probably deserves further study. Flat vanes are so simple and so easy to construct, however, that the airfoil investigation has not been pursued further.

Tests With Flat-Plate Vanes

Vanes used.- The flat vanes used were made from ordinary commercial galvanized iron. Vanes 3 inches or shorter in length were 0.033 inch thick. Except in the 45° tests, where the three central 6-inch vanes were 0.033 inch thick, all vanes longer than 3 inches were 0.052 inch in thickness. The metal was rounded on the leading edge and faired slightly at the trailing edge, but little care was taken in these operations. The galvanized surface of the vanes was rough in comparison with the lacquer-smooth diverging walls of the diffuser and the plate-glass surface of the water table.

A useful feature of the water-table work was the simplicity with which the vanes could be inserted in the flow; they were merely rested upon the glass bottom and steadied from above. Their positions and attitudes could be adjusted at will by simple hand manipulation.

Short vanes at an L/W_1 ratio of 8.- Figure 9(d) shows a water-table diffuser with $L/W_1 \approx 8$ when set at 15°. As discussed earlier, wandering of the main flow can be seen from inspection of the photograph, and the figure, when closely inspected, reveals the three-dimensional separations which occur.

Figure 19(a), with J = A, and figure 19(b), with J = B, show this same 15° diffuser with two 1-inch-long vanes inserted. The downstream jets show that backflow was eliminated at all depths. Although the flow contained more small-scale turbulence, its main flow direction was much steadier so that the flow no longer wandered around in the diffuser. Longer vanes operated even better. Discussion of their action is included below in the discussion of diffusers with larger divergence angles.

Figure 20(a) shows a two-dimensional separation at a diffuser angle of 20°. This separation was larger and more stable than the separation at 17° discussed earlier in connection with figure 9(e). In figure 20(b) an attempt was made to correct the separation by inserting a pair of 2-inch vanes just downstream of the throat. These vanes pushed the point of stall about halfway down the diffuser, but the separation was not entirely eliminated. However, a pair of 3-inch vanes, as shown in figures 20(c) and 20(d), again eliminated the separation at all depths.

At the 30° angle (fig. 21(a)) the separation continued and became more stable. The wedge of stagnant water became larger while the main flow remained at almost a constant width through the length of the diffuser, showing that little or no deceleration or diffusion was taking place. Trials with only a pair of vanes were unsuccessful at this angle; but with three 3-inch vanes (figs. 21(b) and 21(c)) stalls could be eliminated everywhere, although the flow at the outlet near the glass bottom was sluggish. This sluggishness at the center of the outlet could be relieved at the expense of the wall flow by manipulating the vanes at the throat. Thus, the possibility of controlling the shape of the outlet velocity profile was indicated. This ability was demonstrated repeatedly throughout the tests. Longer vanes were found to allow considerable flexibility in the control of outlet velocity profile. As the length of the vanes was decreased, a point was reached where the adjustment of the vanes was extremely critical if stall was to be eliminated throughout the diffuser, there being, sometimes, only one setting at which the vane arrangement would work. Still shorter vanes would then prove incapable of eliminating separation.

The location and attitude of the trio of 3-inch vanes in the 30° diffuser (figs. 21(b) and 21(c)) was critically important to the elimination of separation. The best solution found was to set the vanes so they were equally spaced and oriented to form four small diffusers with divergence angles of $7.5° \pm 0.5°$ within the large 30° diffuser. The

smaller angles within the indicated tolerance, if there were such, always were found between the diverging walls and their adjacent vanes, the central channels being slightly larger. It would seem to be more promising in view of the original purpose of inserting vanes, the injection of momentum into the boundary layer, to have a much smaller angle adjacent to the wall. However, in the prevention of stall and in the production of a square outlet profile, marked unevenness of spacing was decidedly inferior to the nearly equally spaced arrangements described above.

As for exact longitudinal placement relative to the throat, it was found best to have the leading edge from about 1/4 to 1/2 inch downstream from the narrowest throat section, thereby allowing the main stream to diverge slightly before striking the vanes. This dimension was least critical at smallest angles.

At $2\theta = 45^\circ$ (fig. 22(a)) the wedge of stalled water was still larger, and the flow continued to travel down one wall with a nearly constant width. To correct this separation, it was necessary to use five 6-inch vanes which divided the area downstream of the throat into six short 7.5° diffusers (figs. 22(b) and 22(c)). These vanes succeeded in forcing the stalls out of the diffuser, although, owing to the large area ratio involved, flow was sluggish all across the exit. Again the location and orientation of the vanes was extremely critical, indicating that the upper angular limit for application of 6-inch vanes had nearly been reached. Five of the shorter 3-inch vanes, not shown in the figures, were not capable of removing the two-dimensional separation.

Throughout the tests, any increase in turbulence intensity was found to improve the performance of vanes in eliminating separation and to allow greater flexibility in vane orientation and placement. This result was to be expected in view of the previously demonstrated fact that turbulence acts to inhibit two-dimensional separation.

Rationalization of findings on optimum vane placement.- The need for locating vanes immediately downstream of the throat is easily explained. In the first place, this region contains the largest positive pressure gradients found in the diffuser, both because of the wall-curvature effects discussed earlier and because the percentage increase in area in the direction of flow is greatest at some point between the throat and the junction of cylinder and plane wall. Second, at the throat the dynamic pressure and the density of flux of kinetic energy are at their maximum. Thus, with a potentiality for greater loss at the throat than at any other location, the need for good throat flow configuration is of first importance. If corrective action were delayed until some point farther downstream, the damage might already be done. In addition, the very existence of a high availability of energy at the throat enhances the possibility for influencing the behavior of the diffuser; vanes placed farther downstream

simply do not have at their disposal the flow energy required to produce noticeable effects.

The slightly better operation obtained when the leading edges of vanes remained 1/4 to 1/2 inch downstream from the throat also is easy to rationalize. The pressure gradient at the throat is zero since the throat is the point of transition from a negative pressure gradient to a positive one; therefore, it is not necessary to prevent separations from initiating at the throat, though they may start farther downstream and move forward to the throat position. In other words, the slight divergence of the diffuser walls before the flow reaches the leading edges of the vanes is not sufficient to cause separation to occur.

The results concerning the optimum number of vanes and their lengths are more difficult to explain. The water-table flow configurations discussed in the previous section indicated that, for best results, vanes should be approximately evenly spaced within the diffuser and should be numerous enough to form small diffusers in the throat which have angles of divergence $2\theta_V$ approximating those found by other experimenters to give maximum pressure effectiveness in two-dimensional plane-wall diffusers. In addition the length of vane employed L_V had considerable effect on the success of the configuration. Attempts to explain these facts from fundamental principles have not met with success. However, a tenable argument can be presented starting with known facts regarding performance of vaneless diffusers at small angles, and this argument is presented below.

Reid (ref. 7, p. 65) found experimentally that for his test conditions a short, plane-wall diffuser operates at nearly maximum pressure effectiveness at a divergence angle of 7.5°. Gibson's (refs. 2 and 3) results indicated an angle of about 9° for maximum pressure effectiveness. By making use of the results of appendix B, it may be deduced that these pressure effectivenesses are also energy efficiencies, for Reid, and presumably Gibson, had uniform entering velocity profiles. In tests of the air diffuser of the present investigation, as will be seen later, the angle of maximum energy efficiency varied directly with Reynolds number and turbulence intensity from a value of about 9° to about 11°. Reid's value may be lower because of a probably lower turbulence resulting from the use of a damping screen and the existence of a more nearly quiescent reservoir.

Therefore, equal spacing of the vanes at positions near the throat was equivalent to using little diffusers of nearly maximum efficiency in a region where, without vanes, there would have been very poor recovery and efficiency as a result of the bad separation which would have existed on one wall of the large diffuser.

Another criterion results if the point of vane operation, as defined by $2\theta_V$, the angle between the vanes, L_V/W_V, the ratio of vane length to vane spacing at the leading edges, and W_V, the Reynolds number based on vane spacing, is located on the separation graphs, figures 13 or 15. When this was done, it was found that no vane arrangement which resulted in operation above its first stall line a-a was successful since that arrangement itself created separations within the diffuser.

The fact that the successful vane combinations formed little diffusers which should have optimum efficiencies indicates also that the velocity profile at the trailing edges of the vanes must have been nearly uniform. (See appendix A.) This square profile, together with the lateral energy transfer due to the turbulence from the vanes, is believed to be the cause of the improved flow through the remainder of the diffuser. This improved downstream flow, moreover, is essential because, even though the efficiency of flow through the vane section is high, the absolute value of the recovery is still small there owing to the small increase of flow area involved. Therefore, good performance in the remaining length of the large diffuser is essential if overall recovery and efficiency are to be acceptable. Approximation of the L_V/W_V ratios of the vane combinations employed are presented in table VII, and these ratios can be used in conjunction with reference 7, p. 66, to estimate C_{ER} in the vane section of the diffuser and in conjunction with figures 13 and 15 to select vane configurations which will prevent diffuser stall.

This whole line of reasoning concerning the insertion of little diffusers of optimum efficiency is reinforced by the fact that a further increase in the number of vanes, thereby forming inserted diffusers having angles of divergence much smaller than the angle for optimum efficiency, never improved the flow picture. On the contrary, the flow was, in some cases, adversely affected to a marked degree.

At the time of the first successes in eliminating stalls, it was suspected that the drag of the vanes might be the stabilizing influence that slowed the fast-moving mainstream and caused it to spread away from the wall of its choice. However, figure 23, with the diffuser set at 20°, shows that this argument is at variance with the facts. In figure 23(a), where a separation existed on the upper wall of the photograph, one 3-inch vane was placed by the lower wall, yet the flow continued down the same wall with no effect on the separation. When the vane was moved to a position adjacent to the upper wall (fig. 23(b)), the main flow was pulled across the diffuser, and the separation was transferred to the lower wall. It is believed that these photographs demonstrate that the beneficial action of the vanes is not dependent on drag.

This argument does not imply that the vanes themselves do not produce losses. Obviously, motion of a fluid along a flat plate involves friction in the boundary layer, and friction causes losses by transforming the kinetic energy of a steady flow into internal energy. The only implication is that the action of vanes in improving stability and producing a more uniform velocity profile at the diffuser outlet far outweighs the deleterious effects of the added friction.

Long vanes at an L/W_1 ratio of 8.- In the preceding section it was pointed out that vanes somewhat longer than the minimum successful length achieved better results and, in addition, allowed greater flexibility in adjustment. There is, however, a limit to the improvement in performance which can be attained by lengthening the vanes.

Figure 24 shows a 20° diffuser with nearly full length vanes (23 inches long) inserted. The L/W_1 ratio of the vaneless 20° diffuser (fig. 20(a)) was 8.26. In figures 24(a) and 24(b) only one vane was inserted, and in this case the vane divided the 20° diffuser into two 10° diffusers each having an L_V/W_V ratio of approximately 15.35. In figures 24(c) and 24(d), two of the long vanes were placed in the 20° diffuser, thereby forming three 6.7° diffusers having L_V/W_V ratios of about 23. These small-angle diffusers formed by the full-length vanes all have the same area ratio as the original vaneless diffuser.

As expected, the vane insertion provides an improvement in performance over that of the vaneless 20° diffuser. One's first inclination might even be to expect the two parallel 10° channels to show a flow pattern as good as that of the single 10° diffuser of figure 9(a). However, it must be noted that the L_V/W_V ratio of the parallel diffusers formed by the vane (15.35) is about twice the L/W_1 ratio in the configuration of figure 9(a) (8.20). Reference to figure 13 (and using the dashed lines of constant-length Reynolds number R_L shown thereon) shows immediately that the parallel 10° diffusers of figures 24(a) and 24(b) were operated in the three-dimensional separation zone; hence the flow should be represented more closely by the pictures of figure 12. It is not surprising, therefore, to find that at least one of the parallel diffusers, the upper channel in figures 24(a) and 24(b), was badly separated. The flow in the lower channel was much better although it did contain intermittent separations. The flow in the upper channel was an unstable fluctuating one typical of the three-dimensional separation zone defined in figure 13.

It also may be surprising at first to find that the lower channel flow showed less separation than the upper one since the above argument alone would predict separation for it also. However, close inspection

of the throat area reveals that the flow did not divide itself evenly between the two channels,[2] the lower channel getting more than its share. Thus, the throat Reynolds number of the lower channel was higher than that of the upper, but, more importantly, its turbulence seemed to be higher also. This condition would lift the curve b-b of figures 13 and 15, thereby placing the point of operation relatively lower in the three-dimensional zone.

This uneven flow may contribute to a lowering of efficiency through larger absolute losses in energy. More than half the flow, that in the lower channel, would enter with a higher kinetic energy since, by continuity, its velocity at the entrance would be higher, and even the same percentage recovery rate would mean a higher absolute loss.

In the case of the flow of figures 24(c) and 24(d), the coordinates $2\theta_V = 6.7^\circ$ and $L_V/W_V = 23$ put the point of operation below the dashed line of first separation, curve a-a in figure 13. Therefore, it is not surprising to find there were no stalls or backflow anywhere in the three parallel diffusers, although the flow in the corners of the diffusers in figure 24(d) was decidedly sluggish. Note that the parallel diffusers operate at the same length Reynolds number as the vaneless diffuser, but at only one-third the throat Reynolds number. This fact accounts for the necessity of using the dashed, rather than the solid, a-a curve.

The above demonstration that vanes should not be used in lengths which result in operation above the first-stall line suggests that vanes should be just long enough to insure flexible control of the exit velocity profile. While it is true that the performance of a badly separated, vaneless diffuser can often be improved by inserting vanes which operate above line 2-2 in figure 13, the use of these vanes still represents a loss compared with the potentialities of a diffuser with shorter vanes which operate below the first-stall line. The longer vanes not only add friction as a result of their increased surface area but also contribute separations of their own.

These results reemphasize the fact that small angles of divergence alone are no panacea of diffuser ills; long vanes with small angles often produce much worse results than shorter vanes with greater angles. Divergence angle is only meaningful when taken together with L/W_1 ratio, turbulence intensity, and Reynolds number.

---

[2]In figures 24(a) and 24(b), the channels do not appear to be equal in width. This is due to an unfortunate angle of the camera with respect to the support rods which hold the vanes. In reality the channels are equal and the entire flow passage is symmetric to within the measuring accuracy. The same is true in figures 24(c) and 24(d).

Vanes at different L/W_1 ratios.- Experiments were also conducted with vanes in diffusers of other L/W_1 ratios; the results were more or less as expected in view of the conclusions drawn from tests at L/W_1 ratios of about 8. Figure 25 shows the effect of inserting vanes in a 40° diffuser with L/W_1 of about 4. The L_V/W_V ratio here also was 4, and even though the angle between the vanes was as much as 10°, the vane configurations operated well below the first-stall line. Elimination of separation was easily accomplished.

In figure 26 the L/W_1 ratio of the diffuser was 16.44. Three-inch vanes were not effective at this L/W_1 ratio, but 6-inch vanes accomplished the results shown in the figures. The adjustment of these 6-inch vanes, however, was very critical. The L_V/W_V ratio of the 7.5°-throat diffusers formed by the vanes was about 16; thus, the point of operation was below the first-stall line. However, the jet in the corner formed by the upper wall in figure 26(c) was quite sluggish, indicating the approach of first stall. It would have been desirable to have a less critical adjustment usually attained by using a longer vane; however, a substantial lengthening of the vanes would have resulted in pushing the point of operation into the three-dimensional stall zone. Therefore, figure 26 apparently represents very nearly a limiting L/W_1 condition beyond which, with 30° diffusers of the present form, vanes could not be usefully applied.

Figure 27 shows an attempt to extend the use of vanes to $L/W_1 = 24.66$ in a 30° diffuser. In this case the angle between the vanes averaged 7.5°, but the L_V/W_V ratio was about 24 also. Thus, the small-throat diffusers with widest angles probably operated very close to the line of first stall for a Reynolds number of about 1,500 based on the spacing of the leading edges of the vanes W_V. It is not surprising, therefore, that stalls and backflow were encountered in the flow farther along the walls of the large diffuser in both figures 27(b) and 27(c).

General Conclusions From Tests With Vanes Inserted

The results given above indicate clearly that, within limits, wide-angle diffusers of good performance can be constructed using properly designed, short-, flat-vane systems. This fact is borne out by the preliminary air tests cited later in the report. It is hoped that additional quantitative performance data of vaned diffusers will be obtained in the work now being carried out in the air unit to verify the following conclusions.

Tentative design criteria for these vane systems can be stated as follows:

(1) The vanes must be located with leading edges slightly downstream of the diffuser throat.

(2) The number of vanes used should be such that the small passages formed between pairs of vanes and the vanes and walls are little diffusers of maximum efficiency.

(3) The little diffusers formed by the vanes must all operate without stall. It appears that this can be accomplished by designing so that each passage lies well below its line of first stall a-a on figures 13 and 15. The line a-a, of course, should be that for a Reynolds number based on W_V, the vane spacing at their leading edges, rather than on W_1, the throat width. This criterion, then, indicates that vanes should be made as short as possible.

(4) On the other hand, there is also a limit below which vane length cannot be reduced. A definite quantitative criterion for use in determining this limit has not been established. Therefore, a minimum vane length which will insure a degree of exit-velocity-profile control must at present be determined experimentally.

(5) Vanes work best in relatively short diffusers. For given conditions of turbulence, divergence angle, and Reynolds number, there is a maximum L/W_1 ratio beyond which this type of vane system is less effective.

(6) An upper limit to the divergence angle 2θ at which vanes are still effective has not been met. Good results have been obtained in the water-table diffuser at 2θ's as large as 45° when L/W_1 was approximately 8, but the improvement required the insertion of five vanes with L/L_V of approximately 4.

INSERTION OF RODS IN LARGE WATER-TABLE DIFFUSER

First Experiences With Rod Insertions

The fact that large separations could be delayed by inserting rods in the flow ahead of the throat was noted very early in the experimental program. The first rods employed had diameters of 3/4 and $1\frac{1}{8}$ inches, respectively. When inserted in the diffuser, these rods delayed separation more effectively than did the airfoil-profile vanes discussed earlier;

consequently, considerable attention was paid them, and it was planned to expand the rod tests in the present investigation.

Sizes and Placement of Rods Used in Present Work

Rod diameters.- The size of the 3/4- and $1\frac{1}{8}$-inch-diameter rods used at first was so great that the geometry of the entrance section was altered to a marked degree, and it was believed that comparison of results obtained from the different flow through this changed geometry with earlier results might be open to criticism. Smaller rods, of course, will introduce vortices just as well; consequently, it was decided to start work with rods having a diameter of 1/8 inch and to increase this size progressively by doubling the diameter after each series of tests. Thus, tests were run also with rod diameters of 1/4 and 1/2 inch. In this manner it was hoped that a performance trend dependent upon vortex size and, consequently, turbulence scale could be established. After testing these three sizes of rods it was found that a 1/4-inch diameter was slightly better than the others and that 1/2-inch rods produced an effect not much different from that obtained with still larger rods in earlier tests. Because results with the smaller rods largely duplicated previous findings and because the tests with the larger rods were performed less carefully, only results for tests with rod diameters varying from 1/8 to 1/2 inch are presented herein.

Placement.- Tests were run with rods placed both upstream and downstream from the throat. When in their upstream location, the rods always were placed, in plan view, along the approximately 6-inch-long arc of the circle of 4-inch radius having its center on the center line of the diffuser at the throat. This arc, as determined by flux plotting, was very nearly a line of constant velocity potential. The center-line distance between two adjacent rods was never less than twice the rod diameter; thus, the free-flow area at the potential line where rods were placed was never reduced below one-half the free-flow area at the same location with no rods inserted.

In order to check the effect of a 90° shift in the axis of the vortices generated, rods in one-half of the tests were laid horizontally in the flow and in the other half of the tests were suspended vertically. When the rods were placed horizontally in the entrance section, they were bent to agree with the curvature of the aforementioned velocity-potential line and were supported by thin, perforated, sheet-metal strips oriented parallel to the flow. This orientation of the strips resulted, as shown by the bluing jets, in but little disturbance in the incoming stream. When rods were placed vertically in the entrance section, straight rods were used, and these were simply rested on the glass bottom

of the water table and held in position by a brass plate above the surface of the water. This plate had holes drilled at locations where it was desired to fix the location of the rods.

When placed downstream of the throat, vertically alined rods could be supported wherever desired by simply moving the aforementioned brass plates longitudinally along the water table. The greater cross-sectional areas encountered downstream were spanned simply by drilling more holes in the brass plate and using a greater number of rods. Downstream horizontal rods could be placed at only one location for each setting of divergence angle, since the rods used were the same as those inserted upstream, and their fixed lengths would reach entirely across the diverging diffuser at only one longitudinal position.

Results and Discussion of Tests With Rod Insertion

Upstream rods.- Figure 28 shows a few of the flow patterns obtained with rods inserted upstream of the throat. Figure 28(a) shows the 17° diffuser with vertical 1/8 inch rods, and figure 28(b), the flow when these rods were horizontal. The improvement can be appreciated readily if comparison with figure 9(e) is made. Bluing from all downstream jets flowed toward the outlet after the rods were introduced, the large area of stagnant water and the regions of backflow having been eliminated completely. The diffuser angles illustrated were not the largest ones possible with good performance. Those figures presented were selected simply because the contrast obtained in the photographs was more suitable for reproduction than at other angles. In rod work, good photographic contrast is difficult to obtain because the vortices shed by the rods cause strong mixing with the result that the streamlines disappear as the bluing is dispersed through the fluid as a whole.

Figure 28(c) shows the effect of nine, vertical, 1/4-inch rods in a 23° diffuser. At this angle the jet on the upper wall in the picture began to stall intermittently, but the flow, in the main, was well-ordered and proceeded in the proper direction. At higher angles the pattern deteriorated rapidly. Figure 28(d) shows horizontal 1/4-inch rods also just above their maximum angle of good operation. In this case, the flow is still generally well ordered; but the lower wall jet in the picture shows intermittent backflow, and the flow is just beginning to become asymmetric. Figure 20(a) at $2\theta = 20^\circ$ gives an idea of the separated two-dimensional flow which would exist at angles of this order of magnitude without rods or vanes. Figures 20(c) and 20(d) suggest that vanes accomplish the same result, but with less turbulence and disorganization of the flow.

Figures 28(e) and 28(f) show flows at two angles with 1/2-inch rods inserted. Figure 28(e), with a 19° diffuser angle, shows a flow which was on the verge of becoming separated asymmetrically in spite of the inserted vertical rods. Figure 28(f) illustrates very good operation with only two horizontal, 1/2-inch rods at 17°. This angle, however, is just barely into the two-dimensional separation zone, so correction of the poor flow pattern in this case was, not unexpectedly, quite easy.

Table VIII presents the angle for each type of rod arrangement at which asymmetric flow was resumed in spite of rod insertions. The selection of this angle was a good deal more subjective than similar determinations in the cases of flow with and without vanes, and the uncertainty in angle is about ±2°.

As seen in the table, the best arrangement tested was that with nine 1/4-inch rods oriented vertically. With these rods, the angle for two-dimensional flow was extended from about 17° (fig. 9(e)) to about 23° (fig. 28(c)). This angle is denoted by a point Z at $L/W_1 = 8.26$ in figure 15. The point lies 2° below the angle determined earlier for two-dimensional separation with high turbulence (line b-b in fig. 15). The other configurations tested raised the two-dimensional separation line to only 19° or 20°.

Rod insertions also were found to reduce the angle of first separation in the corner to as low as 11°. Thus, this trend also matched in direction the effect of increased turbulence as presented in lines a-a of figure 15. One must remember, however, that the turbulence trend indicated by lines a-a, as discussed earlier, is still in some doubt.

Table VIII includes columns indicating the reduction of flow area and presenting the average flow velocity between the rods as well as a column of Reynolds numbers based on the rod diameter.

The columns on flow-area ratio and velocity are indicative of the cost of creating the vortices. For example, reduction of the flow-area ratio to 0.5 would make the area for flow through the rods equal to the diffuser throat area since the cross-sectional area along the line of rod insertion was just twice the area of the throat. Therefore, the velocity between the rods would equal the average velocity at the throat. With such relatively large accelerations and decelerations, losses of at least the order of magnitude of one velocity head might be expected. Consideration of the possible magnitude of this loss indicates the desirability of keeping the velocity at the rods as low as possible; yet this very act may drastically reduce the effectiveness of the rods in eliminating two-dimensional separation. Furthermore, it seems unlikely that much will be gained from introduction of intense turbulence specifically to combat separation when the diffuser is to be charged with the cost of generating the turbulence. On the other hand, if the entrance geometry

is such that stable Kármán vortices can be generated farther from the throat where velocities and generation losses are smaller, a beneficial effect might still be realized. Final settlement of this point, of course, must await the air-diffuser tests in which it is expected that quantitative performance data will be obtained. Meanwhile, the designer has available the knowledge that a high turbulence already existing in the flow will act to improve performance by delaying two-dimensional separation, though this same turbulence may cause small stalls to exist momentarily at isolated points which shift around the diffuser walls in a random manner.

The column in table VIII of rod-diameter Reynolds numbers is significant in that it indicates the type of turbulence shed by the rod. According to Roshko (ref. 24, p. 36) between $R_d = 40$ and $R_d = 150$, classical stable Kármán streets are formed, whereas between $R_d = 300$ and $R_d = 10{,}000$, the periodic shedding is accompanied by irregular, or turbulent, velocity fluctuations, and the vortices break down very rapidly into a fully turbulent wake. Between these two ranges is a transition zone in which either behavior may occur. In the present application, multiple rods were used; so the limits of the ranges probably were not strictly applicable. Nevertheless, the behavior observed appeared to fit Roshko's classification quite well. The flow of figure 28(a), for example, which had a Reynolds number in the transition zone, showed slowly decaying vortices in the throat. In the flow of figures 28(c) to 28(f), the degeneration was much more rapid because the rods were operated at higher Reynolds numbers.

Since the increase in gains from using vertical rods over those with horizontal rods was disappointingly small, it appears that no "directional effect of vortices" was present. That is, vortices with their axes vertically alined produced little or no better effect in the elimination of separation than did vortices with horizontal axes. This apparent lack of effect may be because the vortices break down immediately into random turbulence. However, there is also the possibility that Kármán streets originating at different points along the same rod are out of phase and therefore add a third dimension to the picture. In other words, it appears unlikely that large u' and v' components of turbulence ever will be present in the free stream without the presence also of an appreciable w' component. This conclusion is, of course, supported by considerations of continuity common to basic turbulence theory. This argument, then, might explain why vortices with horizontal axes can transport energy and momentum toward the diverging walls of the water-table diffuser and retard two-dimensional separation.

The logical conclusion is that any kind of turbulence will act to retard two-dimensional separation in diffusers regardless of whether the turbulence is already in the free stream entering the diffuser, is

caused by artificially roughened walls ahead of the throat, or is the result of decaying vortices generated in any of the many possible ways. It should be noted that the mechanism involved is entirely different from that discussed in connection with the insertion of vanes. This is illustrated clearly by the fact that properly functioning vanes in almost all instances reduced the amount of fluctuations in the flow, usually by a large amount.

These results also lead to speculation concerning a more specialized use of rods to eliminate separations both in vaned and in vaneless diffusers. Recently declassified material shows clearly that airfoil tip vortices can be successfully used for this purpose. It is believed that the mechanism involved in use of such vortices is again mixing. If this is true, then it is natural to ask the question, "would small rods set across the corners at an angle perform the same function as the wing tips, and would these simpler devices perform as efficiently?" To date time has not been available for investigation of this question. However, it is believed that such an investigation would be worthwhile.

Basically, it is felt that, regardless of its origin, any lateral mixing effect introduced near the edge of the boundary layer in the region of a steady stall will be effective in preventing or reducing the stall. Then, if the energy lost in producing the mixing is not too great, an overall improvement in performance will result.

In the present tests, such mixing did not ever appear to eliminate the stall in the sense that the flow was changed into the completely unstalled region. On the contrary, it appeared to eliminate a steady two-dimensional stall in favor of a transitory three-dimensional stall. Whether this would also be true in cases of a small local steady stall, such as in a corner, the present data do not indicate.

The fact that large-scale fluctuations and increased free-stream turbulence sometimes decrease the angle of first stall would tend, at first glance, to be contradictory. However, it is believed that stalls thus created have a shorter lifetime than stalls occurring in a turbulence-free flow. That is to say, the first stalls which appeared in the high-turbulence flows were merely momentary reversals caused by the passage of a large-scale fluctuation. The time average of the effects of such momentary fluctuations is small as is evidenced by the less rapid buildup of a definite backflow which, in turn, is clearly demonstrated by the increase in the angles of steady, two-dimensional separation.

Downstream rods.- Figure 29 shows horizontal 1/8-inch rods inserted downstream of the throat. Rods with two larger diameters were tried also. Both vertical and horizontal alinements were tested. No significant differences in performance were noted as size and orientation were changed; so, for brevity, only 1/8-inch horizontal rods will be discussed.

Figure 29(a) shows the rods placed in a diffuser set at a 20° divergence angle. As may be seen, all backflow in the downstream sections of the diffuser was eliminated. Ahead of the rod section, however, the flow was separated from both diverging walls. There was violent backflow in the separated regions. In figure 29(b), which shows the flow where the diffuser angle has been increased to 30°, the resulting pattern was very similar to the one at 20°. However, flow in the downstream reaches of the diffuser was more sluggish, and the separation ahead of the screen showed more intense, though more concentrated, backflow.

When vertical rods were used and the longitudinal position of rod insertion was varied, it still was easy to prevent separation downstream of the rods, but separation always remained upstream of the rods. As the rod station was moved farther downstream, however, separation would, somewhere along the line, move over to a stable position along one wall.

The work with downstream insertion of rods agreed qualitatively with that of Schubauer and Spangenberg (ref. 22) who inserted screens downstream of diffuser throats. It is worth noting that the present tests tend to shed further light on the question of whether the filling action of screens in diffusers is due to the action of screen resistance in changing the pressure field or to the mixing caused by increased turbulence. The present experience all tends to support the idea of increased lateral transport of momentum by the screen-induced turbulence as the effective mechanism rather than the action of a "filling effect" of the rearranged pressure field.

Comparison of rods with vanes.- Early work with rods showed up well in comparison with the poor results obtained with the short-chord, airfoil-profile vanes discussed earlier. However, newer attainments with flat-plate vanes far surpassed the result for rods in preventing separation and in presenting possibilities for improved energy and pressure performance. In addition, the benefits obtainable from introduction of vortices were found to be no greater than those resulting from the presence of turbulence of different origin. In consequence of these findings, the emphasis was shifted from rod work and concentrated on the effects of vanes.

AIR-DIFFUSER TESTS

As previously stated, the water-table tests just described were used for the following two purposes: (1) To study the flow regimes and governing parameters and (2) to provide a guide for more time-consuming quantitative studies in the air apparatus. Insofar as the first purpose is concerned, the water-table work is in itself highly instructive, but

in regard to the second purpose a definite question arises concerning the conditions of similarity inasmuch as the Reynolds numbers in the water table are lower by one order of magnitude. Furthermore, if the air-apparatus results check the water-table studies in regard to flow regime and parameters, the range of known applicability of the data will be thereby greatly extended.

For these reasons, the following air-apparatus data and test observations are presented. Only a few runs with and without vanes and rods are given. As will be shown, these are sufficient to verify essentially the water-table results. However, it should be strongly emphasized that the quantitative results presented are preliminary. The further studies now in progress will not only embody far more complete data but will also employ, in several respects, more accurate methods of measurement. Consequently, the numerical results presented for the unmodified air diffuser and for the cases with insertion of rods or vanes should definitely be viewed as showing the approximate possibility of the various configurations rather than as definitive data.

APPARATUS

A complete description of the air-apparatus unit is given in appendix H, reference 1. The wall profile is the same as that of the large water-table unit and is shown in figure 1. Other details are shown in figures 30(a) to 30(f). The throat width and exit width as well as the flow rate are all separately variable. Certain other important details are also described below.

OBSERVATIONAL TECHNIQUES AND COMPUTATION OF PARAMETERS

Location of Separations

Visualization of flow using smoke.- The two-dimensional air diffuser was constructed with parallel walls of transparent Plexiglas so that smoke streamlines could be observed within the diffuser. The velocities normally used at the diffuser throat, however, were so high that smoke introduced ahead of the entrance section could not be generated, economically, in quantities large enough to produce streamlines thick enough to be seen and photographed. In later tests, however, it may be possible to achieve better results in the case of stable, asymmetrically separated flow by introducing the smoke through holes in the separated diverging wall, thereby coloring the stagnant wedge only and producing an effect which could be photographed.

Smoke streamers did prove valuable in studying the slower flows ahead of the entrance section, however. Here, the smoke was introduced through holes in a hollow handrailing around the diffuser, and the condition of the flow approaching the entrance was observed. The flow appeared to contain some small-scale turbulence, but no large vortices from projections on other equipment in the laboratory could be discerned. The entrance to the diffuser appeared to be the center of a large, low-velocity vortex which derived its impetus from slow, large-scale circulation around the laboratory. This circulation was supported by the momentum of the air ejected by the blower. In later tests the vortex motion will be reduced by use of an exit duct on the blower.

Visualization of flow using tufts.- A more convenient means of locating separations was found to be the use of tufts. The tufts were made of inch-long pieces of black yarn which were attached to the wall with Scotch tape. Seventy-eight tufts, in all, were distributed evenly over both the diverging and parallel walls of the diffuser. Other tufts were placed at strategic points on the walls of the Plexiglas, two-dimensional plenum. All tufts were located so that their wakes did not cross static-pressure holes.

Three regimes of tuft behavior were noted. First, tufts were seen to lie quietly on the surface of a plate, pointed in the direction of the flow. This behavior indicated a steady flow in a boundary layer either in the laminar sublayer or in a zone where turbulence was too weak to excite tuft vibration. Second, tufts were observed vibrating more or less violently, but still pointing in the downstream direction and still lying against the plate or not far from the plate. This condition indicated strong turbulence in the boundary layer, but no separation or backflow. Third, the tufts rose up from their normal position flat against the plate, reversed their original alinement, and pointed back toward the throat of the diffuser. While in this position the tufts vibrated violently. This tuft condition indicated that separation had occurred and that backflow existed along the wall. Transient stalls are indicated by quick, temporary shifts to the third behavior from one of the first two. Since such behavior did occur, another verification of the transient-stall mechanism is provided.

Determination of Recovery and Efficiency

Location of static-pressure orifices.- Figure 31 shows the locations of the orifices at which static pressure was measured. At the throat, two orifices, numbers 1 and 5, were located on the south and north parallel walls, respectively. Three orifices, numbers 2, 3, and 4, were located on the east and three, numbers 6, 7, and 8, on the west, curved wall of the entrance section. Certain minor errors arise because of the location of taps, the streamline curvature, and the method of computations employed

in these preliminary tests. As shown by the estimate of uncertainties in appendix C and table IX and as discussed in reference 1, these errors are of the order of a few percent and tend to lower the recovery and efficiency. Hence, although the data are not final, the overall conclusions are not seriously affected by these errors.

Measuring and recording static pressure.- Each of the 12 orifices was connected, using a combination of 1/8-inch synthetic rubber tubing and Jessall 1/8-inch plastic Strip-A-Tube tape, to one leg of a vertical, 13-bank, water manometer available in the laboratory. All 12 static pressures were referenced against total atmospheric pressure by leaving the cistern and the thirteenth leg of the manometer open to the atmosphere. The manometer scale was graduated in tenths of an inch, but data were estimated to hundredths of an inch of water.

Photographic recording of data was employed in order to "stop" manometer fluctuations during unsteady flow conditions and insure simultaneity of readings as well as to provide a permanent record of events. Since all manometers were connected to a common cistern, used the same type and length of hookup tubing, and had equal tube diameters, the damping and frequency response of each manometer should be the same. The comparative readings of the various manometers are therefore meaningful even in the very unsteady flow cases. Since the frequencies of the disturbances in the unsteady flow seem to vary over a very wide range, it is not an easy matter to predict the response of the manometer system. In general, it can be remarked that the frequencies are not all high enough to insure a true mean on the manometers, and, consequently, the data in the region of very high fluctuations are less accurate insofar as absolute values are concerned.

Static pressure during different flow regimes.- In the transient three-dimensional stall regime, very large fluctuations of the individual manometers occurred, and momentary differences between comparable manometer readings often varied greatly. This is still further evidence of the transitory nature of the flow in this regime.

In the unstalled regime and the steady two-dimensional stall regime the manometers fluctuated far less. Surprisingly, the static pressures were always much steadier in the case of two-dimensional separation than in the unstalled regime. It is primarily this result which led to the speculation above concerning the existence of very small high-frequency stalls in the region of very low angles.

Computation of recovery and efficiency.- Because of the nonuniformity of the throat static-pressure and velocity profiles discussed above and described in detail in reference 1, it was not possible simply to calculate a pressure recovery and a pressure effectiveness. Instead, the more general concepts of energy recovery and energy efficiency were introduced,

and these values were computed using the following equations:

$$C_{ER} = 1 - 1.2345 \frac{\left(p_o - p_2\right)}{\left(p_o - p_{w_1}\right)} \tag{1}$$

$$\eta_E = C_{ER} / C_{ER_{ideal}} \tag{2}$$

$$C_{ER_{ideal}} = 1 - 0.993\left(1/R^2\right) \tag{3}$$

Equations (1) and (3) apply only to the present diffuser when set at a throat width $W_1 = 3$ inches. The value $W_1 = 3$ inches was used in all these preliminary air-unit tests.

Appendix A discusses in detail the derivation of these equations and the introduction of assumptions, the most critical of which are: (1) A uniform static-pressure profile at the outlet, and (2) throat static-pressure and velocity profiles identical with those obtained in potential flow between cylinders. It is sufficient here merely to point out that equations (1) and (3) are approximate formulas which are employed simply to facilitate the preliminary estimation of the energy performance parameters. The first more accurate data with the diffuser set at $L/W_1 = 8$ and $2\theta = 7^\circ$ show that the approximate determinations are entirely adequate in the sense just discussed.

In equation (1) the quantity $\left(p_o - p_2\right)$ was obtained by averaging readings of the manometers connected to the four static-pressure orifices at the diffuser outlet. Except in cases where stable two-dimensional separation existed, the quantity $\left(p_o - p_{w_1}\right)$ was the average for the manometers connected to the six curved-wall static-pressure orifices at the throat.

For these preliminary estimates two-dimensional separations were treated by assuming that the profiles between the curved flow on the unseparated wall and the center line had the same form as those profiles previously computed using potential flow between cylinders. The quantity $\left(p_o - p_{w_1}\right)$ was then obtained by averaging the readings of the three manometers connected to the three static-pressure orifices in the wall with

unseparated flow. This procedure, admittedly, was much rougher than the procedures assumed when all throat pressures had values of comparable magnitude. However, the recovery and efficiency in the cases of two-dimensional separation were so very low that large errors in their computation were unimportant when the data were to be used merely for comparison with nonseparated cases having much higher recoveries and efficiencies.

AIR DIFFUSER WITHOUT VANES

General Description

Experimental procedure.- The procedure followed in the experiments with the air diffuser without vanes follows. The diffuser was fixed at a throat width $W_1 = 3$ inches, thereby setting L/W_1 at approximately 8. Then, for each angle investigated, the behavior of the tufts was observed through the transparent parallel walls, and the location of any turbulence or separation indicated was noted and recorded. The height of the water columns of the manometer was then photographed several times, with an attempt being made each time to snap the picture when unsteadiness was at a minimum. The whole of this procedure was repeated at four or five different flow rates for each setting of the diffuser divergence angle. Variation of the flow rate was obtained by changing the speed of the centrifugal blower used to evacuate the plenum, thereby changing the pressure p_2 at the diffuser outlet. Finally, the barometric pressure was read, and the wet- and dry-bulb temperatures were determined by holding a sling psychrometer in the airstream ahead of the entrance section.

Data were taken in the above manner for angle-of-divergence settings of $2\theta = 7^\circ$, 10°, 12°, 15°, 20°, 22.5°, 30°, and 45°.

Variation of turbulence.- In these preliminary air-diffuser tests no screen or other turbulence-damping device was employed. Consequently, the increase in flow rate probably entailed an increase in turbulence intensity as well as an increase in Reynolds number. Therefore, when a change in the Reynolds number is mentioned, the reader should recall that the turbulence intensity may also have varied.

Boundary-layer trip.- Unlike the large water-table diffuser, the air diffuser was operated without a boundary-layer trip ahead of the throat. This omission, which will be corrected in later tests, may also have affected the results.

Separation Behavior

Types of separation encountered.- Three main regimes of flow were noted as the diffuser divergence angle was increased through the ranges tested. These zones are the same as those found, for comparable conditions, in the two water-table units.

At the smallest angles tested, as expected, no separations at all were encountered; then, as the angle was increased above a critical value, the tufts began to show small intermittent stalls and separations; these occurred at varying locations on both diverging walls near the outlet. In the water table, most of the first stalls were found to take place in the diffuser corners; however, in the air diffuser it was found that the position of the first stall depended upon the value of the Reynolds number (and turbulence) as determined by the flow rate. Manometer readings were still quite steady at the first-stall angle.

When the divergence was increased still further, the separations began to show a marked preference for one wall or the other, and the main flow became asymmetric. The wall on which most of the separation existed exhibited the pattern shown in figure 32(a). The separations were definitely thicker and more active near the corners. Whereas the upper third of the separated plate became intermittently unseparated at the center of the diffuser, the corners were continuously separated. The lower part of the plate, below the dashed, parabolic-shaped line 3-3 shown in figure 32(a), remained permanently separated with violent and unsteady backflow along the separated wall. This configuration, then, corresponded to the three-dimensional patterns observed in the water-table studies. The throat manometers were very unsteady, especially at the highest flow rates.

At large angles and low flow rates, the configuration idealized in figure 32(b) existed in the diffuser. In the main, the flow was two-dimensional as indicated by the dashed line 2-2. It was not clear whether the line 2-2 was located after the throat as shown or farther forward. As indicated by the tufts near the edges of the plate and those on the Plexiglas walls, the corners became intermittently unseparated, the unseparated flow being maintained all the way to the exit for only a fraction of a second at a time. This corner zone of intermittent unseparation is isolated by the dashed curve 1-1 in figure 32(b). Although the rapid reversals of flow in the corners made the picture seem quite unstable, the static-pressure orifices evidently were not affected, for the manometers were, if anything, steadier than at the very low angles where no separations at all existed. When the air diffuser was operating in this configuration (fig. 32(b)) the pressure recovery was very poor. This indicated that flow was taking place down one wall as it did in the water-table diffuser with two-dimensional flow.

Small diagrams in which the dashed lines have the same significance as those in figure 32 have been spotted on the graph of 2θ versus R_W (fig. 33). Again, each square shows the condition of the separated diverging wall, or in cases where both walls were affected, the wall having the worst separations. The decimal written under each square is the $R_W \times 10^{-6}$ of that particular test. The low-angle zone of no separation and the stable, nearly two-dimensional zone at high angles and low throat Reynolds number (and turbulence) are separated from the zone of three-dimensional separations by the two heavy, jagged lines on the graph. The reader may wish to refer to figure 33 during the following more detailed descriptions of the air-diffuser separation behavior. (All of this air-unit work was conducted at $L/W_1 = 8$.)

Separations at 7° and 10°.- With the diffuser set at 7° and 10°, the tufts showed no vibrations or reversal of direction anywhere in the diffuser; so separations were concluded to be absent. At each angle tests were run at four different R_W settings, the range of R_W for 7° being approximately 127,000 to 360,000 and the range for 10° being between 137,000 and 342,000. Manometers were steady.

Separation at 12°.- At $2\theta = 12°$ the diffuser was operated at five different flow rates. At the lowest of these, $R_W = 138{,}000$, the manometers were steady, and there was no separation anywhere in the diffuser. One tuft, in a corner about midway between throat and outlet, began to vibrate intermittently. Therefore, it was believed that no separation had occurred, although the fluctuations at the single tuft indicated stall to be incipient.

When R_W was increased to 212,000, fluctuations great enough to vibrate the tufts began to appear intermittently over all the walls in the lower half of the diffuser, showing no preference for any particular locality. Separations with backflow began to appear intermittently on the diverging walls near the diffuser outlet with the preferred location being nearer to the center line than to the diffuser corner.

At $R_W = 286{,}000$ the separations preferred the corners and skipped erratically from one corner location to another. However, at $R_W = 364{,}000$ and again at $R_W = 414{,}000$ there seemed to be little preference of location as the separations skipped around on the walls near the outlet. Under these conditions the throat manometers showed momentary unsteadiness, but were, in the main, well behaved.

Separation at 15°.- At $2\theta = 15°$ the patterns noted at 12° continued with the separations becoming stronger and with manometer unsteadiness rising. The separations began to show a marked preference for the east

diverging wall, even though smaller intermittent separations continued to occur also on all other walls of the diffuser. Tests were run at four values of R_W ranging from 142,000 to 414,000.

Separation at 20°.- At $2\theta = 20°$ the separations were limited almost entirely to one diverging wall of the diffuser, although the wall of separation could be selected by using a vane held in the hands to divert the flow to the other wall. The flow was markedly three-dimensional in that the separation in one corner of the diffuser was much worse than in the other corner formed by the same diverging wall. Manometer fluctuation increased. The same pattern was observed throughout the R_W range from 136,000 to 407,000.

Separation at 22.5°.- At $2\theta = 22.5°$ the first nearly two-dimensional flow was encountered with $R_W = 93,000$. The manometers were even steadier than with flows at very small angles. The low throat Reynolds number was caused by a low flow rate which resulted from the poor recovery typical of this type of separated flow. In the corners on the separated plate the flow frequently became momentarily unseparated, but the flow reversals involved did not affect the steadiness of the manometers. The opposite diverging wall was entirely unseparated with not a flicker to be seen in the tufts.

When R_W was increased to 200,000, the two-dimensional separation was replaced by a pattern which was three-dimensional by reason of its greater depth of separation in the corners than at the center of the plate, and this three-dimensional pattern continued at the remaining two R_W settings, 275,000 and 400,000.

The recovery improved markedly when the flow became three-dimensional. This improvement undoubtedly was due to the more or less triangular shaped cross section of the separation which allowed an appreciable amount of diffusion in the portion of the flow which traveled down the center of the diffuser where the separation was thinnest. In contrast, in the two-dimensional cases the main flow, traveling the length of the diffuser with a nearly constant rectangular cross section, was not decelerated and, consequently, was diffused but slightly.

Separation at 30°.- At $2\theta = 30°$ with R_W values of 89,000, 140,000, and 175,000, the pattern was again stable and two-dimensional. At the lowest R_W, the tendency toward becoming momentarily unseparated in the corners was less noticeable than at the higher R_W settings. Manometers were extremely steady, recovery was very poor, and, accordingly, flow rate at fixed blower speed decreased markedly below those obtained even with a three dimensionally separated diffuser.

When R_W was increased to 197,000, the flow returned to a three-dimensional separation regime with its instability and manometer unsteadiness, but with recovery markedly improved. In the higher R_W range between 260,000 and 373,000, the intermittently unseparated zone at the top center of the separated plate extended farther downward toward the outlet as the flow rate increased until, at the highest R_W, it extended nearly halfway down the center of the plate.

Separation at 45°.- The behavior at $2\theta = 45°$ was nearly identical with that at 30°, except that the intermittently unseparated area in the corners virtually disappeared at the lowest R_W, 94,000. At $R_W = 138,000$ and $R_W = 191,000$ nearly two-dimensional separation continued. At R_W values of 321,000 and 349,000 the three-dimensional pattern returned. Recovery, unsteadiness, and the intermittent separations in corners behaved just the same as at $2\theta = 30°$.

Comparison with water-table results.- It has been noted previously that the water-table diffuser has a free surface for one "parallel wall" and a glass bottom for the other. This contrasts with the two parallel Plexiglas walls of the air diffuser. Consequently, when the three-dimensional separation encountered in the two diffusers is studied, it is reasonable that the water-table diffuser be compared with only one-half the air diffuser, either the north or the south half, at one time. That is, the $G/2$ of the water-table diffuser is analogous to only $G/2$ of the air diffuser, not to the whole of G.

In view of the above consideration, the three-dimensional separations of the two diffusers become comparable. In addition, both have zones of operation where there is no separation and zones in which the separations are nearly two-dimensional in form. The main difference noted was in the two-dimensional zone where, in the air diffuser, the corners showed a tendency to become unseparated intermittently at some flow rates. This tendency was not observed in the water-table diffuser.

When, starting in the low-angle unseparated zone, the divergence angles of both diffusers were increased in steps, both diffusers exhibited first stalls at around the same angle, $2\theta = 12°$. Therefore, in this transition the two diffusers even showed good quantitative agreement. When divergence angles were increased still further, the water-table diffuser, operated with low turbulence and with $R_W = 6,000$, reached the region of stable two-dimensional separation at about 17°, but the air diffuser did not demonstrate this transition until somewhere between 20° and 22.5° when the air R_W was 93,000. Larger values of R_W in the air

diffuser resulted in markedly higher angles for transition to stable two-dimensional separation, whereas doubling the R_W of the water-table diffuser, while maintaining a low turbulence intensity, resulted in only a small increase in angle (see fig. 13). The air diffuser's increase in this transition angle when flow rate was increased appears to be more akin to behavior of the water diffuser when increased turbulence caused an appreciable rise in the curve b-b of figure 15.

Figure 34 presents both water-table- and air-diffuser data on a logarithmic plot of 2θ against R_W. On this plot the two-dimensional data points are enclosed in small squares, the three-dimensional ones, in triangles, and the data points for no separation in circles. The different types of separation are then divided by solid curves into the same three zones as those used in figures 13, 15, and 33. The curves are dashed over the range of R_W where no data were obtained.

Reid (ref. 7, pp. 27-28) encountered instances of unsteady manometer behavior similar to those found in the present investigation. The angles he noted for the beginning of unsteadiness and the return of steadiness with increasing flow rate, 10.5° and 15°, respectively, are also shown at $R_W = 426{,}000$ in figure 34. Reid used one 40-mesh screen in the entrance section of his diffuser. Other than this information, nothing is known about the state of his turbulence.

Now, the low-turbulence water-table data exhibit a trend which seems to tie in with the air data at lowest flow rates (low turbulence) and seem to agree closely with the manometer unsteadiness data of Reid. In addition, high turbulence in the water table moved the zone boundaries in the same direction as high flow rate (high turbulence) in the air diffuser. All evidence points to the conclusion that more intense turbulence, rather than increasing Reynolds number, is the cause of the sudden upturn in the two-dimensional transition curve of the air unit shown in figure 34.

In summary, it may be stated that the water-table diffuser and the air apparatus exhibit qualitatively the same changes in flow regime when angle is increased while L/W_1 is held constant at a value of approximately 8. There is even close quantitative agreement as to the angle of occurrence of the first-stall condition; moreover, when flow rate is very low so that turbulence is at a minimum, there appears to be approximate quantitative agreement in the determination of the angle of transition of two-dimensional separation. However, more study of the effect of turbulence on diffuser performance is indicated before a quantitative relationship between the two-dimensional separation points can definitely be proved or disproved. Furthermore, there is a need for further work with the throat of the air unit set at other values of W_1, so that the separation curves for the air diffuser might be defined and compared with those obtained in the water table.

Results and Discussion of Recovery and Efficiency

Tabulated recovery and efficiency data.- The ideal energy recovery factors for the angles employed in the present air-diffuser tests were computed in the manner previously described and are tabulated in table X. These factors were then used in the computation of the energy efficiency.

In table XI, average throat and outlet pressures are presented together with the energy recovery factors and efficiencies computed from the pressures by the approximate methods discussed earlier. These results are the ones to be refined after the detailed profile traverses are completed.

Crossplotting.- The performance parameters tabulated in table XI were plotted against the throat Reynolds number R_W, and a curve was drawn for each of the eight angles at which data were taken during the tests. Then data were picked off these plots in order to obtain the curves of constant R_W shown in figures 35 and 36 which plot energy recovery and efficiency, respectively, against the diffuser divergence angle 2θ. Also shown in the low-angle regions of these graphs are dotted curves of pressure effectiveness and efficiency obtained by Reid.

Comparison with Reid's data.- As shown by the dotted lines in figures 35 and 36 which are drawn through data taken from reference 7, Reid's diffuser gave higher recoveries and efficiencies than the present diffuser at angles below 10°, but at larger angles Reid's values dropped off much more rapidly. The difference in values at the low angles can be explained by the fact that Reid's throat Reynolds number, approximately 426,000, was higher than that of the present diffuser. The difference at larger angles may be due to differences in wall smoothness or to the greater length of Reid's entrance section and, consequently, to a possibly greater thickness of the boundary layer at the entrance to his diffuser.

The most remarkable difference between the data of the two investigations may be noted in the angles at which the maximums of the performance parameters occurred. In the present investigation the maximums of recovery and efficiency (figs. 35 and 36) were found at about 10° and 14°, respectively. Reid's maximums occurred at angles some 3° smaller.

From the trends of the two sets of data and from the points where Reid's manometers returned to steadiness with an increase in angle, it seems likely that his turbulence level was lower than that of the present tests. This may explain the different "optimum angles," but no proof of this conjecture can be given.

Position of maximums with respect to first separation angle.- It is of interest to note that the recovery curves for the present diffuser

(fig. 35) rise for about 3° beyond the angle of occurrence of first separation. Furthermore, the efficiency (fig. 36) begins to drop at angles as much as 2° below that for first separation. This tends to confirm the suspicion (see the conclusion of appendix B) that the squareness of the outlet profile rather than the fact of existence of separation is the primary factor controlling the values of the recovery and the efficiency. Only when separations become large enough to affect the outlet velocity profile materially do they become of importance in overall performance. It is also a mistake, therefore, to assume that the performance parameters do not suffer so long as separation is absent.

Interpretation of recovery and efficiency graphs.- Because both the recovery and the efficiency were found to be affected in the same manner by changes in divergence angle and variation of throat Reynolds number, the curves in figure 35 and those in figure 36 can be covered in the same discussion.

First, consider the train of events which takes place as the angle 2θ is increased in small steps with an attempt being made to hold R_W constant at 200,000.

In the low-angle region there is first an increase in both recovery and efficiency. After the angles for the maximums, 9° to 11° for efficiency and about 14° for recovery, there is a continual decline in the value of the performance parameters as angle is increased. The gradual decrease in performance continues until $2\theta = 30°$ when a transition is reached wherein an increase in angle without a decrease in blower pressure results in an immediate change to a two dimensionally separated flow. Recovery and efficiency at once become very poor, and a decrease in flow rate occurs. In the actual tests R_W dropped abruptly from 200,000 to about 182,000. If, at the same angle, the plenum pressure was now lowered sufficiently by speeding up the blower, the flow rate increased, but the three-dimensional type of separation then returned. The resulting improvement in performance causes R_W to jump to a value considerably higher than 200,000. If, however, the angle is increased with the plenum pressure being adjusted just enough to maintain the new R_W of 182,000, the diffuser will continue to operate with a two-dimensional separation. With this two-dimensional operation, actual tests indicated a gradual increase in C_{ER} and η_E as the divergence angle was increased, but this indication must be used with caution until after the detailed traverses are completed because of doubt concerning the method of computation in this zone of operation.

If the same changes of angle were to be made while holding R_W at 143,000, the events would follow the same sequence, but the transition

to two-dimensional flow, as shown by the dashed lines, would occur somewhere between 20° and 22.5° and R_W would drop to a still lower value of around 91,000.

If the diffuser were to be operated at R_W = 334,000, then it would be possible to extend 2θ to as high as 45°, the highest angle tested, without development of two-dimensional separation. A surprising feature is the relatively large value of the pressure recovery, about 0.63, indicated for this wide angle.

The above descriptions, of course, apply only to the present air diffuser operated without any screens or other turbulence-controlling devices. The hypothesis, as previously stated, is that an increase of turbulence with flow rate is the cause of the unstable jumps from one condition of separation pattern and R_W to another and the cause also of the wide variation in the value of the transition angle as the flow rate is changed. This is also substantiated by the tests with rods given below.

As emphasized previously, a discussion of the effect of angle alone, even within what would at first glance seem to be a homogenous set of data, tends to be very misleading. As shown by figure 35, when the flow rate is adjusted to fix Reynolds number at 334,000 in the present diffuser, the recovery is still high at 45° even though the diffuser is not modified by vanes or other additions. The recovery at 45° is only three points below the frequently referred to "best angle" of 7°. Actually the maximum recovery occurred at 14° to 15° in this series of tests.

AIR DIFFUSER WITH VANES AND RODS

In order to determine whether the excellent results obtained with vanes in the water-table diffuser had possibility of attainment in the air diffuser also, the preliminary air-diffuser work was extended to include a few vane tests. In addition, two brief experiments with rods were tried.

Vanes

Vanes used.- The adjustable vanes which will be used in the air diffuser are still in the process of manufacture at present writing. Therefore, in order to obtain the desired preliminary determinations, two fixed-vane arrangements were quickly constructed. Each arrangement consisted of only two flat-plate vanes made of 16-gage galvanized iron (0.061 inch thick) with rounded leading edges and blunt trailing edges.

One pair of vanes had a length L_V = 3 inches, and the other pair had L_V = 6 inches. Each vane extended the full 24-inch width G of the diffuser, so that a pair of vanes could be held fixed in the diffuser by means of bolts inserted in the Plexiglas walls. The 3-inch-long vanes had between them a fixed angle of divergence $2\theta_V = 7.5^\circ$, but the 6-inch vanes could be set at angles of 7.5°, 10°, or 14°. These fixed angular settings and the practice of bolting the vanes to the diffuser walls greatly limited the flexibility of the vanes as to angular setting and fore and aft position, so there was little opportunity to make small adjustments in attempts to discover optimum settings. Therefore, final results await further experimentation. Nevertheless, some interesting configurations which resulted in appreciable improvement of performance were found.

Diffuser angles investigated.- Vanes were inserted in the air diffuser at $2\theta = 20^\circ$, 22.5°, and 30°. The 22.5° and 30° settings were selected simply because they were fairly large angles and because they each had exhibited both two-dimensional and three-dimensional separations. The 20° angle was included because it allowed investigation of a case of unequal vane spacing when the 7.5° vane arrangement was in use.

Improvement of separation conditions.- When vanes were inserted in a diffuser which, as indicated by 2θ and R_W, ordinarily would have been separated two-dimensionally, the flow pattern always was greatly improved. Although the separation was never completely removed as it was in the water diffuser, separations became much smaller and did not occur so near the throat as in a vaneless diffuser. One case in particular was encouraging. At R_W = 156,000, $2\theta = 30^\circ$, $2\theta_V = 10^\circ$, and L_V = 6 inches, a separation hung on one wall below the trailing edge of the vanes, but the flow returned to the wall after this separation and filled the diffuser cross section at the exit. When it is recalled that best results in the water-table diffuser at $2\theta = 30^\circ$ were obtained only when three vanes were inserted, this result is most encouraging, especially in view of the improvement in performance parameters to be discussed below. The fact that the flow pattern of a two dimensionally separated diffuser was greatly improved by the vanes was clearly demonstrated.

Unfortunately, with three dimensionally separated diffusers the improvement was not so obvious. Although the unsteadiness of manometers was very much reduced, it was not possible to remove the separations from both walls at the same time, although it appeared that separations were thinner and occurred farther from the throat than in diffusers without vanes.

Improvement of performance parameters.- Table XII presents the data obtained in the 15 different instances in which vanes were installed in

the diffuser. Table XIII compares these data with those obtained with the vaneless diffuser operating at the same throat Reynolds number, these latter data having been taken from the crossplotted graphs (figs. 35 and 36).

In every configuration of vanes tried in the diffuser the recovery and efficiency were improved. As already suggested in the discussion of the improvement of the separated flows, the greatest increase was obtained when vanes were used to correct a two-dimensional separation. The best improvement of all was obtained at $2\theta = 30^\circ$ with $R_W = 138{,}000$. Here the energy recovery was improved from 0.18 to about 0.74, a 56-point increase, and the energy efficiency was increased by 60 points.

When the throat Reynolds number was such that the flow would have been three-dimensional without the vanes, the performance was increased less impressively. However, the best case found with the limited vane adjustments available was that at $2\theta = 30^\circ$ and $R_W = 212{,}800$. Here the energy recovery increased from about 0.63 to about 0.745, an 11.5-point increase, and the increase in efficiency was 13.5 percent. An increase of this kind is encouraging not only in itself but also for the indicated possibilities for increase at other angles and flow rates when the means for more careful vane adjustment is provided and when the number of vanes used is increased to the optimum indicated by the water-table tests.

In the two most successful cases quoted above, the angles $2\theta_V$ between the two vanes and between the vanes and the walls all were 10°. Cases were tried also in which $2\theta_V$ between the two vanes was 14° and the angles between vanes and walls were 8°. This arrangement also caused an improvement in the performance parameters, as is indicated in table XIII, but the increases were smaller than in the equal-angle case. These data seem to bear out the water-table indication that equal spacing is about the best. On the other hand, $2\theta = 20^\circ$, where a similar, but less pronounced, uneven spacing was employed, gave slightly better increases than did equal spacing at 22.5°. Usually the overall performance appears to be relatively insensitive to very minor changes in vane configuration. This characteristic is highly desirable from a design point of view.

Rods

Two cases of rod insertion.- In early rod tests in the water table, success in eliminating separation was obtained by placing $1\frac{1}{8}$-inch rods in the entrance section of the diffuser where they reduced the flow area, as measured along a velocity potential line, to a value equal to the area of the throat. This placement was tried also in the air diffuser when

two $1\frac{1}{8}$-inch magnesium rods were suspended in the same position in the entrance section of a 20° diffuser. The rods when placed in this position did not eliminate separation, and the recovery was reduced so drastically that the experiment was abandoned.

However, when the diffuser was separated two dimensionally at an angle of 45°, a single $1\frac{1}{8}$-inch rod was suspended near the entrance lip of the separated diverging wall as shown by A in figure 1. With this configuration the separation conditions improved, and the recovery increased from about 0.30 to around 0.575, a 27.5-point increase. The increase in recovery caused an increase in the flow rate, though the blower speed remained unchanged. In another measurement, the same lone rod gave a 29-point increase in recovery.

Air-diffuser rod indications.- It has been shown that rods can profitably be used to cause a diffuser to generate its own vortices and thereby to improve its own performance. It is suspected that the important point is that rods should be located where the air velocity is low enough to insure low drag, but high enough to cause a rod-diameter Reynolds number which will insure shedding of vortices. A value of $R_d = 50$, which is near the lower limit of the range for generation of classical, stable Kármán streets found by Roshko (ref. 24, p. 36), probably is about optimum.

CONCLUSIONS

Reviews of the literature, work in the water table, and preliminary tests in the air-diffuser apparatus have yielded the conclusions on the effects of vanes and of turbulence on two-dimensional wide-angle subsonic diffusers enumerated below. The water-table results are believed to be accurate and definitive. The results of the air unit, on the other hand, are preliminary, and they should be viewed primarily as confirmation of the water-table results.

1. Water-table results indicate that during increases in the divergence angle 2θ of a diffuser of the present geometry adjusted to a fixed ratio of diffuser length to throat width L/W_1 (or, alternatively, to a constant ratio of diffuser wall length to throat width N/W_1) the flow behavior undergoes three transitions which bound four distinct regimes of operation. In the first regime (small angles), the flow does not separate. Then, as the angle is increased, transient separations begin at a definite and reproducible point. In the water-table diffuser these transient separations usually occur in a corner, the exceptions to

this rule having been noted at extremes of Reynolds number and at very large L/W_1 ratios. As the divergence angle is increased still further, these separations grow larger and more unsteady until a second and definite transition point is reached. At this point a change occurs to a very stable, nearly two-dimensional separated flow in which the main stream travels steadily down one wall with almost constant flow area. A wedge of almost stagnant water fills the remainder of the diffuser. At much larger angles still, a third transition occurs to a jet-type flow separated from both walls. An overlap or hysteresis zone exists at the boundary of the two-dimensional-separation and jet flow regimes. The transition points mentioned above are exactly reproducible in a given diffuser only when at least the free-stream turbulence, wall roughness, throat Reynolds number, ratio of length to throat width, and throat aspect ratio all are held constant.

2. The angles which define the boundaries between the different regimes of flow in the water-table diffuser are strongly affected by the value of L/W_1, the ratio of length to throat width. An increase in L/W_1 causes the first stall and transition to two-dimensional stall to occur at smaller angles. The ratio also affects the angle of transition from two-dimensional separation to jet flow; however, the value of this angle becomes larger as L/W_1 is increased. The plots amply illustrate the futility of attempting to specify diffuser separation as a function of the divergence angle alone.

3. The intensity of turbulence existing in the free stream entering the water-table diffuser is of great importance in determining the angle of separation. At most L/W_1 ratios an increase in turbulence intensity causes a slight lowering of the angle of first stall; however, increased turbulence intensity markedly increases the angle of transition from three-dimensional to two-dimensional separations at all L/W_1 ratios investigated. Turbulence has by far the greatest effect of any of the variables investigated except for divergence angle and L/W_1. The total effect of turbulence is to broaden the three-dimensional separation region at the expense of the unseparated region and the two-dimensional separation regimes. The mechanism appears to be that of directly influencing the boundary layer by transferring momentum toward the wall from the central core of the flow.

4. Changes of throat Reynolds number in the water-table diffuser affect separation angle in the same qualitative sense as does turbulence, but to a much smaller quantitative extent.

5. Changes in aspect ratio exerted only a very minor effect on the performance. In the case of transition from three-dimensional transitory stall to two-dimensional steady separation, the effect, if any existed,

was of approximately the same magnitude as the uncertainty in the data. In the case of transition from unstalled to three-dimensional transitory stall, the effect was slightly larger and hence was discernible, but it still was not of significance for design purposes.

6. In the air diffuser, the existence of the first three zones of operation was verified, but verification of the jet zone was not possible because of geometrical limitations of the apparatus. At $L/W_1 = 8$, the angle of first stall, 12°, was of about the same magnitude as that found in the water-table diffuser; thus quantitative agreement between the two analogs was obtained. The transition to two-dimensional separation, except at very low flow rates, occurred at a much larger angle than it did in the water-table tests, and there was a large variation in this angle with flow rate, the angle becoming markedly larger as the flow rate was increased. This is believed to be due to increased turbulence at higher flow rates. Two-dimensional separation, though very steady in operation, may cause recovery to drop to nearly zero. Three-dimensional separations, though unsteady in their operation, often give acceptable recovery factors, especially when the turbulence intensity is high.

7. Flat-plate vanes are effective in preventing stall and separation when carefully located within a definite range of positions in the water-table diffuser. Maximum effect is obtained when vanes are nearly equally spaced angularly and when the divergence angle between the vanes $2\theta_V$ is near the angle which gives maximum efficiency in a two-dimensional plane-wall diffuser operating under similar conditions. Vanes are most effective when placed immediately downstream of the throat so that the leading edges are just ahead of the position where the walls of the diffuser first reach a total divergence angle of around 10°. In the extreme case of successful application of vanes, all separations and stalls were removed from a 45° diffuser of $L/W_1 = 8$ by using five equally-spaced 6-inch vanes with their leading edges almost at the throat.

8. The vane configurations developed in the water table also produce a beneficial effect in the air diffuser. Separations, however, were not removed as completely as in the water-table diffuser. This shortcoming was believed to be the result of the employment of a makeshift vane arrangement having very little flexibility of adjustment. Better results can be achieved after installation of larger numbers of the more easily adjustable vanes now in process of manufacture. In one test of a 30° diffuser, a two-dimensional separation was changed to a three-dimensional one by inserting a pair of vanes, and the recovery factor rose from about 0.18 to about 0.74, a 56-point increase, while efficiency exhibited a 60-point rise. When the separation was three-dimensional at a higher flow rate in this 30° diffuser, the improvement obtainable was smaller, but still the recovery was raised about 11.5 points from 0.63 to nearly 0.745 while the efficiency increased 13.5 points. Because of results

such as the above, it is believed that vane configurations of this type hold real promise as a means for producing efficient wide-angle diffusers.

9. Many combinations of rods inserted upstream of the throat were tried in the water-table diffuser, but none of the configurations tried was much better than the average. Even though rods furnish vortices rather than random turbulence, these vortices soon break down into random oscillations which have much the same effect as turbulence from any other source. When rods were inserted downstream of the throat, separation downstream of the point of rod insertion often was eliminated, but separation continued to exist between the throat and the rods. It appeared that the effectiveness of separation with rods was again the result of the turbulence created rather than the pressure drop introduced at the rods as has sometimes been proposed. To cure all the separation in the diffuser, it was necessary to advance downstream rods well into the high-speed flow region where pressure loss undoubtedly would be excessive.

10. One case of rod placement in the air diffuser showed that the upstream location employed in the water-table diffuser would cause excessive losses in high-velocity flows. However, it was found that even one $1\frac{1}{8}$-inch rod properly located in a lower speed region of the entrance section produced marked improvement in the air-diffuser performance by changing the separation from the two-dimensional to the three-dimensional regime. Considering all factors, it does not appear that insertions of rods or other turbulence-producing devices offer nearly so much possibility for improvements as those offered by proper use of vanes. The rod results are mainly of interest in illuminating the role of turbulence in diffuser performance.

Stanford University,
Stanford, Calif., September 1, 1955.

APPENDIX A

DEFINITION AND DERIVATION OF ENERGY PARAMETERS AND THEIR COMPARISON WITH PRESSURE PARAMETERS

ENERGY RECOVERY FACTOR

In order to define performance parameters, the flux of energy is considered through the control volume bounded by the walls of the diffuser and the dashed lines labeled 1-1 and 2-2 in figure 4(a) and having a thickness G in the z-direction.

The rate of flux of kinetic energy into the diffuser is represented by the integral

$$Ik_1 = \int_{-W_1/2}^{W_1/2} \left(\rho v_1^2/2\right) v_1 G \, dx \tag{A1}$$

and the rate at which flow work is being done on the control volume is

$$Iw_1 = \int_{-W_1/2}^{W_1/2} p_1 v_1 G \, dx \tag{A2}$$

The rate at which flow work is being done by the control volume in expelling the flow is

$$Iw_2 = \int_{A_2} p_2 v_2 \, dA_2 \tag{A3}$$

An integral to be used for manipulation later in the development also is defined:

$$Io = \int_{-W_1/2}^{W_1/2} p_o v_1 G \, dx = p_o \int_{-W_1/2}^{W_1/2} v_1 G \, dx \tag{A4}$$

where p_o is the reservoir pressure or the total pressure in a flow where all streamlines have the same Bernoulli constant.

Continuity for an incompressible flow yields:

$$\int_{A_2} v_2 \, dA_2 = \int_{-W_1/2}^{W_1/2} v_1 G \, dx$$

If the pressure p_2 is constant over the outlet, considerable simplification results. In test runs on the air diffuser, a few cases were found where bad three-dimensional separations existed at high flow rates. In these few cases the maximum deviation of any one of four different static-pressure readings from their average was nearly 8 percent. However, in the great majority of cases the deviation from the average of these four outlet pressures was less than 3 percent. Since an even smaller error in C_{ER} is induced by this error in p_2, an assumption of constant static pressure everywhere in the exit plane is entirely justifiable.

Assuming that p_2 = Constant and substituting the above continuity relationship into equation (A3) yield:

$$Iw_{2a} = p_2 \int_{-W_1/2}^{W_1/2} v_1 G \, dx \tag{A5}$$

This eliminates the need for use of the exit velocity profile.

The energy recovery factor is now defined by

$$C_{ER} = \frac{Iw_2 - Iw_1}{Ik_1} \tag{A6}$$

where the integrals indicated are from the first three equations of this appendix. For greatest accuracy each integral is evaluated directly from measured pressure and velocity profiles.

Thus the energy recovery factor is defined as the ratio of the increase in the rate at which the medium does flow work to the rate of influx of kinetic energy; or, equivalently, the energy recovery factor is the fraction of the incoming kinetic energy per pound of fluid flowing which is converted by the diffuser into flow work.

It is anticipated that subsequent work on this subject will include the use of the accurate formulas. However, the purposes of the present paper are more adequately served by deriving a simple approximation.

The energy recovery factor is now defined approximately:

$$C_{ER} = \frac{Iw_{2a} - Iw_1}{Ik_1} \tag{A6a}$$

This assumes, as noted, that p_2 is constant across the exit plane. The integral defined by equation (A4) is now added to and subtracted from the numerator on the right-hand side of equation (A6a). This gives:

$$C_{ER} = \frac{(Io - Iw_1) - (Io - Iw_{2a})}{Ik_1}$$

Reference to equations (A1), (A2), and (A4) shows that outside the boundary layer, which in the present air apparatus has a displacement thickness of the order of 0.01 inch,

$$Ik_1 = Io - Iw_1$$

Therefore, it is assumed that this relationship holds for the whole entrance plane. Substituting and regrouping terms, one obtains:

$$1 - C_{ER} = \frac{Io - Iw_{2a}}{Ik_1} \tag{A7}$$

In the preliminary estimates of performance reported in the present paper, the entering profile was assumed to be that for flow between cylinders as discussed in appendix A of reference 1. Equations (A6) and (A12) from reference 1, when combined, furnish the following expression for the velocity profile at the diffuser entrance:

$$v_1 = (v_{w1})\frac{W_1 r_s}{a^2 - x^2} \tag{A8}$$

When this expression is substituted for v_1 in the integrals which form the terms of equation (A7) and the constants are factored out, the following equation results:

$$1 - C_{ER} = \frac{(p_o - p_2)}{\left(\rho v_{w_1}^2/2\right)(r_s W_1)^2} \frac{\int_{-W_1/2}^{W_1/2} \frac{dx}{a^2 - x^2}}{\int_{-W_1/2}^{W_1/2} \frac{dx}{(a^2 - x^2)^3}} \tag{A9}$$

Along any streamline outside the boundary layer at the throat, the velocity and pressure are related by the Bernoulli equation:

$$\left(\rho v_{w_1}^2/2\right) = p_o - p_{w_1}$$

Equation (A9), therefore, is more conveniently expressed as

$$1 - C_{ER} = \left(\frac{p_o - p_2}{p_o - p_{w_1}}\right)\left[\frac{1}{(r_s W_1)^2}\right]\left(\frac{I_n}{I_d}\right) \tag{A9a}$$

Where I_n is the integral in the numerator and I_d the integral in the denominator of equation (A9). The ratio $(p_o - p_2)/(p_o - p_{w_1})$ is the ratio of the manometer readings of the difference between reservoir pressure and the static pressure at wall orifices. The other variables, including the two integrals I_n and I_d, are determined by the geometry and dimensions of the diffuser.

In particular, the integral in the numerator of equation (A9) can be evaluated as

$$I_n = (2/a)\tanh^{-1}\left(W_1/2a\right) \tag{A10}$$

and the integral in the denominator becomes

$$I_d = \frac{1}{4a^2} \frac{(W_1/2)}{\left[a^2 - (W_1/2)^2\right]^2} + \frac{3}{8a^4} \frac{(W_1/2)}{a^2 - (W_1/2)^2} + I_n \tag{A11}$$

With a throat width W_1 of 3 inches and a value of r_s of $4\frac{1}{4}$ inches the following quantity can be evaluated:

$$\left[1/(r_s W_1)^2\right]\left(I_n/I_d\right) = 1.2345 \tag{A12}$$

and the expression for the energy recovery factor (A9a) becomes simply:

$$C_{ER} = 1 - 1.2345\left(\frac{p_o - p_2}{p_o - p_{w_1}}\right) \tag{A13}$$

where $p_o - p_{w_1} = q_{w_1}$ in the frictionless flow just outside the boundary layer. For other throat widths a reevaluation of the coefficient 1.2345 in equation (A13) is required.

ENERGY EFFICIENCY

The energy efficiency is, by definition:

$$\eta_E = C_{ER} \Big/ \left(C_{ER_{ideal}}\right) \tag{A14}$$

where $C_{ER_{ideal}}$ is the energy recovery factor which would be obtained if the flow between sections 1 and 2 in figure 4 were a potential one and the exit velocity v_2 were a constant. The reason for requiring v_2 to be a constant is discussed in appendix B.

Applying continuity to steady, incompressible, ideal flow through the control volume of figure 4(a), where the area ratio is R, yields:

$$V_2 R G W_1 = \int_{-W_1/2}^{W_1/2} v_1 G \, dx \tag{A15}$$

Again the velocity profile at the throat is described by equation (A8), and introducing this into equation (A15) gives

$$V_2 R W_1 = v_{w_1} W_1 r_s \int_{-W_1/2}^{W_1/2} \frac{dx}{\left(a^2 - x^2\right)}$$

or

$$V_2 = v_{w_1}(r_s/R) I_n \tag{A16}$$

For ideal flow

$$p_o - p_2 = \left(\rho V_2^2/2\right) = \left(\rho v_{w_1}^2/2\right)\left(r_s/R\right)^2 I_n^2 \tag{A17}$$

Substitution of equation (A17) into equation (A9) yields:

$$C_{ER_{ideal}} = 1 - \left(1/R^2\right)\frac{I_n^3}{W_1^2 I_d} \tag{A18}$$

Substituting the expressions from equations (A10) and (A11) for I_n and I_d in equation (A18) when $W_1 = 3$ inches and $r_s = 4.25$ inches gives:

$$C_{ER_{ideal}} = 1 - 0.993\left(1/R^2\right) \tag{A19}$$

Again, the coefficient in this equation must be evaluated for each new setting of the throat width W_1.

COMPARISON OF ENERGY WITH PRESSURE PARAMETERS

If the entering velocity is uniform and parallel, the energy integrals of equations (A2), (A4), and (A5) degenerate to the following:

$$Iw_1 = p_1 V_1 G W_1$$

$$Io = p_o V_1 G W_1$$

$$Iw_{2a} = p_2 V_1 G W_1$$

When equation (A7) is revised by replacing Ik_1 by $Io - Iw_1$ and the terms are rearranged, the result is

$$C_{ER} = 1 - \frac{Io - Iw_{2a}}{Io - Iw_1} \tag{A20a}$$

Substitution of the above-listed values for these integrals gives

$$C_{ER} = 1 - \frac{p_o - p_2}{p_o - p_1} \tag{A20b}$$

Comparison with equation (A13) shows the coefficient in that equation now has become 1. Further simplification of equation (A20b) while noting that $q_1 = p_o - p_1$ yields

$$C_{ER} = \frac{p_2 - p_1}{q_1} \tag{A20c}$$

Also, the second parenthetical expression in equation (A18) becomes equal to 1 and the equation degenerates to

$$C_{ER_{ideal}} = 1 - \left(1/R^2\right) \tag{A21}$$

Thus, in equations (A20c) and (A21), expressions have been obtained which are identical with the expressions for the pressure recovery C_{PR} and $C_{PR_{ideal}}$ as derived at the beginning of appendix B. The pressure recovery and the pressure effectiveness, therefore, are shown to be special cases of the more general energy parameters.

In comparing these formulas, it is of interest to note that the term $1 - C_{ER}$ based on flow between cylinders and the assumption of a constant value of v_2 varies from an equivalent one-dimensional flow by 23 percent as is seen by comparing equations (A20b) and (A13).[1] On the other hand the term $1 - C_{ER_{ideal}}$ varies by only 0.7 percent. It then follows that, for C_{ER} = 75 percent, η_E would be altered approximately 7 percent by the effect of velocity profile. These figures are all indicative only, and, as stated previously, vary considerably with circumstances. They are sufficient to show that the effect of velocity variation at the inlet cannot be ignored in careful calculations.

---

[1]The 23-percent variation is primarily due to the form of equation used. In particular, if the average throat pressure is used, instead of the wall pressure which is used in equation (A13), the coefficients will be nearly the same. However, the comparison shown clearly indicates the errors which may arise from use of wall pressure taps.

APPENDIX B

EFFECT OF EXIT-VELOCITY-PROFILE SQUARENESS ON PRESSURE RECOVERY AND PRESSURE EFFECTIVENESS

The following examples and analysis demonstrate the effect of exit-velocity-profile squareness on pressure recovery and pressure effectiveness.

The pressure recovery is defined as

$$C_{PR} = \left(p_2 - p_1\right)/q_1 \tag{B1}$$

In the first case the flow is assumed steady, one-dimensional, incompressible, and frictionless.

The Bernoulli equation (for ideal flow) is introduced

$$p_1 + q_1 = p_2 + q_2 \tag{B2}$$

and equation (B1) is solved for the pressure recovery:

$$C_{PR} = 1 - \left(q_2/q_1\right) \tag{B3}$$

Continuity for an incompressible flow gives

$$A_1V_1 = A_2V_2 \tag{B4}$$

and by definition

$$\frac{q_2}{q_1} = \frac{V_2^2}{V_1} = \frac{A_1^2}{A_2} = \frac{1}{R^2} \tag{B5}$$

For this ideal flow, the pressure recovery becomes, by combining equations (B3) and (B5):

$$C_{PR_{ideal}} = 1 - \frac{1}{R^2} \tag{B6}$$

Next the boundary layer is considered and steady incompressible flow with no friction in the core is assumed. By definition, $2\delta + c = W$ as shown in figure 4(b). Continuity for an incompressible flow gives

$$A_1V_1 = Uhc + 2\int_0^{\delta} uh\,dy$$

$$= UhW + 2\int_0^{\delta} uh\,dy - 2Uh\delta$$

$$= UhW + 2\int_0^{\delta} uh\,dy - 2\int_0^{\delta} Uh\,dy$$

$$= AU - 2Uh\int_0^{w/2}\left[1 - (u/U)\right]dy \qquad (B7)$$

The integral is the boundary-layer displacement thickness by definition; consequently,

$$A_1V_1 = AU - 2Uh\delta^*$$

At the outlet of the diffuser, since $U_1 = V_1$

$$A_1U_1 = A_1V_1 = U_2\left(A_2 - 2h\delta_2^*\right)$$

and

$$\frac{U_2}{U_1} = \frac{A_1}{A_2 - 2\delta_2^*h} \qquad (B8)$$

Since the core is assumed frictionless, the pressure recovery is again as defined by equation (B1) and, provided only that the streamline curvature is small,

$$C_{PR} = \frac{p_2 - p_1}{q_1} = 1 - \left(U_2/U_1\right)^2 \qquad (B9)$$

Combining equations (B8) and (B9) gives

$$C_{PR} = 1 - \left(\frac{A_1}{A_2 - 2h\delta_2^*} \right)^2 \tag{B10}$$

and the pressure effectiveness is given by

$$\eta_p = \frac{C_{PR}}{C_{PR_{ideal}}} = \frac{1 - \left(\frac{A_1}{A_2 - 2h\delta_2^*} \right)^2}{1 - \frac{1}{R^2}} \tag{B11}$$

Thus, both pressure recovery and pressure efficiency are found to be inverse functions of the displacement thickness of the boundary layer. Both are a maximum when δ_2^* is zero.

The investigation of the effect of the outgoing velocity profile can be carried still further by recognizing that the rate of momentum efflux at the diffuser exit represents a loss in possibility of pressure recovery. The rate of momentum efflux is represented as follows:

$$\frac{\text{Diffuser outlet rate of momentum flux}}{h} = \int_0^{W_2} \rho u^2 \, dy \tag{B12}$$

Obviously this integral is a minimum when the velocity u is zero throughout the profile, but this situation does not satisfy continuity as represented by the integral

$$\int_0^{W_2} \rho u \, dy = \text{Constant} = \frac{\rho A_1 V_1}{h} \tag{B13}$$

The minimization of the momentum integral, equation (B12), while observing the side condition of continuity, equation (B11), is a simple isoperimetric problem of the calculus of variations. See, for example, Weinstock (ref. 25, pp. 48-50).

A new integral is formed by adding to the momentum integral the function u, multiplied by a Lagrange multiplier λ, and then proceeding as if the integral formed by this new function were the one for which the minimum is desired. Accordingly,

$$\rho \int_0^{W_2} \left(u^2 - \lambda u\right) dy = A \text{ minimum} \tag{B14}$$

Now, as shown in Weinstock, if equation (B14) is a minimum, then the function which forms this integral becomes zero when operated upon by the Euler-Lagrange equation as follows:

$$\frac{\partial f^*}{\partial u} - \frac{d}{dy} \frac{\partial f^*}{\partial u'} = 0 \tag{B15}$$

where $f^* = (u^2 - \lambda u)$. Because u' is absent, the second term of equation (B15) makes no contribution. The first term, however, yields

$$2u + \lambda = 0 \qquad \text{or} \qquad u = \frac{\lambda}{2} = \text{Constant}$$

The value of λ is found by substituting back into the continuity equation (B13)

$$\int_0^{W_2} \frac{\lambda}{2} \, dy(1) = A_1 V_1 / h$$

$$\lambda = 2V_1 \frac{A_1}{A_2} \tag{B16}$$

and

$$u = \lambda/2 = V_1 \frac{A_1}{A_2} = V_2$$

where V_2 is the velocity for ideal flow.

Thus, provided there is still a frictionless core at the exit, the pressure effectiveness and pressure recovery depend only on the area ratio and displacement thickness of the boundary layer. For a given area ratio the maximum of both pressure effectiveness and pressure recovery will occur when the displacement thickness is zero, and the smaller the displacement thickness, that is, the squarer the velocity profile, the higher both the pressure effectiveness and the pressure recovery will be.

The following example illustrates an extreme case of an unsquare velocity profile in order to show the size of the effect which could be created. An artificially conceived flow is considered in which the frictionless core occupies one-third of the channel width at the outlet. The area ratio is 1.5 and the velocity profile in the wall boundary layers is linear (fig. 4(c)). Solving for the velocity in the core by continuity gives

$$V_1A_1 = (1/3)U_2A_2 + (2/3)A_2\left(U_2/2\right)$$

$$V_1A_1 = (2/3)U_2A_2$$

but

$$A_2 = (3/2)A_1$$

Hence

$$U_2 = V_1$$

and

$$C_{PR} = 0$$

by virtue of equation (B9). But for this area ratio

$$C_{PR_{ideal}} = 1 - \left(1/R^2\right) = 0.56 \tag{B6}$$

and consequently

$$\eta_p = \frac{C_{PR}}{C_{PR_{ideal}}} = 0$$

This extreme example makes it easy to believe that the first losses in effectiveness when the angle is increased above the angle of maximum efficiency are not caused directly by incipient separation or even by small separations actually in being. A small departure from squareness of the outlet profile is influential enough to be solely responsible for the modest downward trends actually experienced. Furthermore, it is indicated that even when large stable separations are generated at still higher angles, the detrimental effect of separation on effectiveness and recovery is a result of creation of a nonuniform outlet profile and not an intrinsic quality of the separation itself.

APPENDIX C

ACCURACY

The accuracy of measurements and computations of the present investigation will be described in terms of the "uncertainty," following the simple and systematic procedure described by Kline and McClintock (ref. 26). In the work that follows, it should be noted that it is the uncertainty which is estimated rather than the error.

The terms employed in the discussion are defined below and a brief outline of the procedure is presented. For a detailed discussion of the term "uncertainty" and for a treatment of the accuracy of engineering experiments from the present viewpoint reference 26 should be consulted.

Variable: A variable is a basic quantity observed directly in the laboratory.

Result: A result is a value obtained by making corrections to or calculations with the recorded values of the variables.

Error: The error in a given reading is the true value minus the observed value. For present purposes the word "error" represents the total effect of the fixed errors, accidental errors, and mistakes.

Uncertainty: The uncertainty is a possible value the error might have.

Percentage uncertainty: One hundred times the uncertainty, divided by the value of the variable or result for which the specification is made is termed the percentage uncertainty.

BRIEF DISCUSSION OF PROCEDURE

Although a large amount of data was collected in the course of the present investigation, repeated runs were not made at the same point of operation, and the errors of these single sample observations cannot be treated statistically. However, the uncertainty, or what it is thought the error might have been, is a statistical variable in this same observation and can be treated, in part, by the methods of statistics.

Though a great mass of data was not available, the experimenter still was able to estimate the uncertainty well enough to provide a useful evaluation of the results. These estimates were based on experience, judgment, and detailed knowledge concerning the construction and design

of the equipment, as well as on the actual operation of the instruments and equipment during the experiments.

Most experimenters are aware that it is something of a fiction to state that the "maximum error" is a certain amount, for it is plain that if the experiment is repeated indefinitely, any reasonable value stated for this maximum might someday be exceeded. It is far more realistic to use an uncertainty interval based on suitable odds. This is done as follows:

$$W_2 = 10.00 \pm 0.05 \text{ inches (20 to 1)} \tag{C1}$$

In equation (C1) the first number is the best estimate of the observed value of the variable W_2. The second number is the uncertainty S_{W_2}. The numbers in parentheses indicate that the experimenter believes the odds are 20 to 1 that the true value lies within ±0.05 inch of the estimated value. The odds selected for the uncertainty specification are the result of the experimenter's intuitive evaluation of the needs and possibilities of the particular situation. The percentage uncertainty in the variable can then be computed as follows:

$$\frac{S_{W_2}}{W_2} = \frac{0.05}{10} = 0.005 \text{ or } 0.5 \text{ percent} \tag{C2}$$

The uncertainty in a result β caused by uncertainties in variables x_n can be computed from the equation

$$S_\beta = \left[\left(\frac{\partial\beta}{\partial x_1} S_1\right)^2 + \left(\frac{\partial\beta}{\partial x_2} S_2\right)^2 + \ldots + \left(\frac{\partial\beta}{\partial x_n} S_n\right)^2\right]^{1/2} \tag{C3}$$

And the percentage uncertainty can again be found by forming S_β/β.

If a result is computed from variables combined as products and ratios in a single group, it is often convenient to take logarithms before differentiating. If the square root of the sum of the squares of these derivatives is then taken in a manner similar to the process indicated by equation (C3), the percentage uncertainty is obtained directly.

Reference 26 points out that equation (C3) assumes β to be a linear function of the independent variables x_n, each of which would be normally distributed if large amounts of data were available. When these conditions are met, then the odds on the uncertainty in the

result computed from the equation are the same as the odds selected for stating the uncertainty of the variables. Considerable deviation from exact conformation to the conditions stated may be tolerated without seriously altering the odds.

For example, let it be stated that

$$W_1 = 3.00 \pm 0.05 \text{ inches (20 to 1)} \tag{C4}$$

For a strictly two-dimensional channel, the area ratio R can be computed from $R = W_2/W_1$. After computing the partial derivatives, the uncertainty in the area ratio is obtained as follows:

$$S_R = \left\{\left[\left(-W_2/W_1\right)S_{W_1}\right]^2 + \left[\left(1/W_1\right)S_{W_2}\right]^2\right\}^{1/2}$$

$$= \left\{\left[(10/9)0.05\right]^2 + \left[(1/3)0.05\right]^2\right\}^{1/2}$$

$$= 0.058 \tag{C5}$$

Since $R = 3.33$ in this example, the percent uncertainty is then

$$S_R/R = 0.058/3.33 = 1.74 \text{ percent}$$

When this computation was repeated for other W_2 settings employed in the air-diffuser tests, S_R/R was found to vary from 1.7 to 1.9 percent. When listed below with the other uncertainties, these values were simply rounded off to 2.0 percent.

ACCURACY OF PRESENT DATA

It is believed that, with odds of 20 to 1, the variables and the results of the present experiments have uncertainties or percentage uncertainties as listed in table IX. Accuracy is indicated only for those variables and results actually used in computation and presentation of the experimental data.

Usually one or the other of the two methods of designation remains nearly constant over the range of values of a variable or a result. Therefore, a considerable saving in presentation space results from choosing, for each item, the more nearly constant designation. When the value shown in table IX is a percentage uncertainty, it is so designated. All the values in table IX(b) are percentage uncertainties. Simple uncertainties have an indication of the dimensions used in reading the variable.

REFERENCES

1. Moore, Carl A., Jr.: Some Effects of Vanes and of Turbulence on Two-Dimensional Wide-Angle Subsonic Diffusers. Ph. D. Thesis, Stanford Univ., Sept. 1955.

2. Gibson, A. H.: On the Flow of Water Through Pipes and Passages Having Converging or Diverging Boundaries. Proc. Roy. Soc. (London), ser. A, vol. LXXXIII, no. 563, Mar. 2, 1910, pp. 366-378.

3. Gibson, A. H.: On the Resistance to Flow of Water Through Pipes of Passages Having Divergent Boundaries. Trans. Roy. Soc. (Edinburgh), vol XLVIII, pt. 1, art. no. 5, 1913, pp. 97-116.

4. Jones, J. B., and Binder, R. C.: Boundary Layer Flow in the Corner of a Diffuser. Res. Ser. No. 116, Eng. Exp. Station Bull., Purdue Univ., Mar. 1952.

5. Tults, Harold: Flow Expansion and Pressure Recovery in Fluids. Proc. Am. Soc. Civ. Eng., vol. 80, separate no. 567, Dec. 1954, pp. 567-1 - 567-26.

6. Patterson, G. N.: Modern Diffuser Design. Aircraft Eng., vol. X, no. 115, Sept. 1938, pp. 267-273.

7. Reid, Elliott G.: Performance Characteristics of Plane-Wall Two-Dimensional Diffusers. NACA TN 2888, 1953.

8. Vedernikoff, A. N.: An Experimental Investigation of the Flow of Air in a Flat Broadening Channel. NACA TM 1059, 1944. (Translation of CAHI Rep. No. 137, 1926.)

9. Nikuradse, Johann: Untersuchungen über die Strömungen des Wassers in konvergenten und divergenten Känalen. Forsch.-Arb. Geb. Ing.-Wes., Bd. , Nr. 289, 1929.

10. Demontis, Jean: Recherches sur l'influence de l'angle d'ouverture d'un ajutage divergent sur l'écoulement á deux dimensions de l'air á traverse cet ajutage. Pub. sci. et tech. du Ministère de l'air, no. 87, 1936.

11. Polzin, J.: Flow Investigations in a Two-Dimensional Diffuser. R.T.P. Translation No. 1286, British Ministry of Aircraft Production. (Translation from Ing.-Archiv, Bd. 11, Heft 5, Oct. 1940, pp. 361-385.)

12. Rouse, Hunter, and Hassan, M. M.: Cavitation-Free Inlets and Contractions. Mech. Eng., vol. 71, no. 3, Mar. 1949, pp. 213-216.

13. Shapiro, Ascher H.: The Dynamics and Thermodynamics of Compressible Fluid Flow. Vol. I. The Ronald Press Co. (New York), 1953.

14. Johnston, I. H.: The Effect of Inlet Conditions on the Flow in Annular Diffusers. C. P. No. 178, Aero. Res. Council Tech. Rep., Ministry of Supply, 1954.

15. Robertson, J. M., and Ross, Donald: Effect of Entrance Conditions on Diffuser Flow. Proc. Am. Soc. Civil Eng., vol. 78, separate no. 141, July 1952; discussion, vol. 79, separate No. D-141, June 1953.

16. Copp, Martin R.: Effects of Inlet Wall Contour on the Pressure Recovery of a 10°, 10-Inch-Inlet-Diameter Conical Diffuser. NACA RM L51E11a, 1951.

17. Little, B. H., Jr., and Wilbur, Stafford W.: Performance and Boundary-Layer Data From 12° and 23° Conical Diffusers of Area Ratio 2.0 at Mach Numbers up to Choking and Reynolds Numbers up to 7.5×10^6. NACA Rep. 1201, 1954. (Supersedes NACA RM's L9H10, L9K10, and L50C02a. NACA RM L9H10 contains information pertinent to the present paper.)

18. Peters, H.: Conversion of Energy in Cross-Sectional Divergences Under Different Conditions of Inflow. NACA TM 737, 1934.

19. Hamel, G.: Spiralformige Bewegungen zaher Flussigkeiten. Jahresber. Mathem. Vereinigung, Bd. 25, 1916, p. 34.

20. Fluid Motion Panel of the Aeronautical Research Committee and Others (S. Goldstein, ed.): Modern Developments in Fluid Dynamics. Vol. 1. The Clarendon Press (Oxford), 1938.

21. Dryden, Hugh L., and Schubauer, G. B.: The Use of Damping Screens for Reduction of Wind-Tunnel Turbulence. Jour. Aero. Sci., vol. 14, no. 4, Apr. 1947, pp. 221-228.

22. Schubauer, G. B., and Spangenberg, W. G.: Effect of Screens in Wide-Angle Diffusers. NACA Rep. 949, 1949. (Formerly NACA TN 1610.)

23. Eckert, B., and Pflüger, F.: The Resistance Coefficient of Commercial Round Wire Grids. NACA TM 1003, 1942.

24. Roshko, Anatol: On the Development of Turbulent Wakes from Vortex Streets. NACA Rep. 1191, 1954. (Supersedes NACA TN 2913.)

25. Weinstock, Robert: Calculus of Variations. McGraw-Hill Book Co., Inc., 1952.

26. Kline, S. J., and McClintock, F. A.: Describing Uncertainties in Single-Sample Experiments. Mech. Eng., vol. 75, no. 1, Jan. 1953, pp. 3-8.

TABLE I.- SUMMARY OF TWO-DIMENSIONAL DIFFUSER RESEARCH

Source of data	Medium	L/W_1	2θ, deg	R	G/W_1	W_1, in.
Gibson (refs. 2 and 3)	Water	2.4-7.2	10-30	2.25	1.0	1.33
		4.4-34.4	5-40	4.00	1.0	1.33
		5.7-45.9	10-90	9.00	2.25	.59
Vedernikoff (ref. 8)	Air	10.0	0-26	1.0-7.77	1.0	3.94
Nikuradse (ref. 9)		33.3	0-8	1.0-5.65	25.0	
Demontis (ref. 10)		3.5	0-31	1.0-2.94	1.0	
Polzin (ref. 11)		15.0	0.44	1.0-11.9	1.0	
Reid (ref. 7)	Air	5.50	8.0-17.4	1.75-2.625	8.0	4.0
		7.75	6.0-18.9	1.8-3.5	8.0	4.0
		11.00	5.4-15.9	2.0-4.0	8.0	4.0
		15.25	3.8-15.2	2.0-5.0	8.0	4.0
		21.75	2.7-10.7	2.0-5.0	8.0	4.0
Jones and Binder (ref. 4)	Air	4.0	8.0	1.55	1.0	8.0
Tults (ref. 5)	Water	[a]5.8	[a]0-40	1.0-2.05	1.0	7.83
Present investigation[b]		24.16-24.78	0-50	1.0-22.45	9.0 and 3.0	1.0
		16.11-16.52	0-50	1.0-15.30	6.0 and 3.0	1.5
		8.10-8.26	0-45	1.0-7.45	3.0 and 1.5	3.0
Large water-table diffuser	Water	6.07-6.20	0-45	1.0-5.84	2.25	4.0
		4.06-4.13	0-40	1.0-3.88	1.5	6.0
Small water-table diffuser	Water	15.3-3.1	0-180	1.0-37.8	18.0	.5
		7.7-6.5	0-90	1.0-12.8	9.0	1.0
		3.8-3.2	0-90	1.0-6.9	4.5	2.0
Air diffuser	Air	8.10-8.26	7-45	1.99-7.45	8.0	3.0

[a]Tults used an asymmetric diffuser in which only one wall diverged. Divergence angle of this one wall and the ratio L/W_1 shown in this table have been changed so that his values could be compared with others in the table.

[b]In the present investigation dimensions of diverging wall were fixed; L/W_1 and R were changed by varying throat width W_1. Thus, both L/W_1 and R could be made to increase indefinitely by causing W_1 to approach zero. Values shown are merely those settings within which data actually were taken.

TABLE II.- COMPARISON OF WALL AND CENTER-LINE VELOCITIES AND DYNAMIC PRESSURES AT THROAT

W_1	$\frac{v_w}{v_c}$	$\frac{q_w}{q_c}$
1	1.059	1.121
2	1.118	1.250
3	1.177	1.385
4	1.235	1.525
5	1.294	1.674
6	1.353	1.831

TABLE III.- COMPARISON OF VALUES DERIVED FROM FLUX PLOTS WITH FLOW BETWEEN CYLINDERS

$[W_1 = 3$ in.$]$

Values derived from -	2θ, deg	$\frac{v_w}{v_c}$	$\frac{q_w}{q_c}$
Flux plots	7	1.115	1.24
	30	1.150	1.32
Flow between cylinders	--	1.177	1.383

TABLE IV.- SEPARATION ANGLES AND CONDITIONS

FOR LOW TURBULENCE

(a) Occurrence of first stall

W_1, in.	2θ, deg	L/W_1	R	G/W_1	V_1, ft/sec	R_W	R_L
6	22	4.13	2.61	1.50	0.22	11,600	47,800
6	20	4.13	2.46	1.47	.11	5,930	24,500
3	13	8.22	2.85	2.86	.23	6,020	48,900
3	12	8.22	2.70	3.00	.39	10,830	86,200
3	14	8.23	2.99	1.46	.24	5,990	49,300
1.5	9	16.38	3.54	5.74	.25	3,135	51,400
1.5	8	16.35	3.26	5.86	.48	6,000	98,000
1.5	9	16.38	3.54	2.93	.49	5,990	98,100
1.0	8	24.57	4.40	8.60	.25	2,280	56,000
1.0	6	24.53	3.56	8.70	.69	5,920	145,000
1.0	7	24.55	3.98	2.90	.72	6,000	147,200

(b) Occurrence of transition from three-dimensional to two-dimensional separation

W_1, in.	2θ, deg	L/W_1	R	G/W_1	V_1, ft/sec	R_W	R_L
6	24	4.13	2.75	1.47	0.11	5,930	24,500
6	26	4.12	2.89	1.50	.22	11,600	47,800
3	16	8.24	3.29	2.93	.23	6,020	49,600
3	17	8.25	3.45	3.00	.43	11,150	92,100
3	16	8.24	3.29	1.46	.24	5,990	49,400
1.5	12	16.4	4.40	5.74	.25	3,270	53,600
1.5	13	16.5	4.69	5.86	.48	6,000	98,000
1.5	13	16.43	4.69	2.93	.49	5,990	98,100
1.0	10	24.61	5.25	8.60	.25	2,280	56,300
1.0	11	24.64	5.68	8.70	.69	6,090	150,000
1.0	12	24.65	6.11	2.90	.72	6,000	147,800

TABLE V.- SEPARATION ANGLES AND CONDITIONS

FOR HIGH TURBULENCE

(a) Occurrence of first stall

W_1, in.	2θ, deg	L/W_1	R	G/W_1	V_1, ft/sec	R_W	R_L
6	17	4.13	2.22	1.45	0.13	6,050	25,000
4	15	6.18	2.61	2.18	.20	6,050	34,700
3	11	8.21	2.56	2.94	.26	5,980	49,100
[a]3	12	8.22	2.70	3.00	.43	9,750	80,200
1.5	9	16.38	3.54	5.80	.53	6,050	99,000
1	7	24.55	3.98	8.60	.81	6,120	150,000

(b) Occurrence of transition from three-dimensional to two-dimensional separation

W_1, in.	2θ, deg	L/W_1	R	G/W_1	V_1, ft/sec	R_W	R_L
6	40	4.08	3.88	1.47	0.13	5,980	24,400
4	28	6.18	4.05	2.20	.20	5,950	36,750
[b]4	38	6.16	5.10	2.28	.32	9,650	59,500
3	26	8.24	4.78	2.94	.26	5,980	49,300
[a]3	22	8.25	4.22	3.00	.43	9,750	80,500
1.5	20	16.50	6.85	5.80	.53	6,050	99,800
1	18	24.76	10.33	8.80	.79	5,980	148,000

[a]Turbulence intensity lower than for remainder of data.

[b]Turbulence intensity much higher than for remainder of data.

TABLE VI.- CRITICAL ANGLES IN SMALL WATER-TABLE DIFFUSER OPERATED AT LARGE ANGLES

(a) Transition from two-dimensional separation to jet flow when angle is being increased

W_1	N/W_1	R_W	Critical 2θ, deg
2.0	4.33	3,690	75
2.0	4.30	6,330	70
1.0	8.87	3,695	90
1.0	8.87	5,860	90
.5	20.18	3,650	180

(b) Transition from jet flow to two-dimensional separation when angle is being decreased

W_1	N/W_1	R_W	Critical 2θ, deg
2.0	4.20	3,690	55
2.0	4.16	6,240	50
1.0	8.46	3,640	60
1.0	8.39	5,780	55
.5	17.06	3,650	65

TABLE VII.- RATIO OF LENGTH TO LEADING-EDGE SPACING OF VANES L_v/W_v FOR EQUALLY SPACED ARRANGEMENTS

[All values are only approximate since W_v varies slightly as leading edge of vane is moved fore and aft; $W_v = W_1/(m + 1)$ where m is number of vanes]

L_v	m	W_1 = 6 in.; L/W_1 = 4		W_1 = 3 in.; L/W_1 = 8		W_1 = 1.5 in.; L/W_1 = 16		W_1 = 1 in.; L/W_1 = 24	
		W_v	$\frac{L_v}{W_v}$	W_v	$\frac{L_v}{W_v}$	W_v	$\frac{L_v}{W_v}$	W_v	$\frac{L_v}{W_v}$
1	2	2	0.5	1	1	0.5	2	0.33	3
2	2	2	1.0	1	2	.5	4	.33	6
2	3	1.5	1.3	.75	2.7	.38	5.3	.25	8
3	2	2	1.5	1	3	.5	6	.33	9
3	3	1.5	2.0	.75	4	.38	8	.25	12
3	5	1.0	3.0	.5	6	.25	12	.17	18
6	2	2	3.0	1.0	6	.5	12	.33	18
6	3	1.5	4.0	.75	8	.38	16	.25	24
6	5	1.0	6.0	.5	12	.25	24	.17	36
23	1	3.0	7.7	1.5	15.4	.75	46	.5	46
23	2	2.0	11.5	1.0	23	.5	69	.33	69

TABLE VIII.- DETAILS AND RESULTS OF UPSTREAM ROD INSERTIONS

Rod diameter, in.	Number of rods	Placement	$\frac{\text{Flow area}}{\text{Free flow area}}$	Average velocity[a] between rods, ft/sec	Rod-diameter Reynolds number	Two-dimensional separation angle, deg
1/8	21	Vertical	0.562	0.213	222	20
1/8	23	Horizontal	.522	.229	239	20
1/4	9	Vertical	.626	.191	388	23
1/4	5	Horizontal	.792	.151	315	20
1/4	7	Horizontal	.709	.169	352	20
1/2	5	Vertical	.583	.205	855	19
1/2	4	Horizontal	.667	.179	755	20

[a]Average velocity at this potential line before rod insertion was about 0.12 ft/sec.

TABLE IX.- UNCERTAINTIES IN VARIABLES AND RESULTS

(a) Uncertainties in variables

Variable	Water-table diffusers		Air diffuser
	Large	Small	
z-direction fluid dimension, h, in.	0.05	0.05	0.05
Jet height, J, in.	0.15	0.15	----
Diffuser length, L, in.	0.03	0.10	0.03
Vane length, L_v, in.	0.03	----	0.03
Length of plane wall, M, in.	0.20	0.20	0.20
Diverging wall length, N, in.	0.05	0.05	0.05
Average of six throat manometers, $(p_o - p_{w_1}) = q_w$, percent			
No separation	----	----	3
3-dimensional separation	----	----	15
3-dimensional separation with vanes	----	----	5
2-dimensional separation	----	----	0.5
Average of four outlet manometers, $(p_o - p_2)$, percent			
No separation	----	----	1
3-dimensional separation	----	----	10
3-dimensional separation with vanes	----	----	5
2-dimensional separation	----	----	0.5
Weight of water, lb	0.5	0.5	----
Cylinder radius, r_o, in.	0.03	0.03	0.05
Time, t, sec	0.2	0.2	----
Throat width, W_1, in.	0.05	0.05	0.05
Outlet width, W_2, in.	0.03	0.10	0.05
Vane leading-edge spacing, W_v, in.	0.10	----	0.03
[a]Diffuser angle, 2θ, deg	0.3	0.5	0.3
Temperature, °F	1.0	1.0	0.2
Wet-bulb temperature, °F	----	----	0.2

[a]Uncertainty indicated for 2θ includes only geometrical uncertainty of measuring angle. Additional uncertainty due to subjective nature of separation-angle determination is discussed separately in text wherever question arises.

TABLE IX.- UNCERTAINTIES IN VARIABLES AND RESULTS - Concluded

(b) Uncertainties in results

Uncertainty, percent, in -	Water-table diffusers		Air diffuser, W_1 = 3 in.
	Large	Small	
[a]Energy recovery factor, C_{ER}			
No separation	---	---	1.5
3-dimensional separation	---	---	6
3-dimensional separation with vanes	---	---	2.5
2-dimensional separation at 7°	---	---	2.0
2-dimensional separation at 45°	---	---	1.5
$C_{ER_{ideal}}$	---	---	0.05
Ratio of length to throat width, L/W_1			
$L/W_1 = 4$	1	---	
$L/W_1 = 24$	5	---	1.7
Ratio of wall length to throat width, N/W_1			
$N/W_1 = 4$	---	3	----
$N/W_1 = 16$	---	10	----
[a]Reynolds number, R_W			
No separation	4	4	8
3-dimensional separation	4	4	11
3-dimensional separation with vanes	4	4	8
2-dimensional separation	4	4	8
Area ratio, R	---	---	2
[a]Efficiency, η			
No separation	---	---	2.0
3-dimensional separation	---	---	6.0
3-dimensional separation with vanes	---	---	3.0
2-dimensional separation	---	---	2.5
Mass density	---	---	6.5
Viscosity	2.7	2.7	1.1

[a]In addition to percentage uncertainties given, these results are subject to uncertainty introduced by assumption of flow between cylinders which was used to determine entering profiles. The effect of this assumption will not be known until completion of detailed traverses now in progress. For details regarding this assumption see appendix A and section entitled "Diffuser Geometry and Entrance Velocity and Pressure Profiles."

TABLE X.- OUTLET WIDTH W_2, AREA RATIO R, AND IDEAL ENERGY RECOVERY AS FUNCTIONS OF DIVERGENCE ANGLE 2θ FOR THROAT WIDTH W_1 = 3 INCHES

2θ	W_2	R	$C_{ER_{ideal}}$
0	3.00	1.00	-----
7	5.98	1.99	0.750
10	7.25	2.42	.830
12	8.11	2.70	.864
15	9.42	3.14	.899
20	11.79	3.93	.936
22.5	12.86	4.29	.946
30	16.00	5.33	.965
45	22.35	7.45	.982

TABLE XI.- PERFORMANCE OF VANELESS AIR DIFFUSER

2θ, deg	p_{c_1} Plexiglas orifices, in. water	p_{w_1} curved wall, in. water	p_2, in. water	V_1, ft/sec	R_w	C_{ER}	η_E
Unseparated diffusers							
7	1.43	1.97	0.59	84	126,900	0.630	0.840
7	3.16	4.34	1.27	125	188,300	.638	.851
7	5.72	8.05	2.26	170	256,200	.653	.870
7	11.30	15.9	4.40	239	360,600	.658	.877
10	1.61	2.30	.54	91	137,000	.710	.855
10	3.68	5.33	1.15	138	208,600	.733	.883
10	6.46	9.42	2.04	184	277,800	.732	.882
10	9.92	14.35	2.98	227	342,200	.742	.894
12	1.75	2.32	.52	92	138,000	.723	.837
Diffusers separated three dimensionally							
12	4.01	5.50	1.09	141	212,000	.76	.87
12	7.27	9.96	1.97	190	285,500	.76	.87
12	11.15	16.14	2.81	242	363,700	.78	.91
12	15.3	20.83	3.52	276	414,000	.79	.92
15	1.84	2.50	.53	95	142,100	.74	.82
15	4.26	5.95	1.10	146	219,400	.77	.86
15	7.79	10.96	2.03	198	297,300	.77	.86
15	14.75	21.1	4.15	276	413,500	.76	.84
20	1.66	2.22	.56	89	135,500	.69	.74
20	3.77	5.50	1.16	140	213,000	.74	.79
20	3.84	5.65	1.20	142	216,000	.74	.79
20	7.51	11.34	2.09	201	306,000	.77	.83
20	6.96	10.14	2.03	190	289,000	.75	.80
20	13.35	20.25	4.1	269	408,600	.75	.80
20	15.5	20.0	4.26	268	406,100	.74	.79
[a]22.5	[a].64	[a].70 [a]1.10	[a].64	[a]63	[a]93,400	[a].28	[a].30
22.5	3.54	5.07	1.20	136	200,800	.71	.75
22.5	3.66	5.21	1.28	138	203,800	.70	.74
22.5	6.21	9.40	2.06	185	273,300	.73	.77
22.5	6.17	9.62	2.06	187	276,300	.74	.78
22.5	6.24	9.18	2.21	182	269,800	.69	.73
22.5	6.30	9.63	2.22	187	276,300	.72	.76
22.5	13.5	20.7	4.40	274	405,800	.74	.78
22.5	11.8	19.2	4.66	265	391,700	.75	.79
22.5	12.2	20.3	4.47	272	402,000	.73	.77
[a]30	[a].63	[a].67 [a].97	[a].65	[a]58	[a]89,000	[a].17	[a].18
[a]30	[a]1.48	1.53 2.38	1.33	92	140,500	.31	.32
[a]30	[a]2.46	4.68	[a]1.45	[a]129	[a]196,600	[a].62	[a].64
[a]30	[a]2.40	[a]2.38 [a]3.72	[a]2.45	[a]115	[a]175,500	[a].18	[a].19
30	4.41	8.13	2.27	170	259,500	.66	.68
30	6.5	13.2	3.6	217	330,200	.66	.69
30	-----	16.8	4.5	245	373,000	.67	.69
[a]45	[a].65	[a].60 [a]1.10	[a].60	[a]63	[a]94,050	[a].22	[a].23
[a]45	[a]1.42	[a]1.36 [a]2.37	[a]1.36	[a]93	[a]138,300	[a].29	[a].30
[a]45	[a]3.10	[a]2.70 [a]4.55	[a]2.51	[a]128	[a]191,400	[a].31	[a].32
45	5.48	12.8	3.6	215	321,000	.65	.67
45	7.6	15.1	4.6	234	348,600	.62	.64

[a]Two-dimensional separation, with different p_w's on east and west curved walls.

TABLE XII.- PERFORMANCE OF AIR DIFFUSER WITH TWO VANES INSERTED

2θ, deg	L_v, in.	$2\theta_v$, deg	p_{c_1} Plexiglas orifices, in. water	p_{w_1} curved wall, in. water	p_2, in. water	V_1, ft/sec	R_W	C_{ER}	η_E
20	6	6.25-7.5-6.25	1.53	2.40	0.47	93	140,600	0.758	0.810
20	6	6.25-7.5-6.25	3.96	6.29	1.16	150	227,800	.772	.825
22.5	3	7.5-7.5-7.5	1.47	2.27	.51	90	136,400	.723	.765
22.5	3	7.5-7.5-7.5	3.21	5.25	1.20	137	207,000	.730	.771
22.5	3	7.5-7.5-7.5	6.53	10.68	2.06	196	295,100	.762	.805
22.5	6	7.5-7.5-7.5	1.48	2.42	.50	93	141,900	.754	.796
22.5	6	7.5-7.5-7.5	3.24	5.56	1.17	141	215,400	.740	.782
22.5	6	7.5-7.5-7.5	4.52	7.59	1.54	164	251,300	.749	.791
30	6	10-10-10	1.37	2.60	.54	102	156,600	.743	.785
30	6	10-10-10	3.06	5.86	1.21	144	221,500	.745	.787
30	6	10-10-10	5.36	10.58	2.18	194	298,000	.745	.787
30	6	10-10-10	1.16	2.26	.52	90	138,000	.716	.757
30	6	10-10-10	2.70	5.39	1.29	138	212,800	.704	.744
30	6	10-10-10	5.02	10.02	2.28	189	290,200	.719	.760
30	6	10-10-10	7.54	15.50	3.28	235	361,000	.732	.774

TABLE XIII.- IMPROVEMENTS IN PERFORMANCE OBTAINED BY INSERTING TWO VANES INTO AIR DIFFUSER

2θ, deg	L_v, in.	$2\theta_v$, deg	R_w	With vanes		Without vanes		Increase in C_{ER}	Increase in η_E
				C_{ER}	η_E	C_{ER}	η_E		
20	6	6.25-7.5-6.25	140,600	0.758	0.810	0.69	0.74	0.07	0.07
20	6	6.25-7.5-6.25	227,800	.772	.825	.73	.78	.04	.045
22.5	3	7.5-7.5-7.5	136,400	.723	.765	.30	.32	.42	.45
22.5	3	7.5-7.5-7.5	207,000	.730	.771	.70	.74	.03	.03
22.5	3	7.5-7.5-7.5	295,100	.762	.805	.725	.765	.04	.04
22.5	6	7.5-7.5-7.5	141,900	.754	.796	.30	.32	.45	.48
22.5	6	7.5-7.5-7.5	215,400	.740	.782	.71	.75	.03	.03
22.5	6	7.5-7.5-7.5	251,300	.749	.791	.715	.735	.035	.035
30	6	10-10-10	156,600	.743	.785	.18	.186	.56	.60
30	6	10-10-10	221,500	.745	.787	.63	.65	.115	.135
30	6	10-10-10	298,000	.745	.787	.65	.675	.095	.11
30	6	8-14-8	138,000	.716	.757	.18	.186	.54	.57
30	6	8-14-8	212,800	.704	.744	.625	.65	.08	.095
30	6	8-14-8	290,200	.719	.760	.65	.675	.07	.085
30	6	8-14-8	361,000	.732	.774	.68	.705	.05	.07

TABLE XIV.- LONGITUDINAL LOCATION OF 3/8-INCH DIVERGING-WALL PROBE HOLES

[Tolerances on dimensions are 0.010 in.]

Holes numbered from curved end of plate	Distance from trailing edge of aluminum plate measured along inner surface of aluminum plate, in.
1	26.000
2	25.667
3	25.333
4	25.000
5	24.667
6	24.333
7	24.000
8	23.000
9	22.000
10	21.000
11	20.000
12	19.000
13	18.000
14	17.000
15	15.000
16	13.000
17	11.000
18	9.000
19	7.000
20	5.000
21	3.000
22	1.000

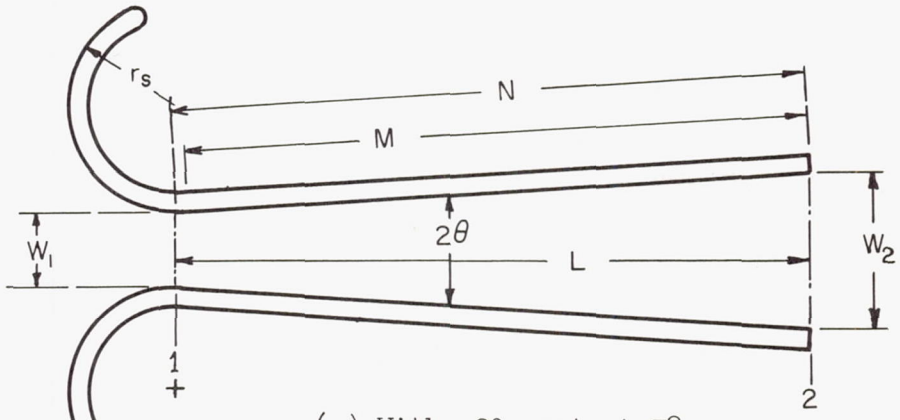

(a) With 2θ set at 7°.

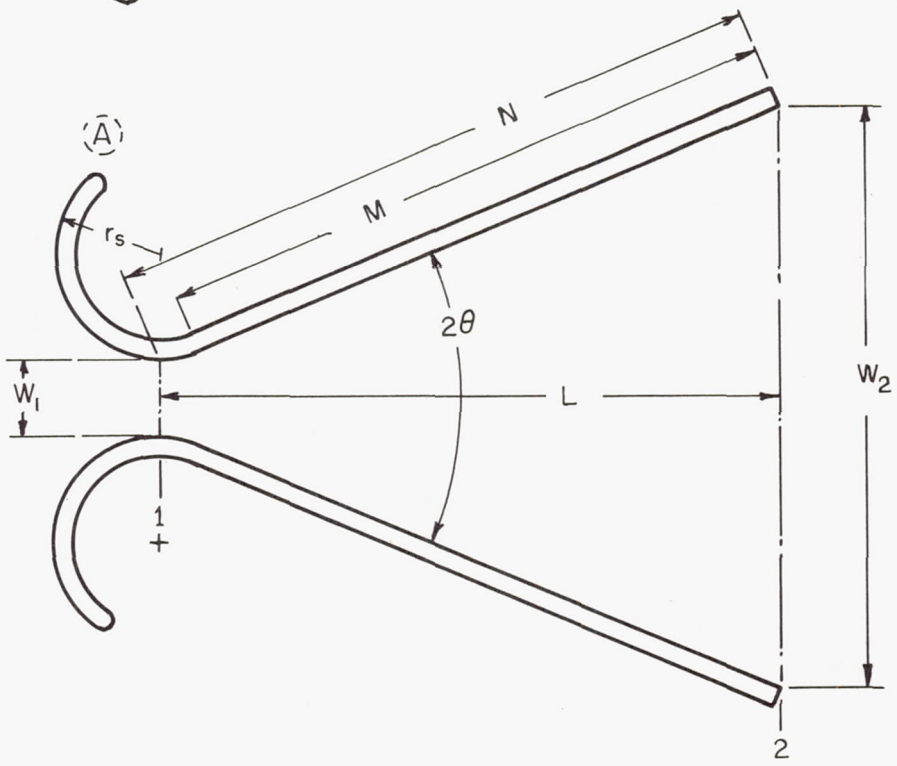

(b) With 2θ set at 45°.

Figure 1.- Geometry of diffusers and entrance sections. W_1 and 2θ are independently variable; L depends on 2θ and W_2, on 2θ and W_1; N depends on 2θ; and M and r_s are fixed.

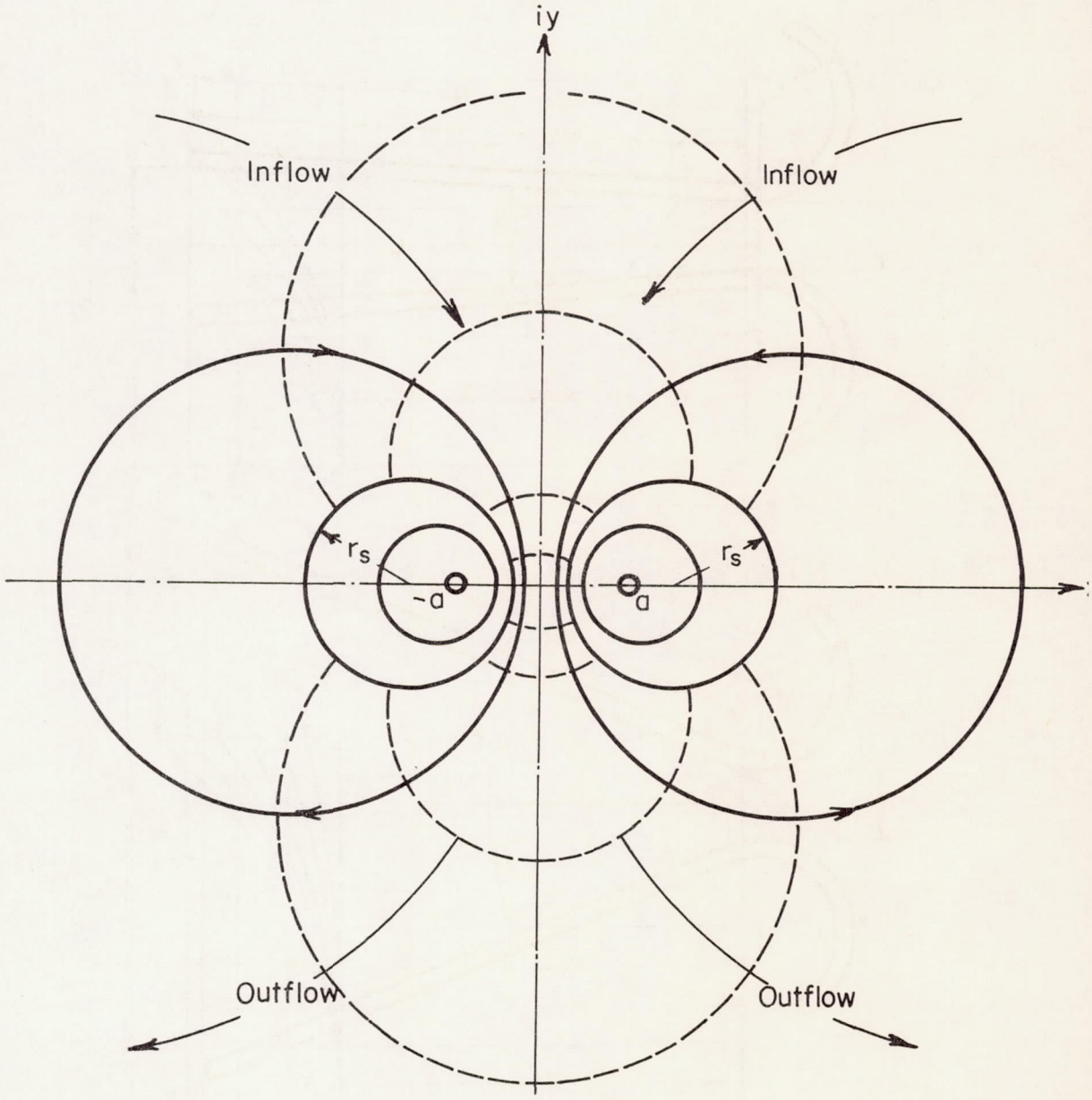

Figure 2.- Vortices of opposite sign at a and -a representing flow between two cylinders. Potential function $X = i\gamma \log_e(z - a) - i\gamma \log_e(z + a)$, where $z = x + iy$ and $X = \phi + i\psi$; streamlines ψ are shown as solid circles; and velocity-potential lines ϕ are shown as dashed arcs of circles.

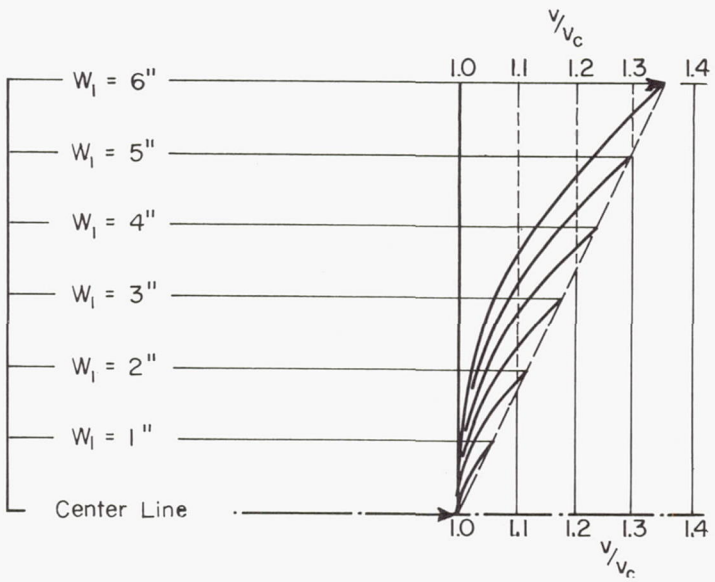

(a) Half throat width $W_1/2$ shown double scale.

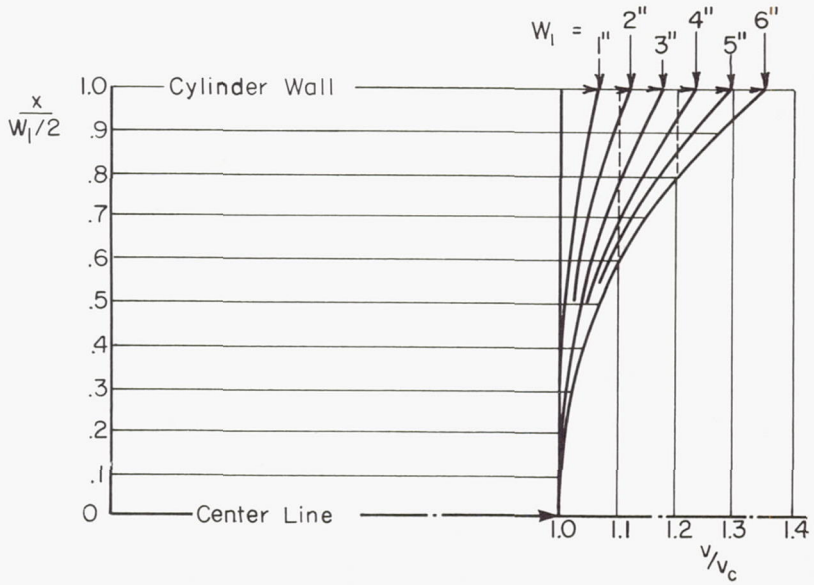

(b) Dimensionless throat width.

Figure 3.- Velocity profiles at throat for two-dimensional flow between cylinders.

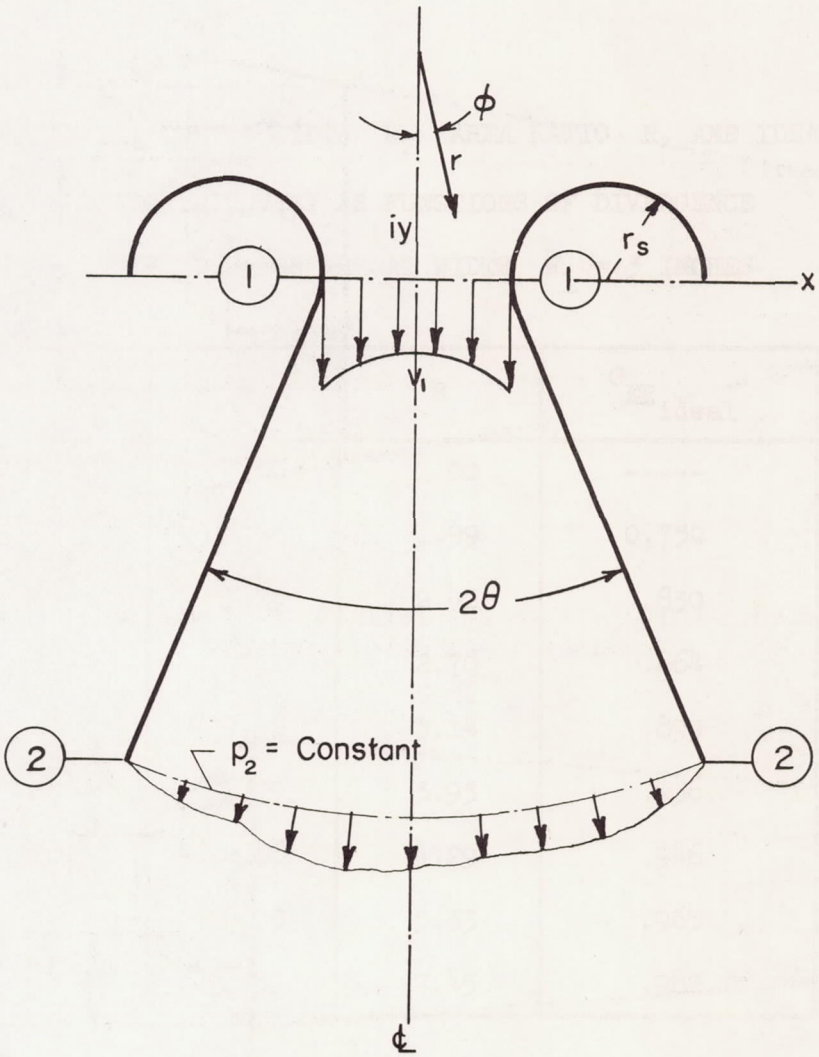

(a) Control volume for energy parameter definition. z axis is perpendicular to paper.

Figure 4.- Control volumes. ①, inlet section; ②, outlet section.

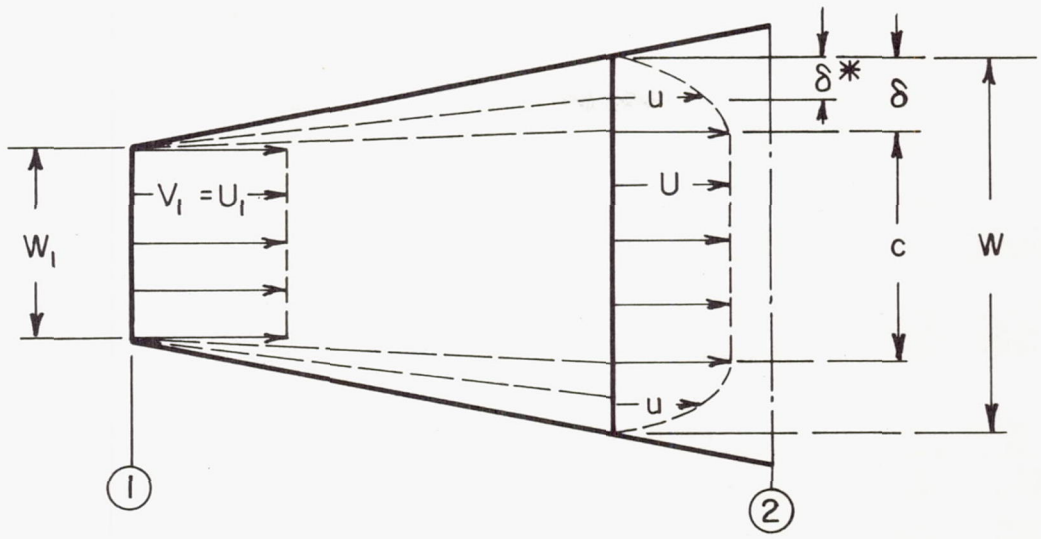

(b) Idealized control volume for definition of variables used in boundary-layer developments.

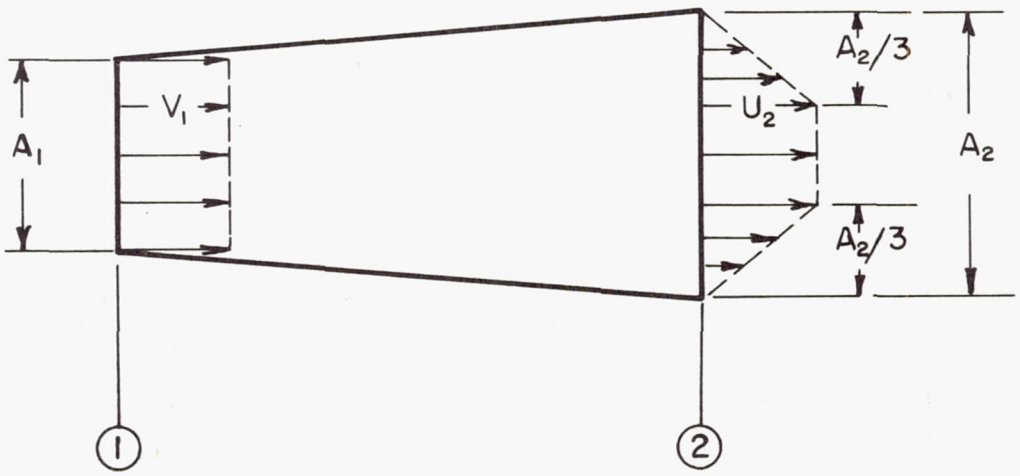

(c) Idealized control volume with artificially conceived flow.

Figure 4.- Concluded.

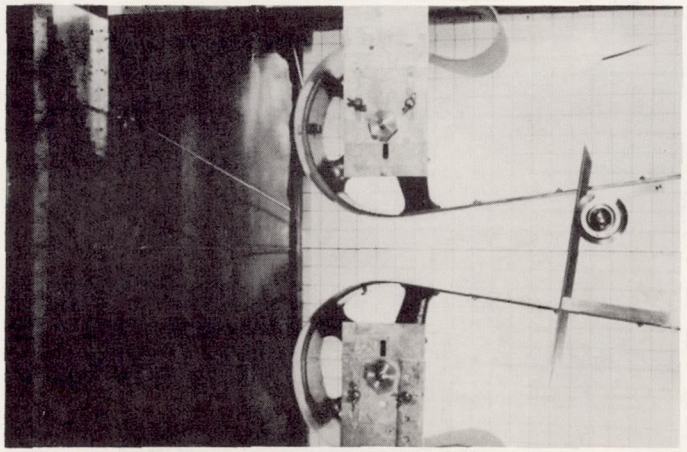

(a) Large diffuser in water table.

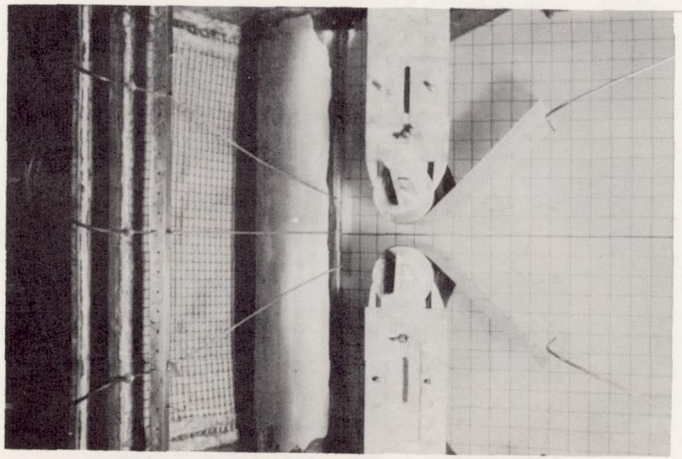

(b) Small diffuser in water table.

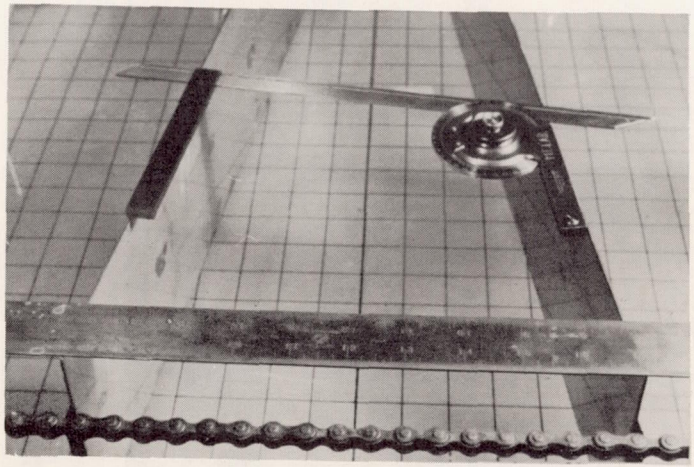

(c) Exit section of large diffuser; protractor and scale in place.

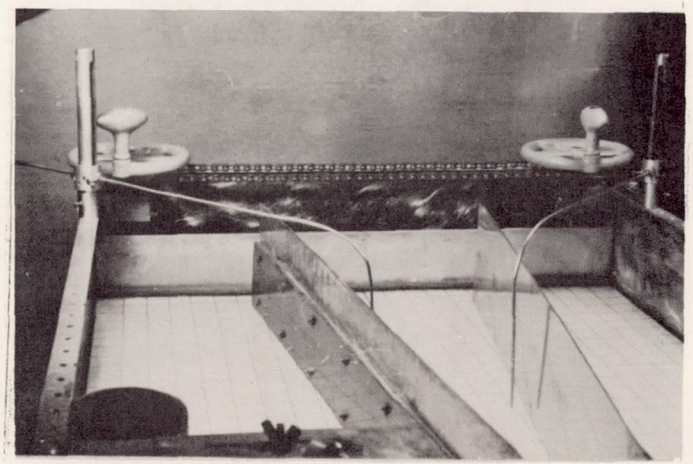

(d) Downstream end of water table.

L-58-1349

Figure 5.- Water table used in tests.

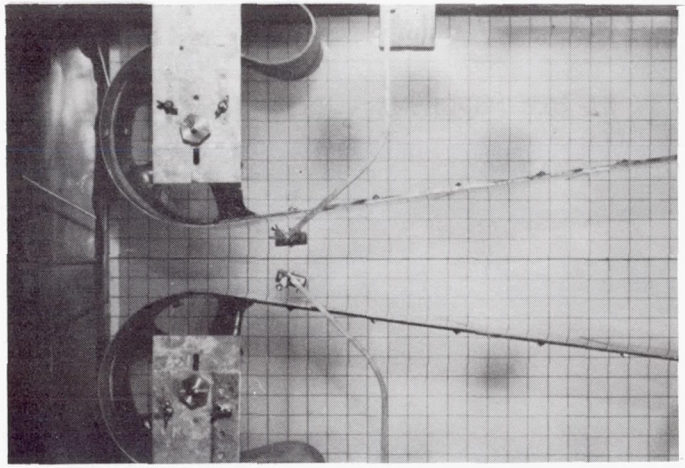

(e) Vane holders in place.

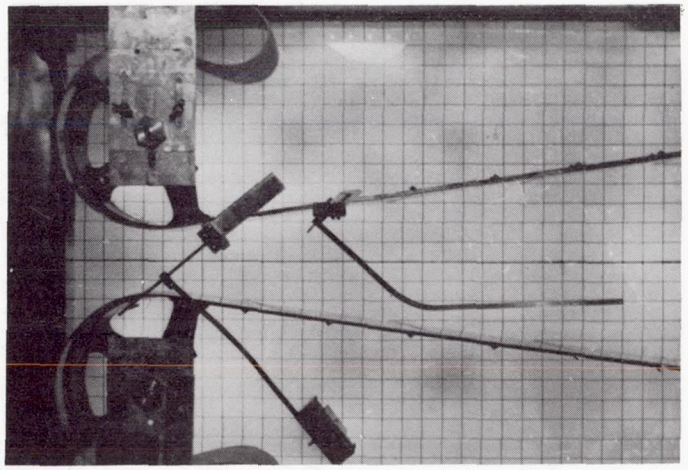

(f) Vane holders removed.

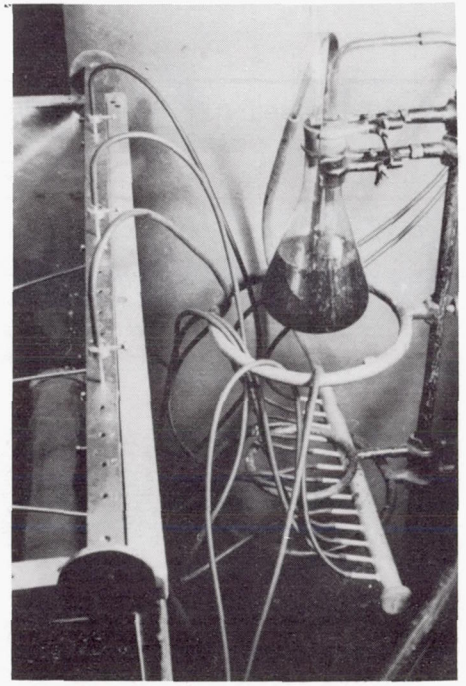

(g) Ink distribution system.

Figure 5.- Concluded.

L-58-1350

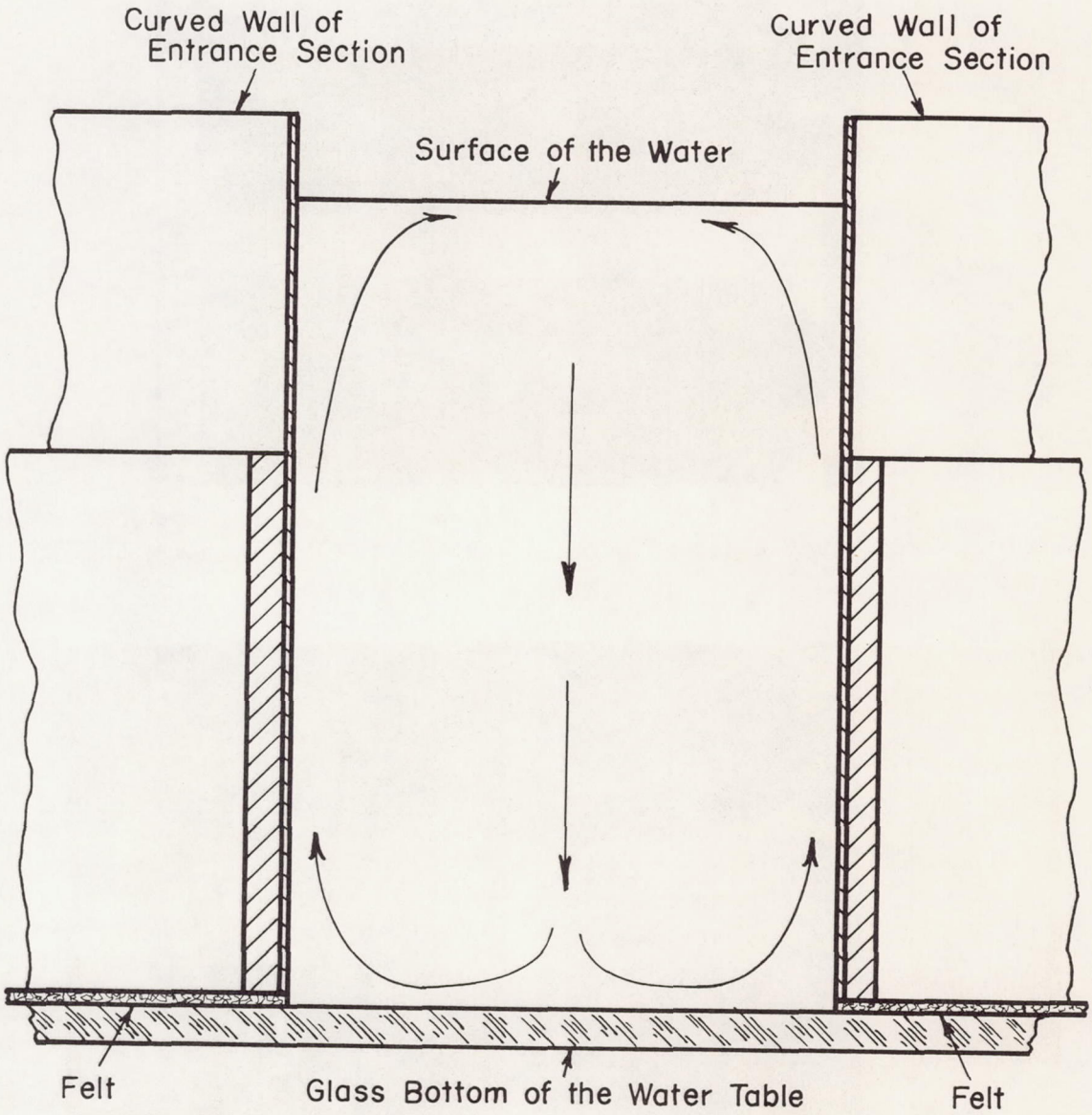

Figure 6.- Secondary flow observed both upstream and downstream of diffuser throat section. Arrows show observed secondary flow directions.

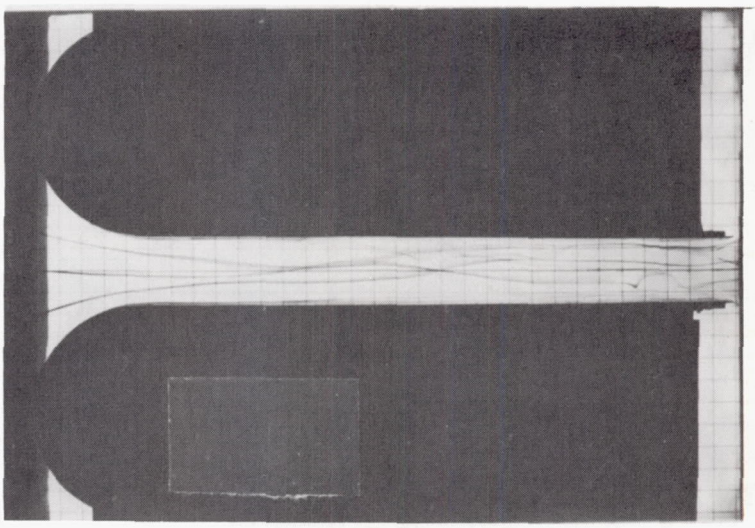

(a) Flow with low-turbulence screens installed. $L/W_1 = 8.12$; $T = 76^\circ$ F.

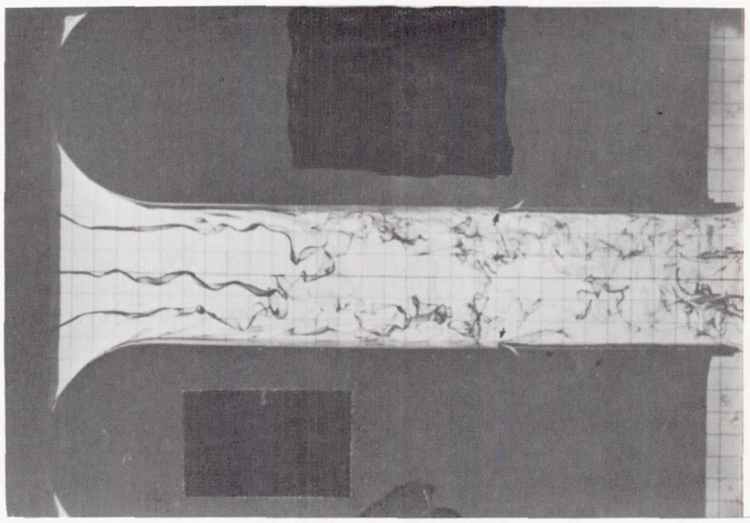

(b) High-turbulence inflow, no screens. $L/W_1 = 4.06$.

Figure 7.- Difference in turbulence at entrance caused by addition of screens. $2\theta = 0^\circ$; $R_W = 6,750$; J = B; H = 4 inches; $(G/2)_{cl} = 4.4$ inches; and Q = 1.5 lb/sec.

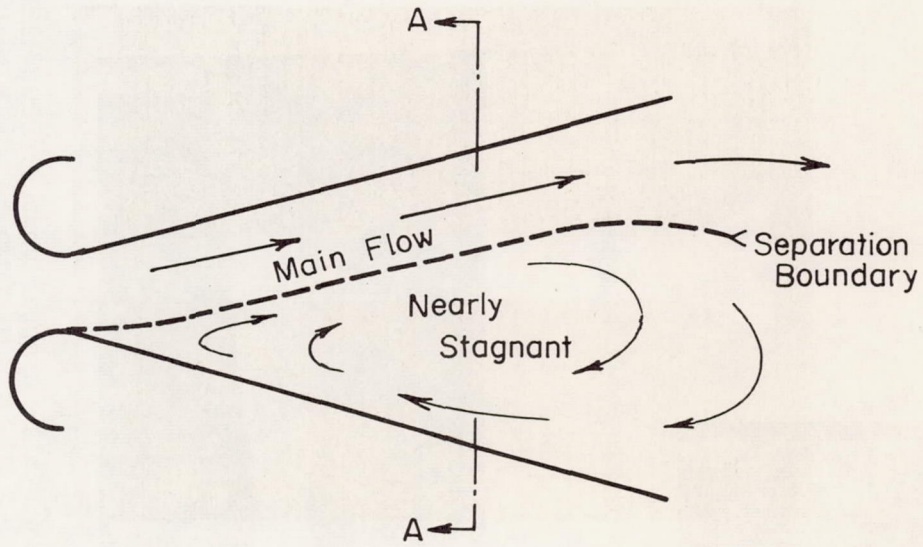

(a) Top view; dashed line shows boundary of separation; arrows show direction of water motion.

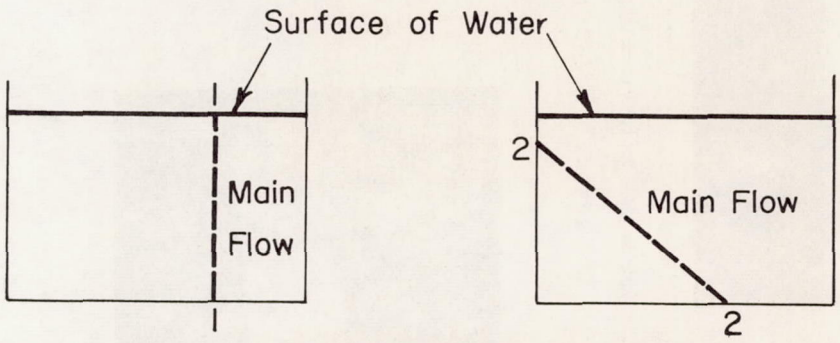

(b) Cross section A-A; separation boundary as seen in two-dimensional separation.

(c) Cross section A-A; separation boundary as seen in three-dimensional separation.

Figure 8.- Flow separation in water-table diffuser.

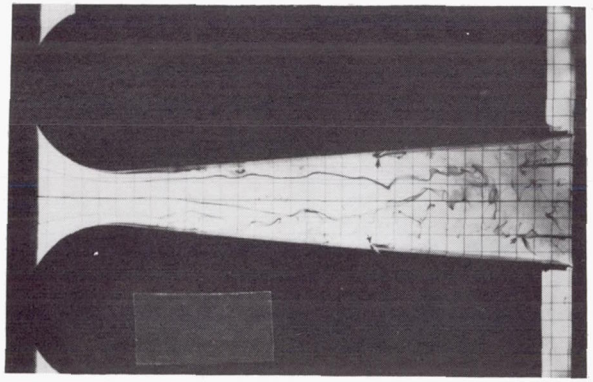

(a) No stalls. $2\theta = 10^{\circ}$; $L/W_1 = 8.2$; J = B; $(G/2)_{cl} = 4.4$ inches; Q = 2.3 lb/sec; T = 70° F.

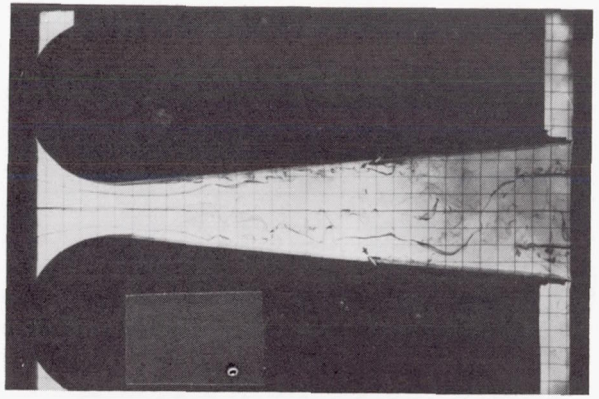

(b) No stalls. $2\theta = 11^{\circ}$; $L/W_1 = 8.21$; J = B; $(G/2)_{cl} = 4.4$ inches; Q = 2.3 lb/sec; T = 70° F.

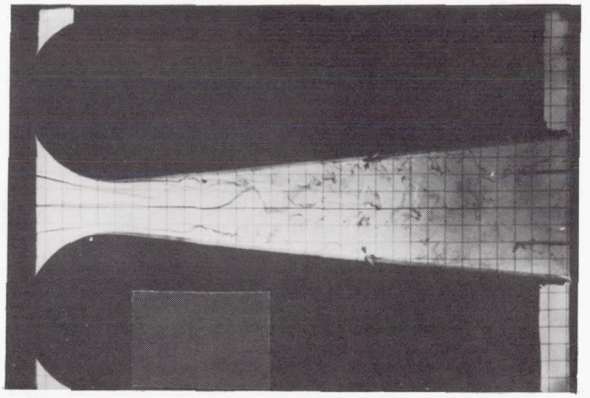

(c) First stall in upper corner. $2\theta = 12^{\circ}$; $L/W_1 = 8.22$; J = B; $(G/2)_{cl} = 4.4$ inches; Q = 2.3 lb/sec; T = 70° F.

Figure 9.- Changes in flow configuration from $2\theta = 10^{\circ}$ where no separation occurred to $2\theta = 17^{\circ}$ where there was stable asymmetric configuration of two-dimensional flow. H = 4 inches.

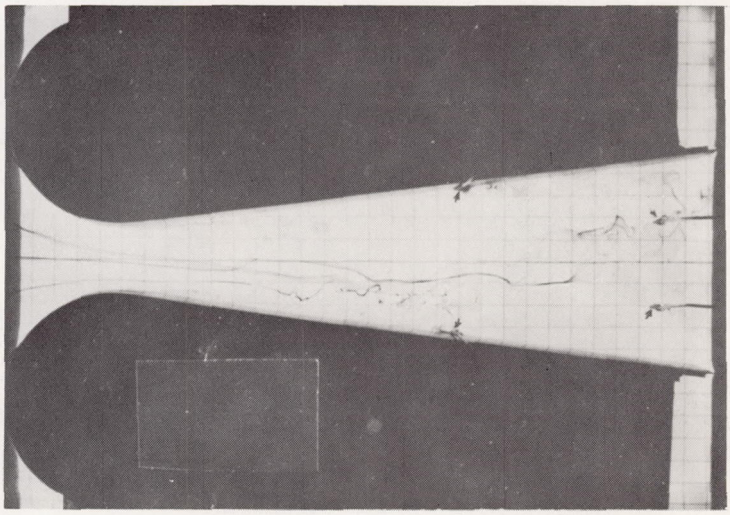

(d) Unsteady three-dimensional separation at lower middle arrow. $2\theta = 15^{\circ}$; $L/W_1 = 8.23$; J = B; $(G/2)_{cl} = 4.5$ inches; Q = 2.5 lb/sec; $T = 79^{\circ}$ F.

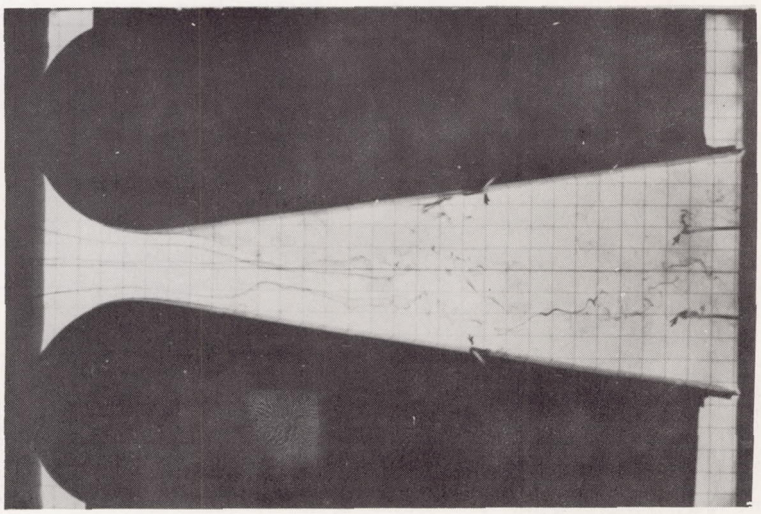

(e) Stable two-dimensional separation. $2\theta = 17^{\circ}$; $L/W_1 = 8.25$; J = A; $(G/2)_{cl} = 4.5$ inches; Q = 2.5 lb/sec; $T = 77^{\circ}$ F.

Figure 9.- Concluded.

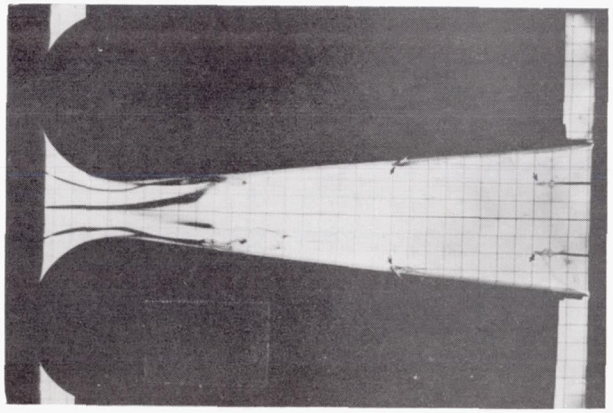

(a) No stalls. $2\theta = 12^{\circ}$; $L/W_1 = 8.22$; J = C.

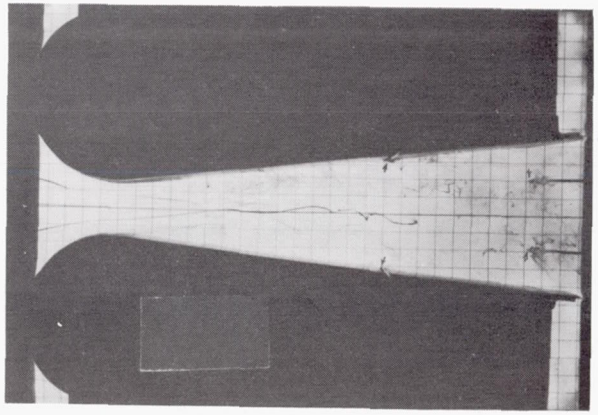

(b) First stall in upper corner. $2\theta = 13^{\circ}$; $L/W_1 = 8.22$; J = B.

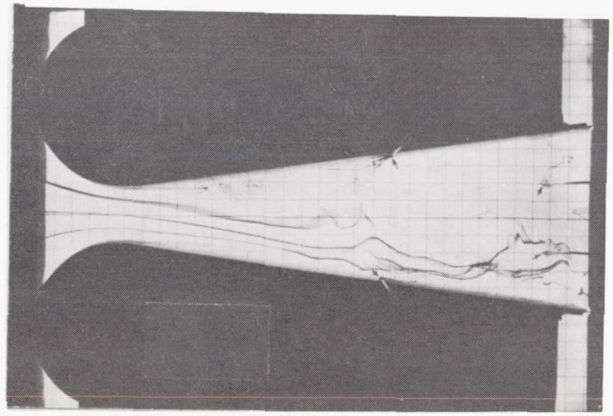

(c) Stable two-dimensional separation. $2\theta = 16^{\circ}$; $L/W_1 = 8.24$; J = A.

Figure 10.- Effect of lowering throat Reynolds number to about 6,000 by diminishing flow rate on angle at which flow becomes two dimensional. H = 4 inches; $(G/2)_{cl} = 4.4$ inches; Q = 1.3 lb/sec; T = 77° or 78° F.

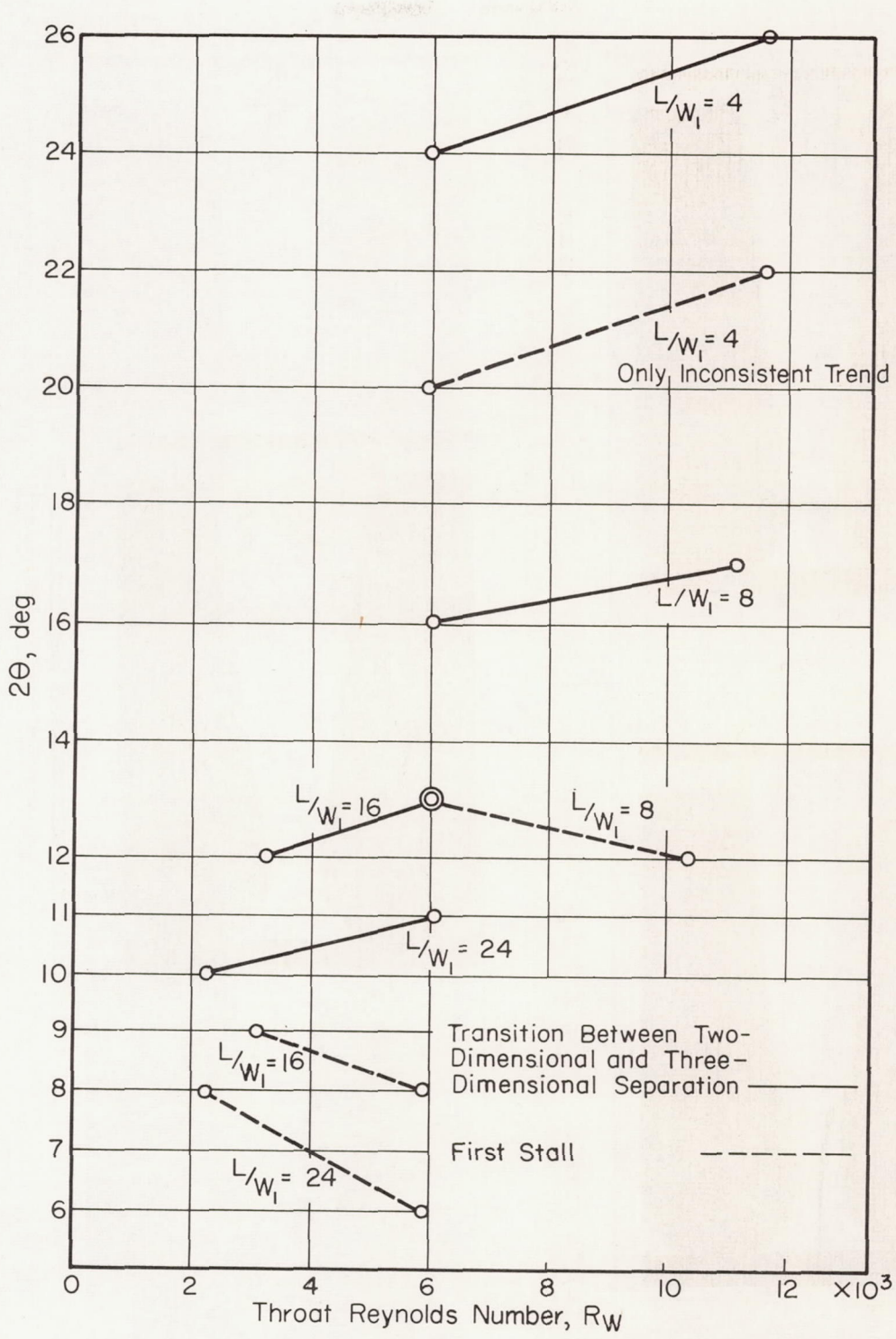

Figure 11.- Effect of Reynolds number on angles of separation.

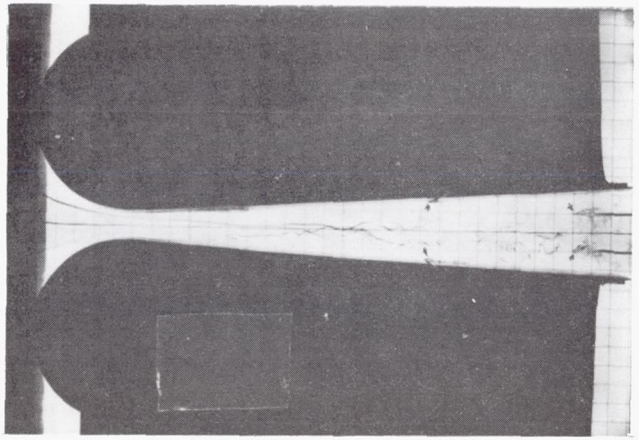

(a) No stalls. $2\theta = 7^{\circ}$; $L/W_1 = 16.37$; J = B.

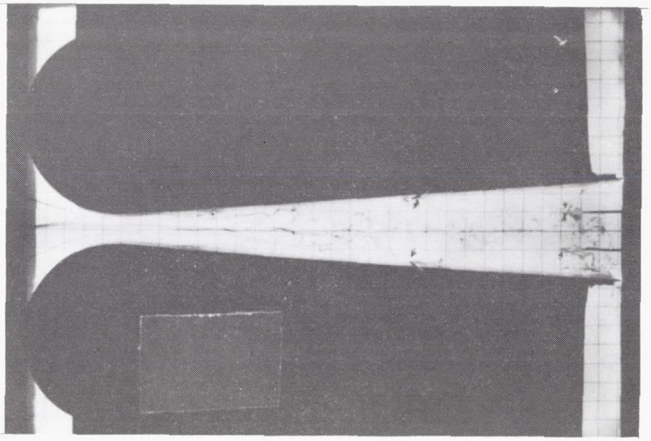

(b) First stall at upper arrow. $2\theta = 8^{\circ}$; $L/W_1 = 16.38$; J = B.

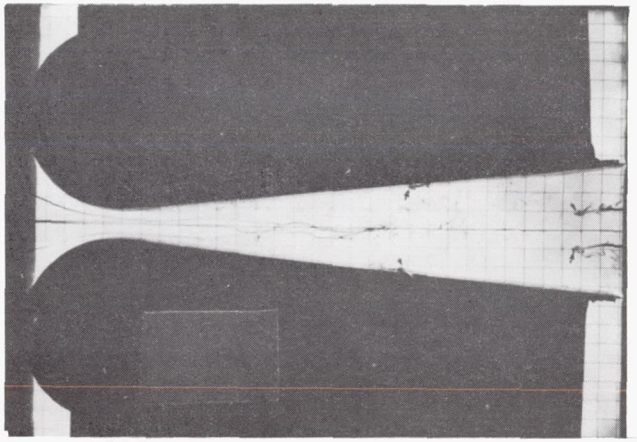

(c) Unsteady three-dimensional separation at lower arrow. $2\theta = 12^{\circ}$; $L/W_1 = 16.43$; J = A.

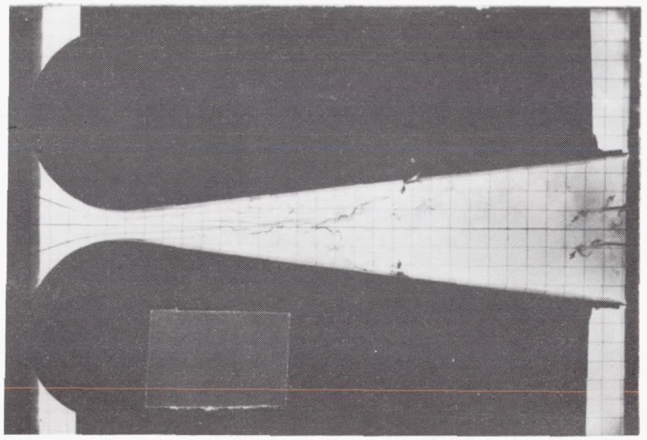

(d) Stable two-dimensional separation. $2\theta = 13^{\circ}$; $L/W_1 = 16.45$; J = A.

Figure 12.- Effect of doubling L/W_1 to about 16 on first separation angle and angle at which flow becomes two dimensional. H = 4 inches; $(G/2)_{cl} = 4.4$ inches; Q = 1.35 lb/sec; T = 75° F.

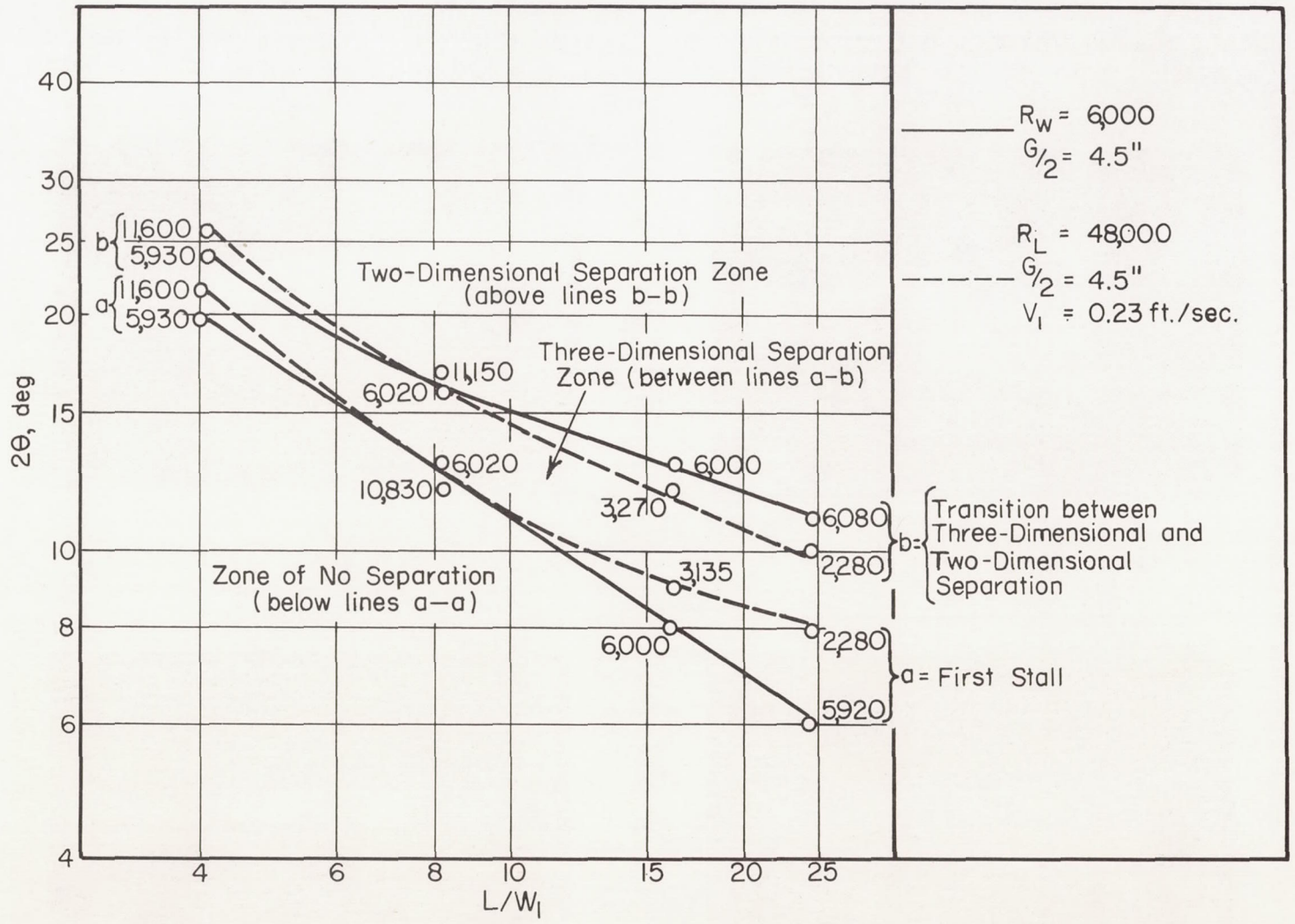

Figure 13.- Separation angles against L/W_1 at low turbulence. Numbers adjacent to data circles give throat Reynolds numbers R_W.

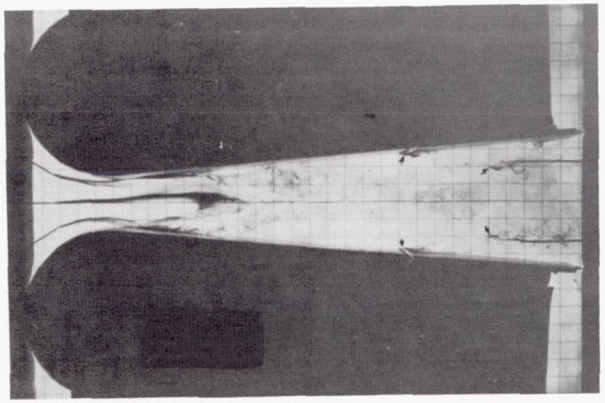

(a) No stalls. $2\theta = 10^{\circ}$; $L/W_1 = 8.20$; $J = C$; $(G/2)_{cl} = 4.4$ inches.

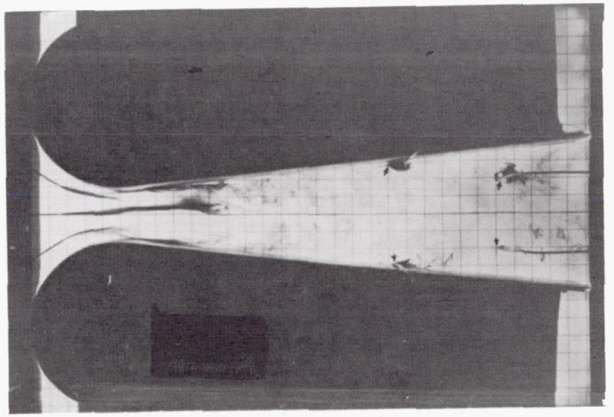

(b) First stall. $2\theta = 12^{\circ}$; $L/W_1 = 8.22$; $J = C$; $(G/2)_{cl} = 4.4$ inches.

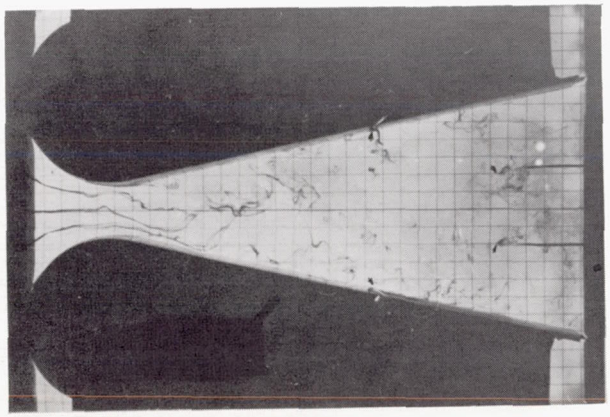

(c) Three-dimensional separation. $2\theta = 25^{\circ}$; $L/W_1 = 8.25$; $J = A$; $(G/2)_{cl} = 4.4$ inches.

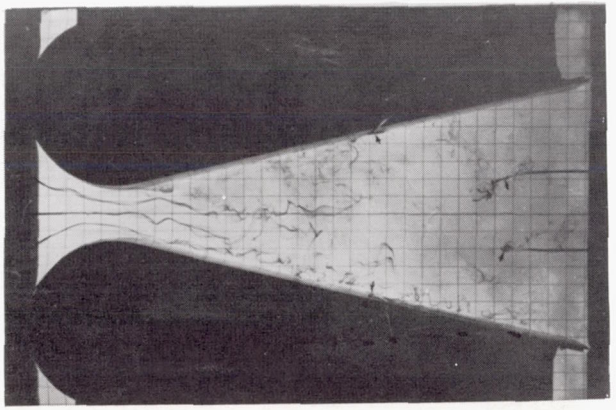

(d) Two-dimensional separation. $2\theta = 26^{\circ}$; $L/W_1 = 8.25$; $J = A$; $(G/2)_{cl} = 4.4$ inches.

Figure 14.- Diffuser flows with high-turbulence entrance conditions. H = 4 inches; Q = 1.5 lb/sec.

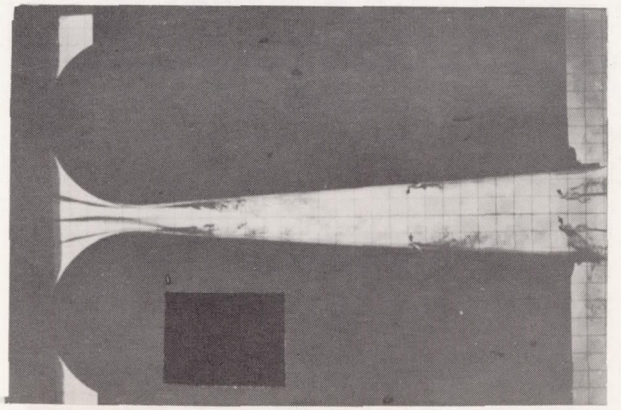

(e) No stalls. $2\theta = 8^{\circ}$; $L/W_1 = 16.41$; $J = C$; $(G/2)_{cl} = 4.35$ inches.

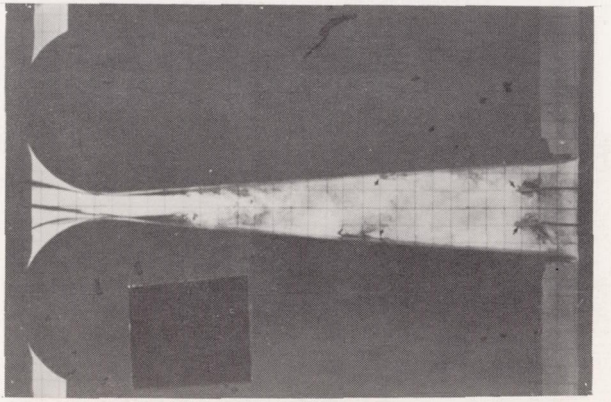

(f) First stall in lower corner. $2\theta = 9^{\circ}$; $L/W_1 = 16.42$; $J = C$; $(G/2)_{cl} = 4.35$ inches.

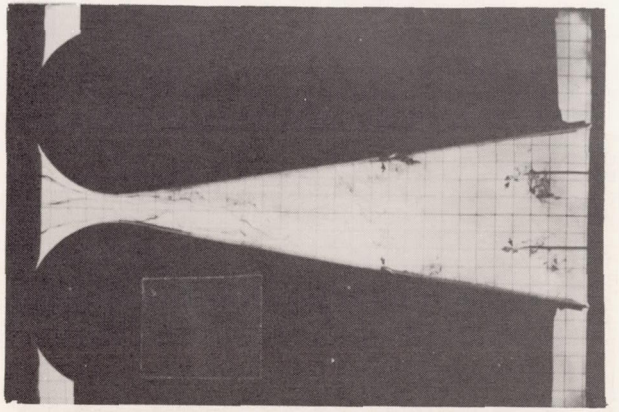

(g) Three-dimensional separation. $2\theta = 19^{\circ}$; $L/W_1 = 16.51$; $J = A$; $(G/2)_{cl} = 4.6$ inches.

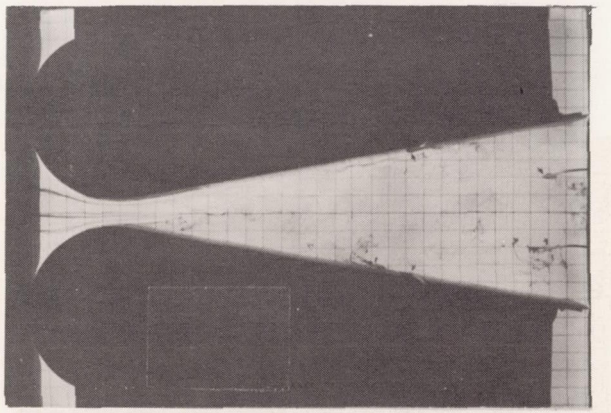

(h) Two-dimensional separation. $2\theta = 20^{\circ}$; $L/W_1 = 16.52$; $J = A$; $(G/2)_{cl} = 4.35$ inches.

Figure 14.- Concluded.

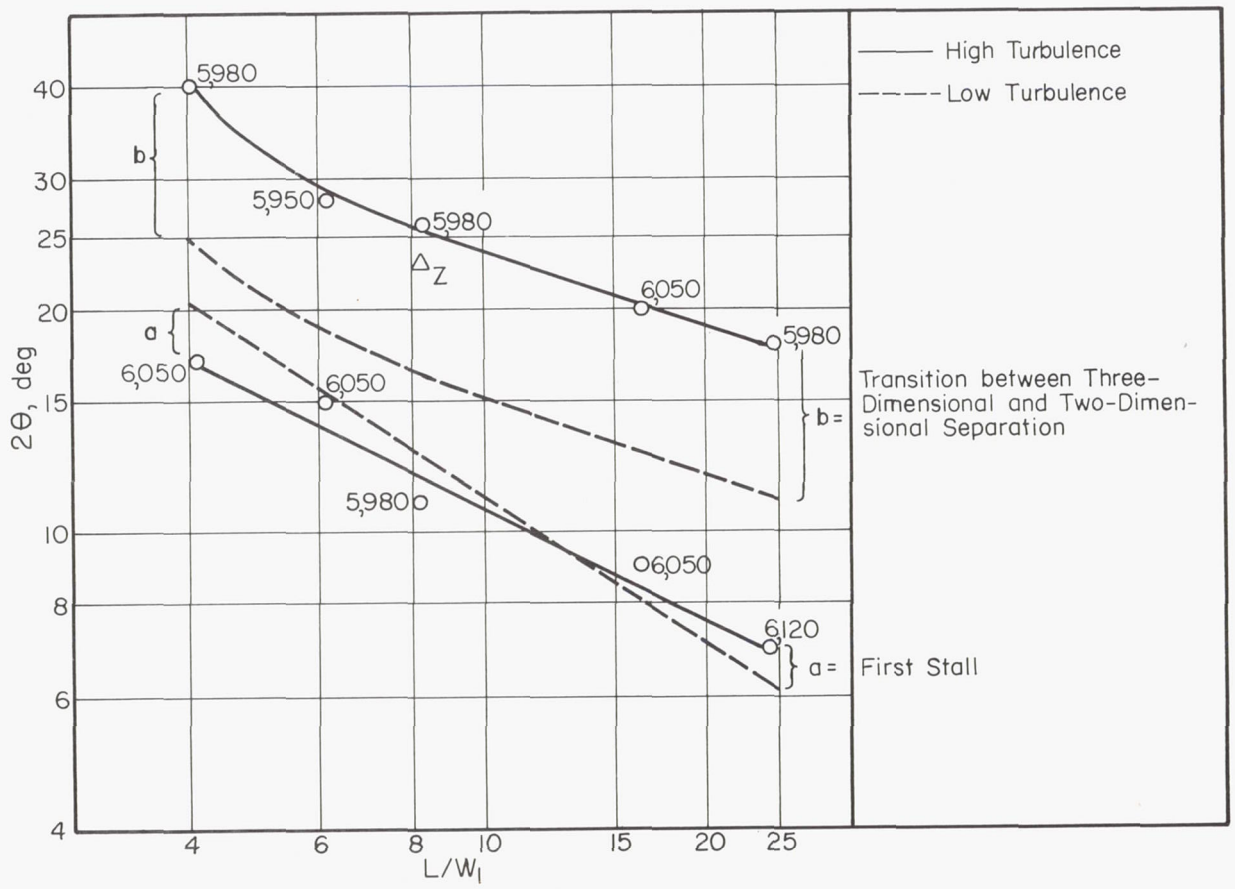

Figure 15.- Separation angles plotted against L/W_1; comparison of high- and low-turbulence results. $R_W \approx 6{,}000$; $G/2 = 4.5$ inches. Numbers adjacent to data circles give throat Reynolds numbers R_W. ΔZ is largest b-b transition angle reached with prethroat rods.

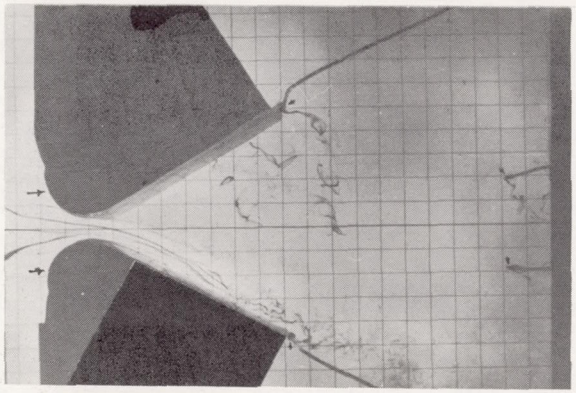

(a) Stable two-dimensional separation. $2\theta = 65^{\circ}$; $N/W_1 = 8.53$.

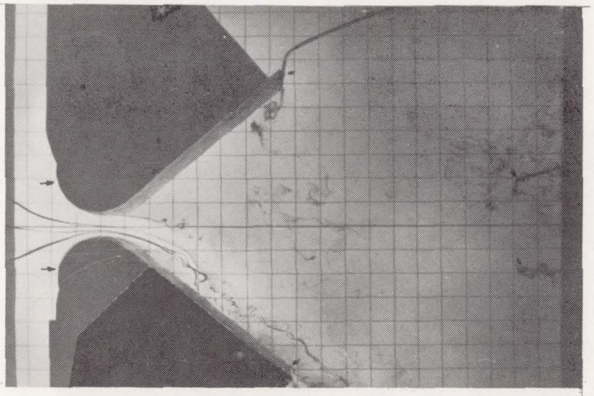

(b) Stable two-dimensional separation. $2\theta = 80^{\circ}$; $N/W_1 = 8.74$.

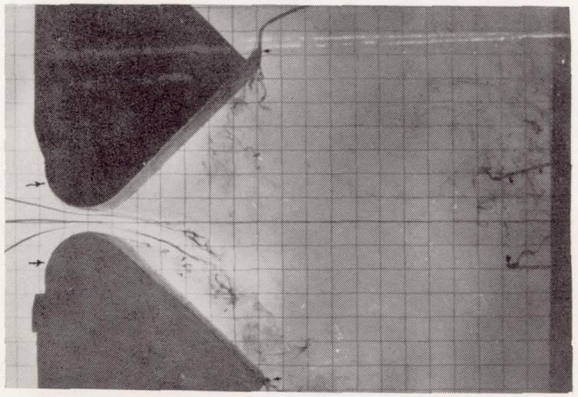

(c) Main flow leaves wall. $2\theta = 90^{\circ}$; $N/W_1 = 8.87$.

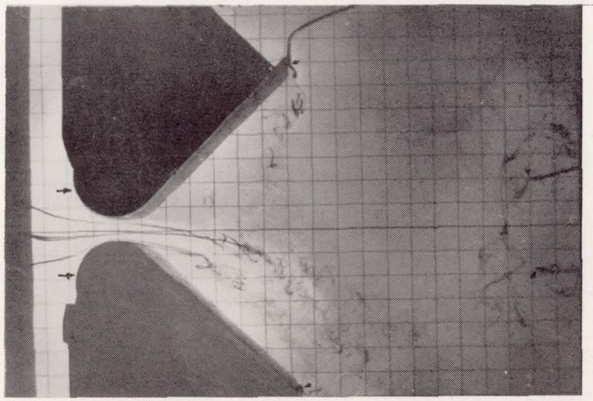

(d) Main flow slowly straightens. $2\theta = 90^{\circ}$; $N/W_1 = 8.87$.

Figure 16.- Behavior of small water-table diffuser at very large angles. J = A; H = 4.0 inches; $(G/2)_{cl}$ = 4.4 inches; Q = 0.75 lb/sec; and T = 82° or 83° F.

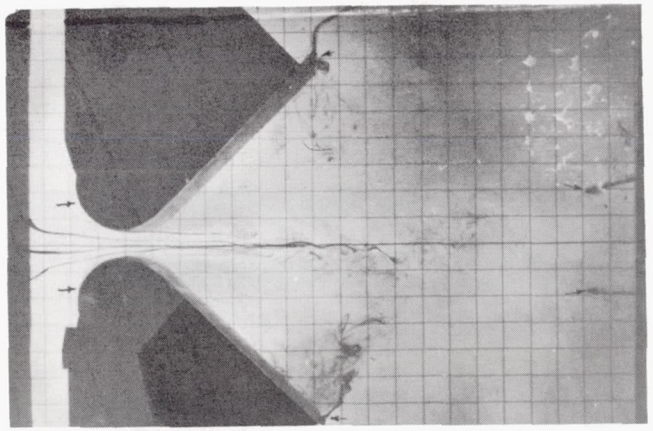

(e) Jet flow. $2\theta = 90^{\circ}$; $N/W_1 = 8.87$.

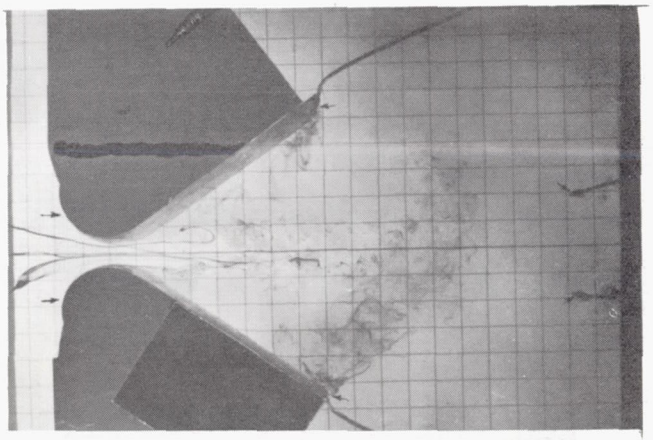

(f) Jet flow. $2\theta = 70^{\circ}$; $N/W_1 = 8.60$.

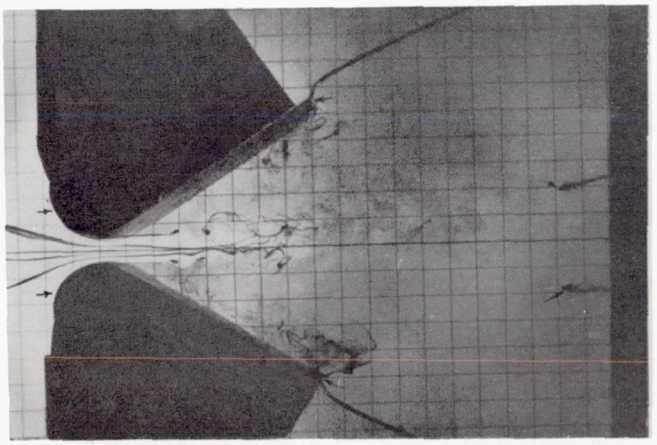

(g) Jet flow. $2\theta = 65^{\circ}$; $N/W_1 = 8.53$.

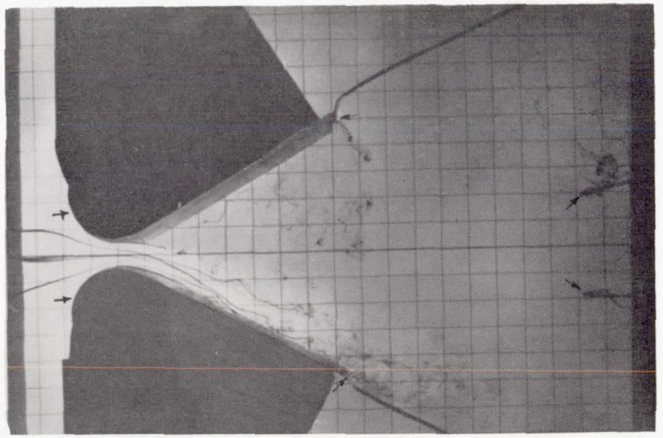

(h) Main flow snaps from jet to wall position. $2\theta = 60^{\circ}$; $N/W_1 = 8.46$.

Figure 16.- Concluded.

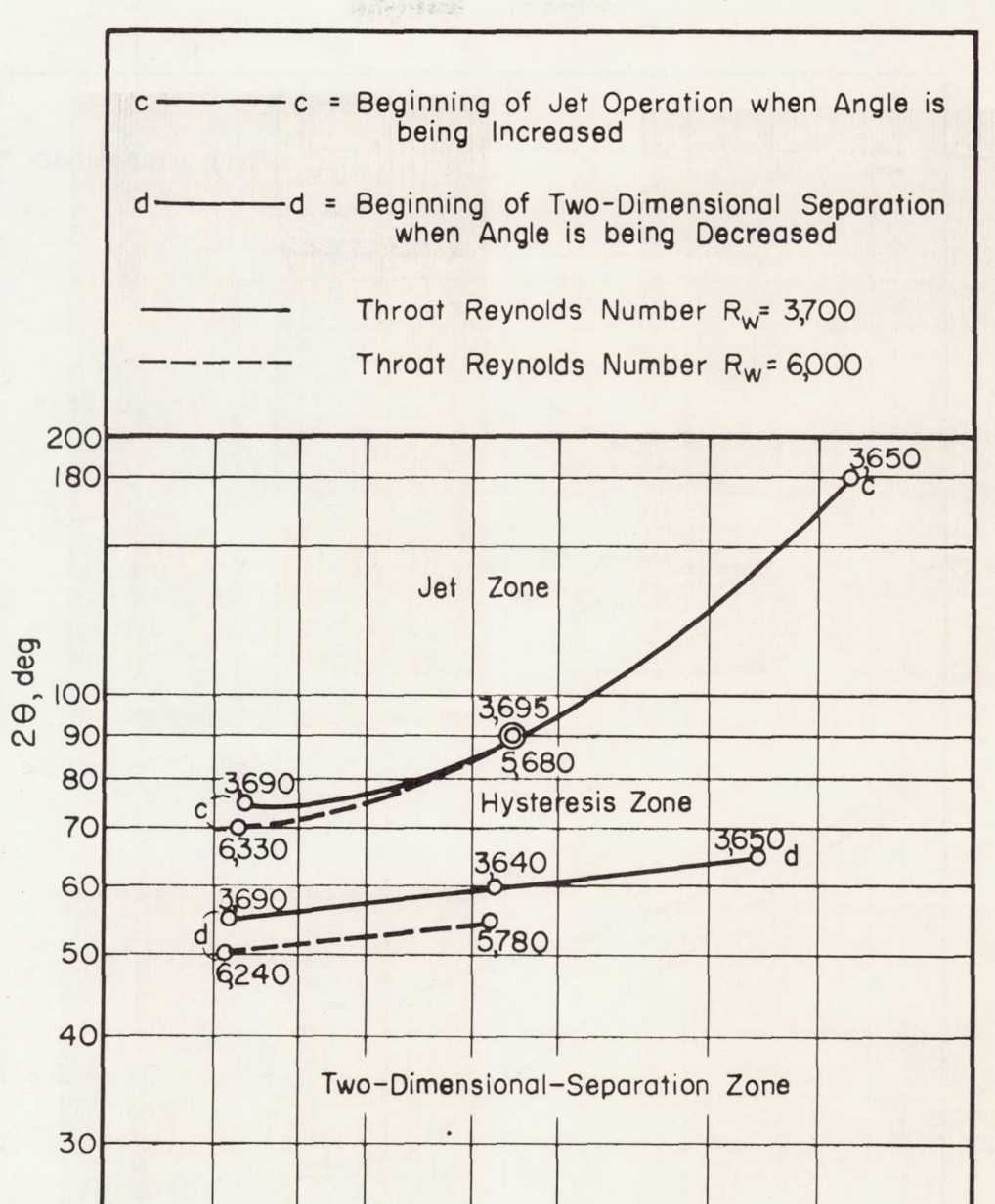

Figure 17.- Results for small water-table diffuser at very large angles. Numbers near data circles give throat Reynolds numbers.

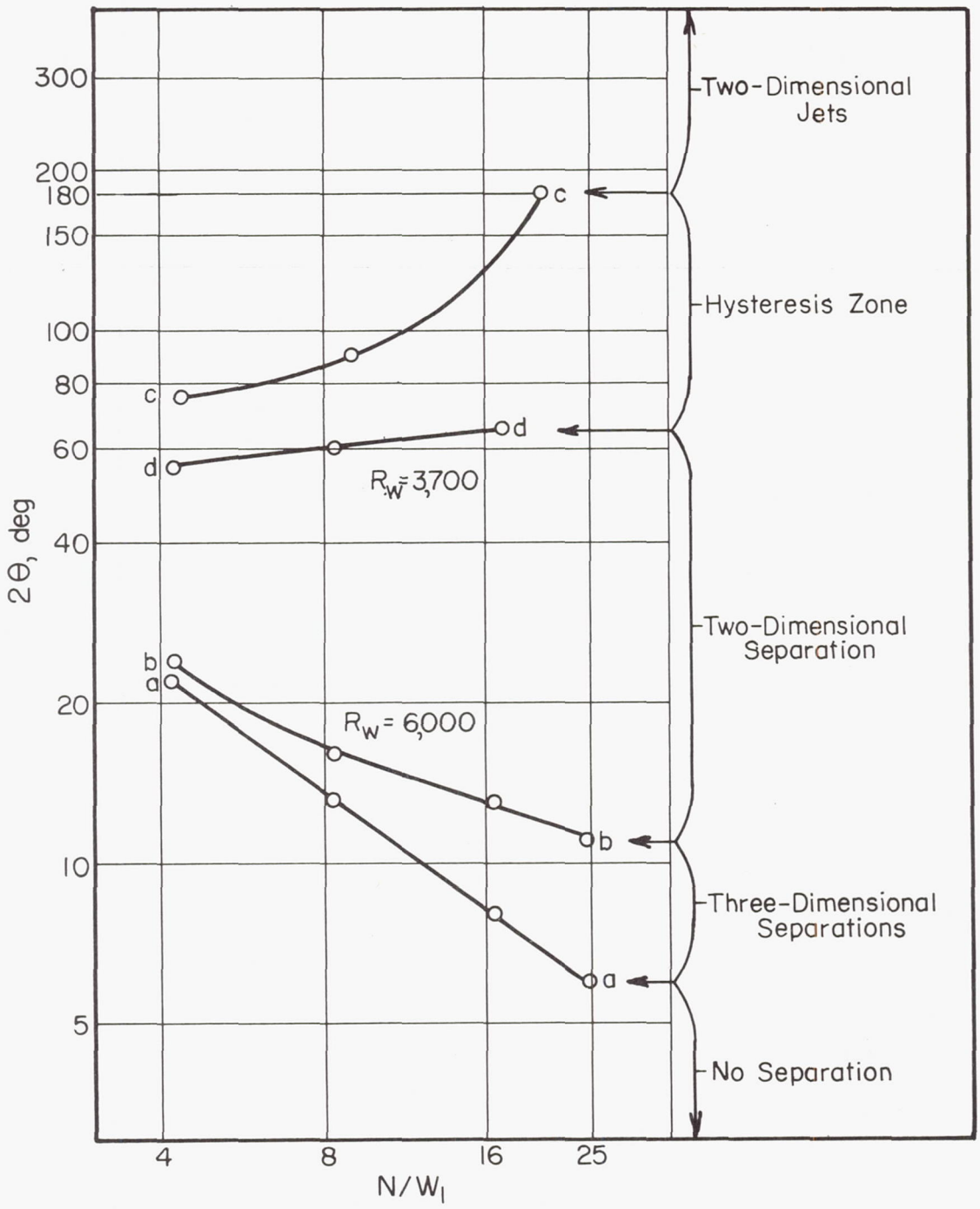

Figure 18.- Superimposed plots of results from large and small water-table diffusers. Top two curves are for small diffusers.

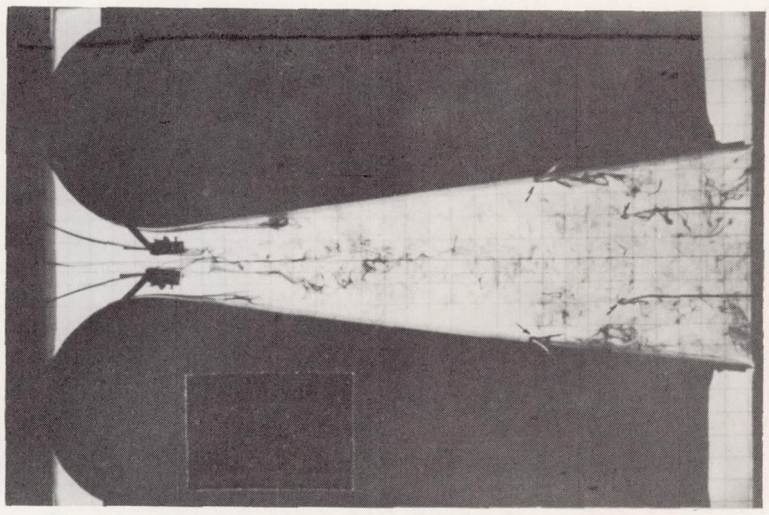

(a) J = A.

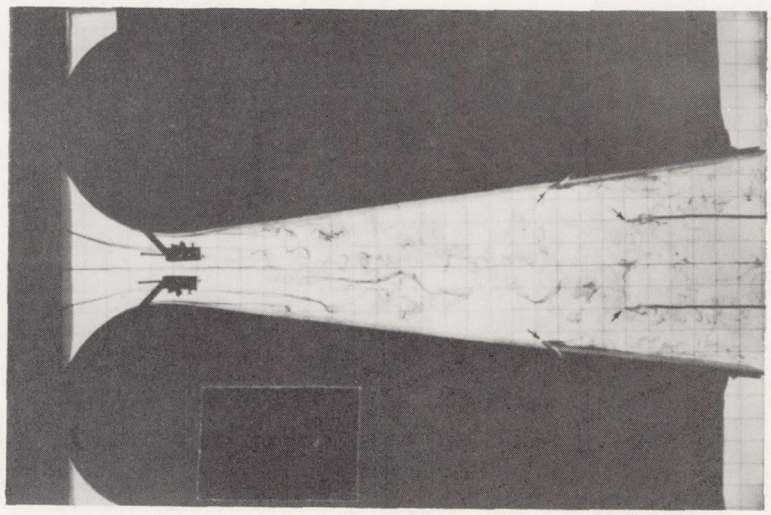

(b) J = B.

Figure 19.- 15° diffuser of figure 9(d) with two 1-inch-long vanes inserted to eliminate separation. $L_V/W_V = 1$; H = 4 inches; $(G/2)_{cl} = 4.35$ inches; Q = 1.35 lb/sec; and T = 72° F.

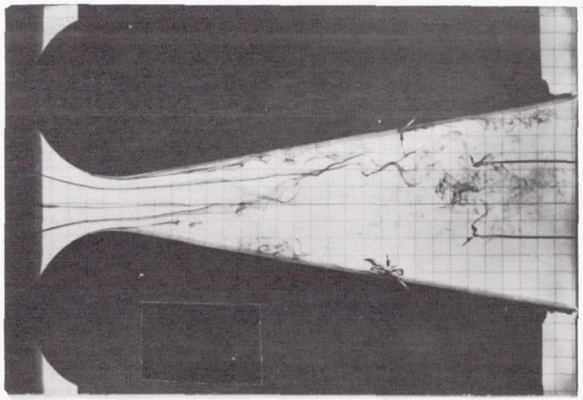

(a) Stable two-dimensional separation with no vanes inserted. $L/W_1 = 8.26$; J = A.

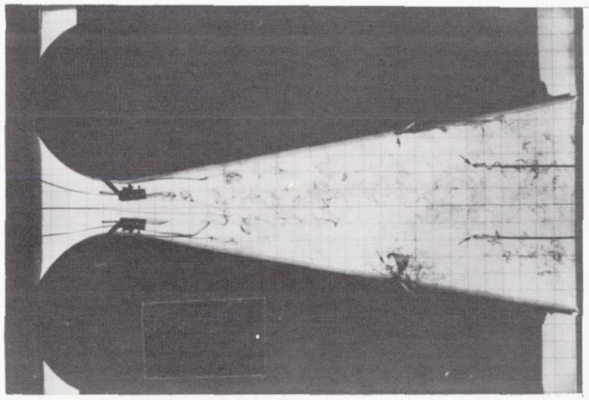

(b) Separation diminished by two 2-inch-long vanes. $L_V/W_V = 2$; J = A.

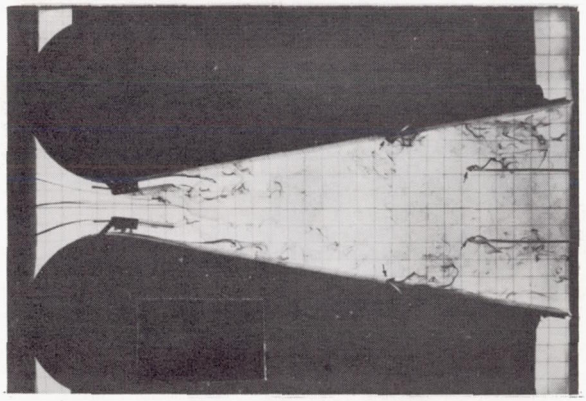

(c) Separation eliminated by two 3-inch-long vanes. $L_V/W_V = 3$; J = A.

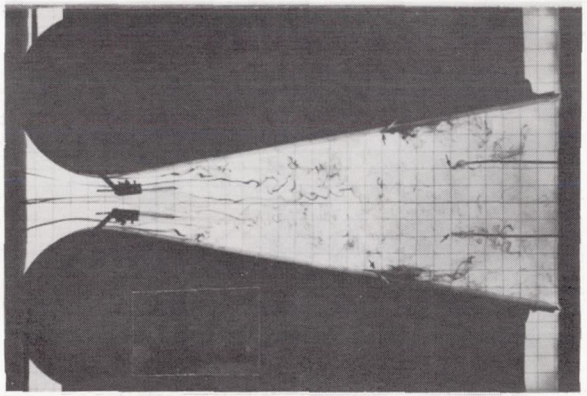

(d) Separation eliminated by two 3-inch-long vanes. $L_V/W_V = 3$; J = B.

Figure 20.- 20° diffuser with two 2- and 3-inch-long vanes inserted to eliminate separation. H = 4 inches; $(G/2)_{cl} = 4.35$ inches; Q = 1.35 lb/sec; and T = 69° F.

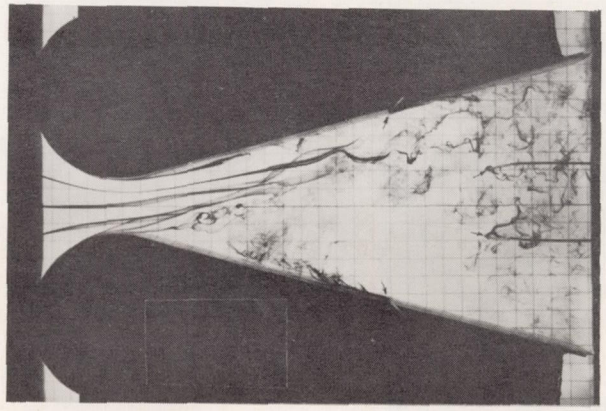

(a) Stable two-dimensional separation with no vanes inserted. $L/W_1 = 8.22$; J = A.

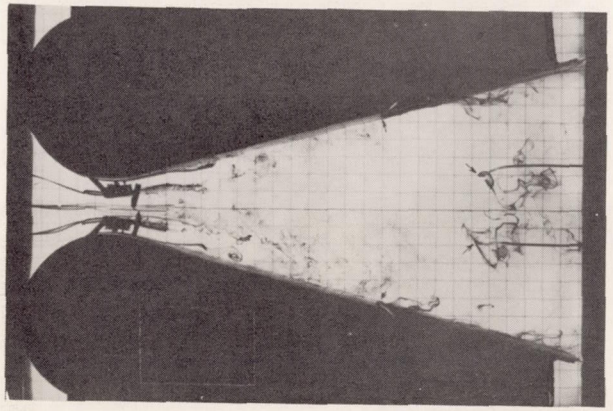

(b) Separation eliminated by three 3-inch-long vanes. $L_V/W_V = 4$; J = A.

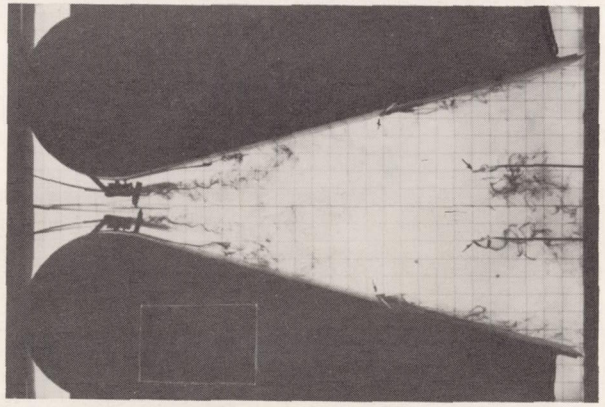

(c) Separation eliminated by three 3-inch-long vanes. $L_V/W_V = 4$; J = B.

Figure 21.- 30° diffuser with three 3-inch-long vanes inserted to eliminate separation. H = 4 inches; $(G/2)_{cl} = 4.35$ inches; Q = 1.35 lb/sec; and T = 69° F.

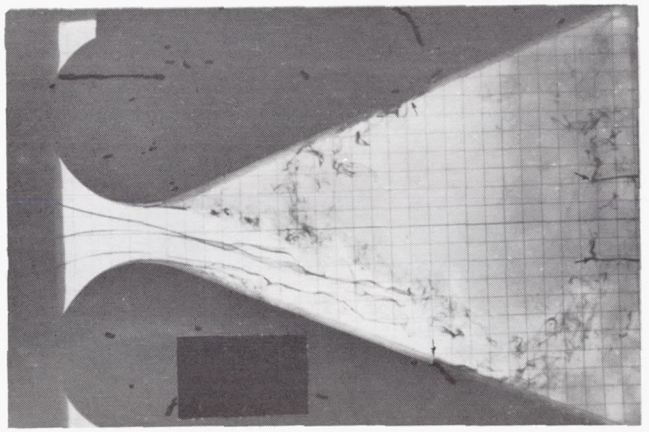

(a) Stable two-dimensional separation with no vanes inserted. $L/W_1 = 8.10$; J = A.

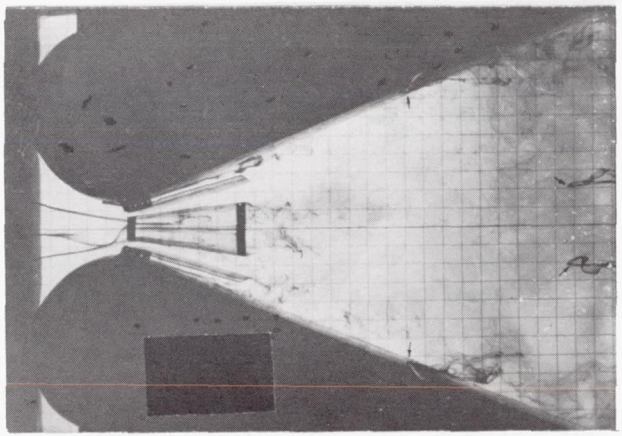

(b) Separation eliminated by five 6-inch-long vanes. $L_V/W_V = 12$; J = A.

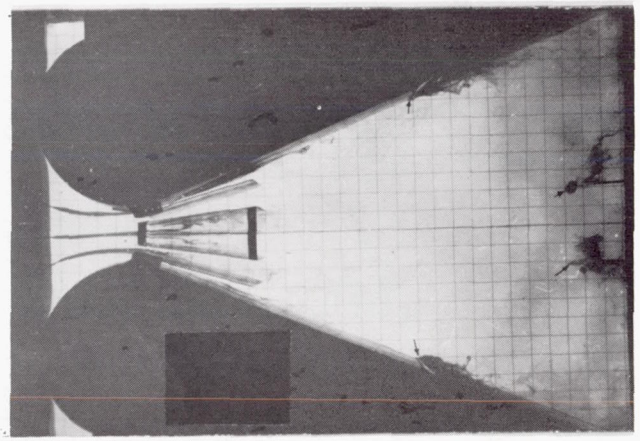

(c) Separation eliminated by five 6-inch-long vanes. $L_V/W_V = 12$; J = B.

Figure 22.- 45° diffuser with five 6-inch-long vanes inserted to eliminate separation. H = 4 inches; $(G/2)_{cl} = 4.35$ inches; Q = 1.35 lb/sec; and T = 72° F.

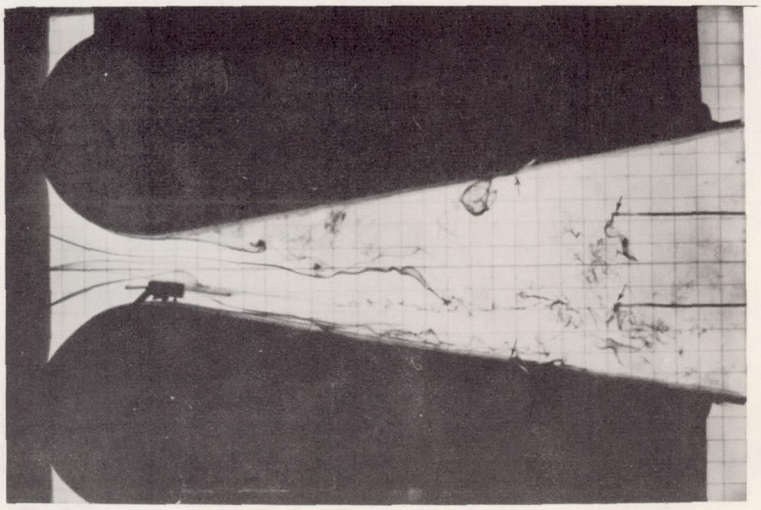

(a) One vane near lower wall had little effect on main flow.

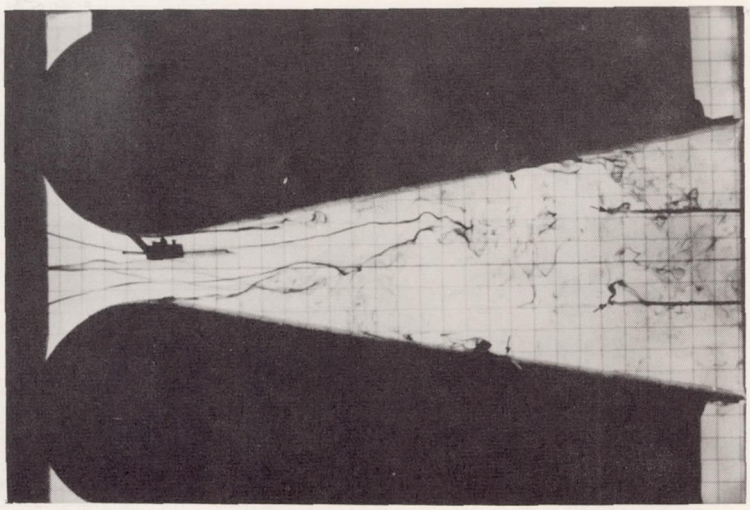

(b) Moving vane to upper wall shifts main flow to upper wall.

Figure 23.- 20° diffuser with 3-inch-long vane inserted to show that beneficial action of vanes is not dependent on drag. J = A; H = 4 inches; $(G/2)_{cl}$ = 4.35 inches; Q = 1.35 lb/sec; and T = 69° F.

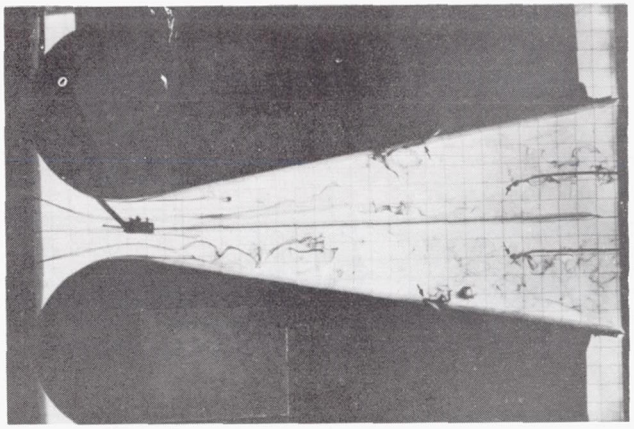

(a) Separation in upper channel with one vane inserted. $L_V/W_V = 15.35$; J = A.

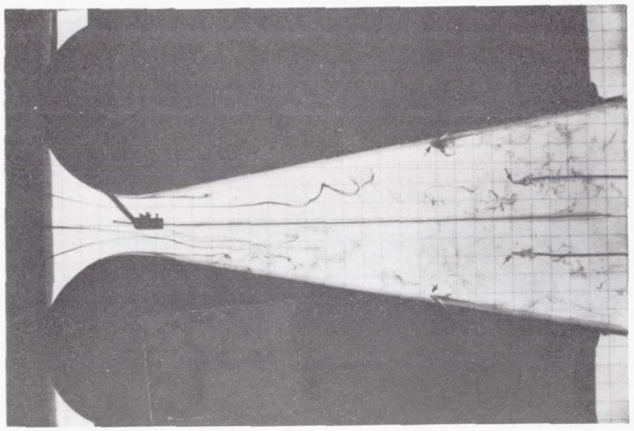

(b) Separation in upper channel with one vane inserted. $L_V/W_V = 15.35$; J = B.

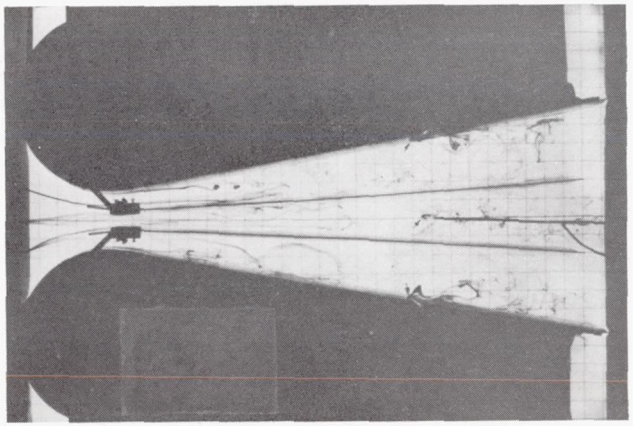

(c) Separation eliminated at height A with two vanes inserted. $L_V/W_V = 23$; J = A.

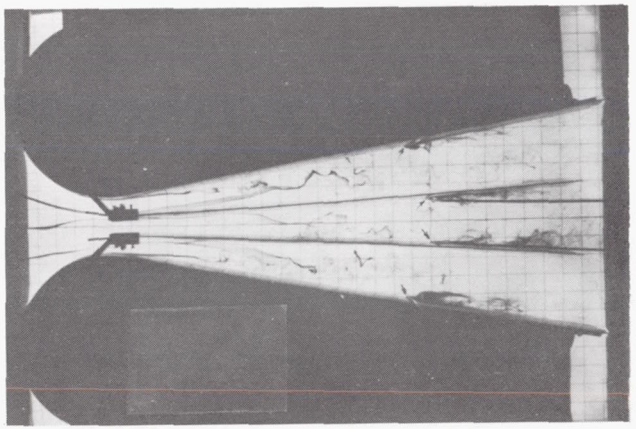

(d) Separation eliminated but corners sluggish with two vanes inserted. $L_V/W_V = 23$; J = B.

Figure 24.- 20° diffuser with 23-inch-long vanes inserted to eliminate separation. H = 4 inches; $(G/2)_{cl} = 4.35$ inches; Q = 1.35 lb/sec; and T = 72° F.

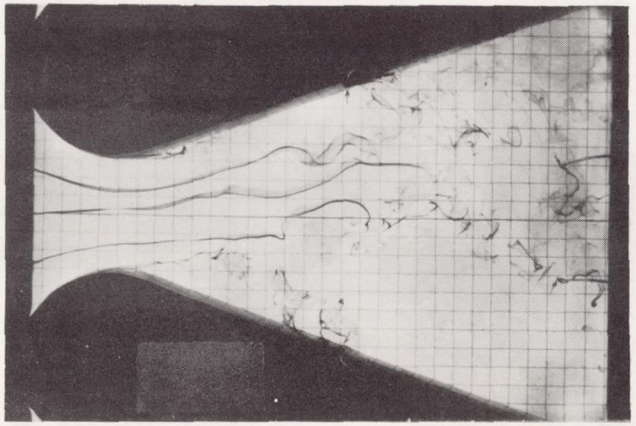

(a) Stable two-dimensional separation with no vane inserted. $L/W_1 = 4.07$; J = A.

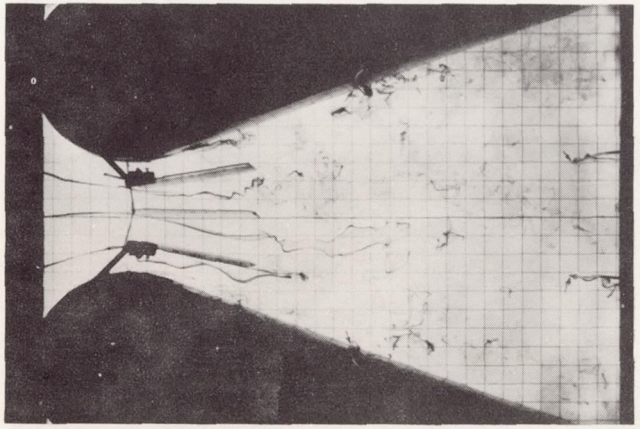

(b) Separation eliminated by three vanes. $L_V/W_V = 4$; J = A.

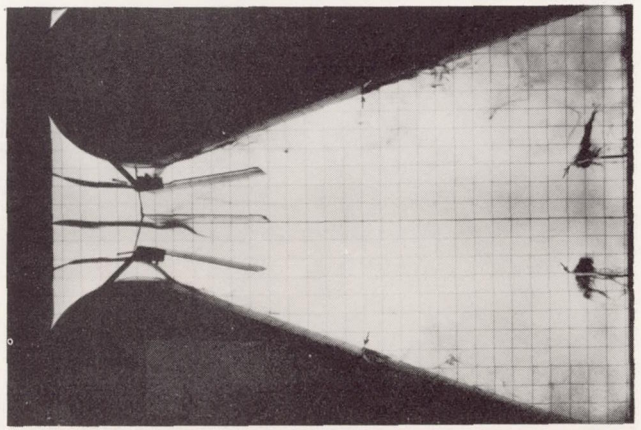

(c) Separation eliminated by three vanes. $L_V/W_V = 4$; J = C.

Figure 25.- 40° diffuser with $L/W_1 \approx 4$ with 6-inch-long vanes inserted to eliminate separation. H = 4 inches; $(G/2)_{cl} = 4.4$ inches; and Q = 1.35 lb/sec.

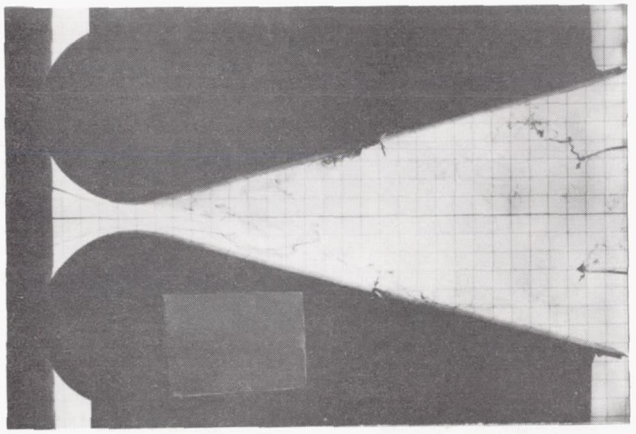

(a) Stable two-dimensional separation with no vanes inserted. J = A.

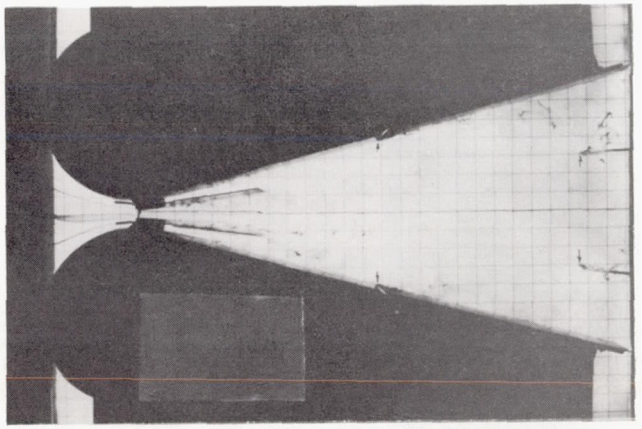

(b) Separation eliminated at height A with three vanes inserted. $L_V/W_V = 16$; J = A.

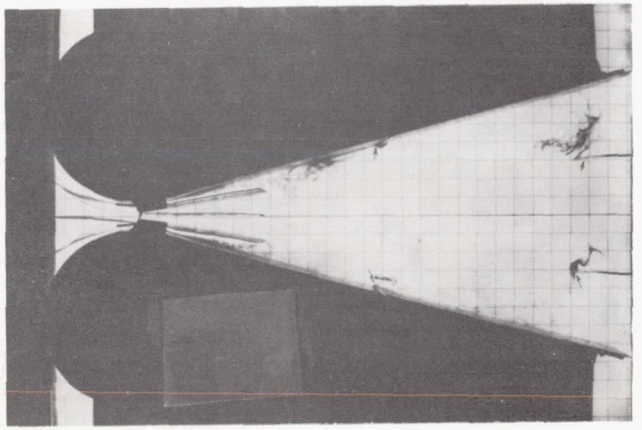

(c) Three vanes fail to unseparate corners. $L_V/W_V = 16$; J = C.

Figure 26.- 30° diffuser with $L/W_1 = 16.44$ with 6-inch-long vanes inserted to eliminate separation. H = 4 inches; $(G/2)_{cl} = 4.4$ inches; Q = 1.35 lb/sec; and T = 77° F.

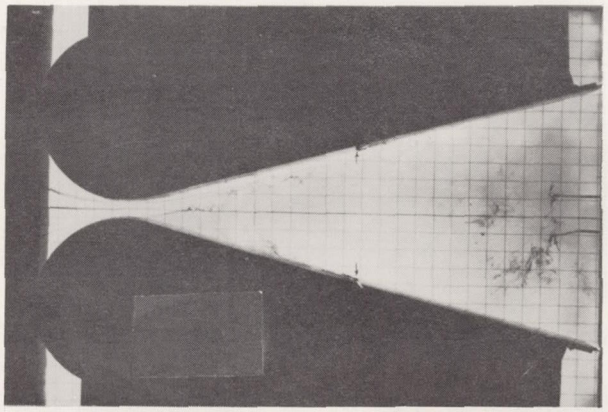

(a) Stable two-dimensional separation with no vanes inserted. J = A.

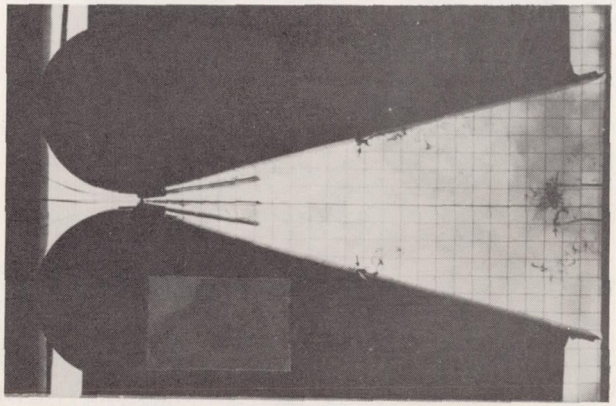

(b) Flow very sluggish, some jets stalled, with three vanes inserted. $L_V/W_V = 24$; J = A.

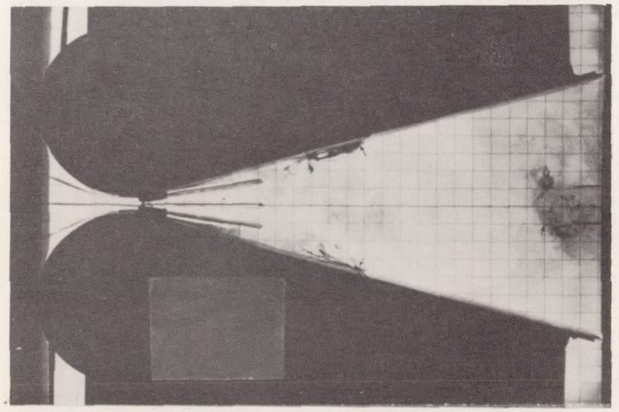

(c) Three vanes leave bad corner separations. $L_V/W_V = 24$; J = C.

Figure 27.- 30° diffuser with $L/W_1 = 24.66$ with 6-inch-long vanes inserted to eliminate separation. H = 4 inches; $(G/2)_{cl} = 4.35$ inches; Q = 1.35 lb/sec; and T = 78° F.

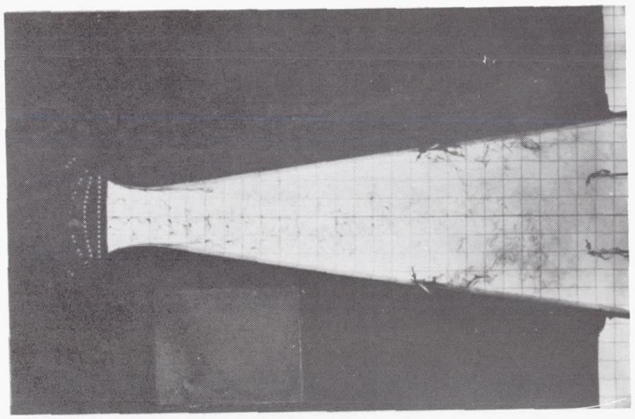

(a) 17° diffuser; 7 vertical 1/8-inch rods.

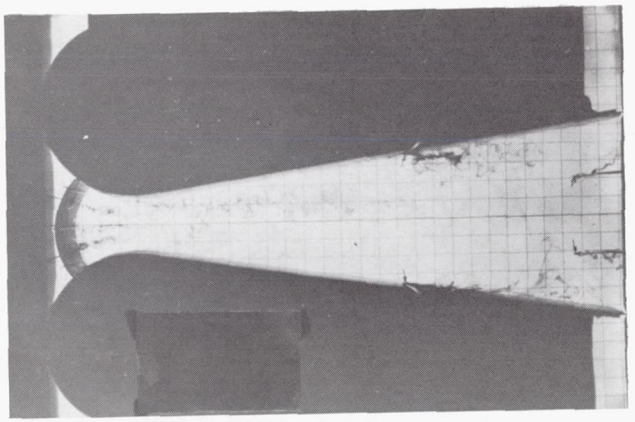

(b) 17° diffuser; 23 horizontal 1/8-inch rods.

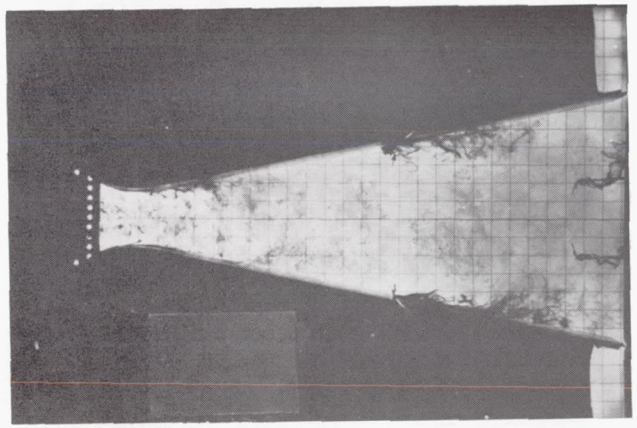

(c) 23° diffuser; 9 vertical 1/4-inch rods.

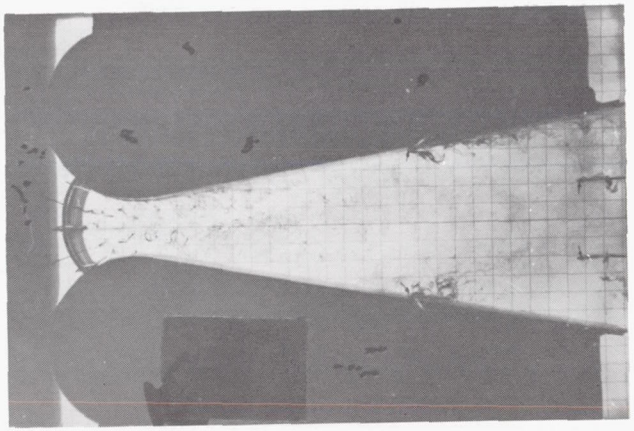

(d) 20° diffuser; 7 horizontal 1/4-inch rods.

Figure 28.- Flow patterns obtained with rods inserted upstream of throat. J = 3 inches; H = 4 inches; $(G/2)_{cl}$ = 4.35 inches; Q = 1.35 lb/sec; and T = 71° to 74° F.

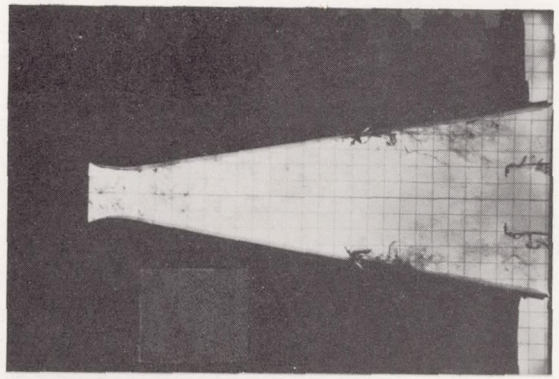

(e) 19° diffuser; 5 vertical 1/2-inch rods.

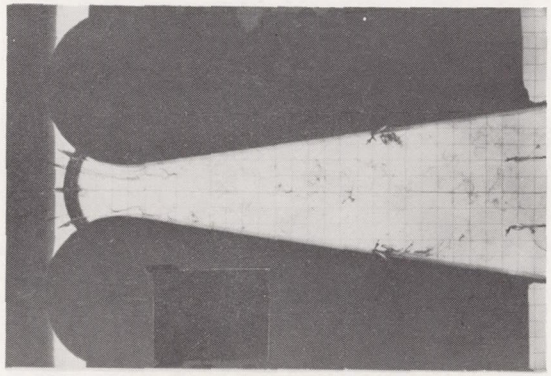

(f) 17° diffuser; 2 horizontal 1/2-inch rods.

Figure 28.- Concluded.

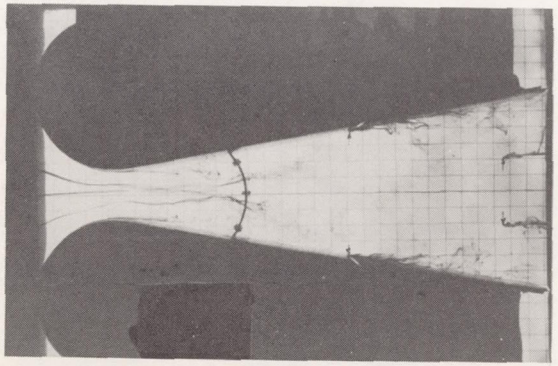

(a) 20° diffuser; 15 horizontal 1/8-inch rods.

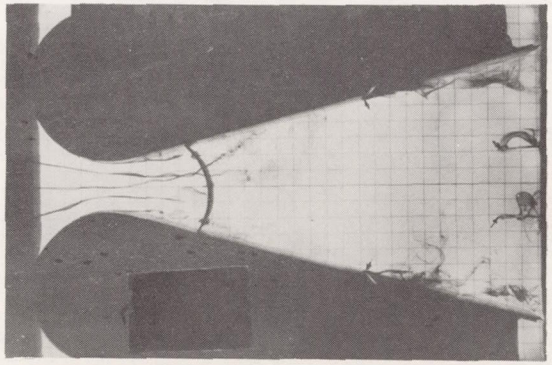

(b) 30° diffuser; 23 horizontal 1/8-inch rods.

Figure 29.- Flow patterns obtained with rods inserted downstream of throat. J = 3 inches; H = 4 inches; $(G/2)_{cl}$ = 4.35 inches; Q = 1.35 lb/sec; and T = 71° to 74° F.

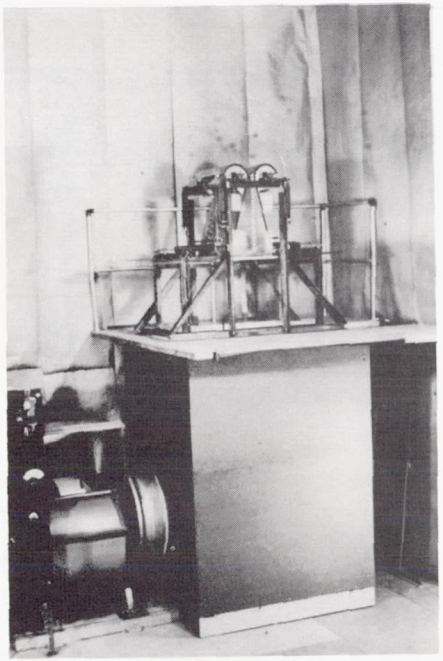

(a) Air-diffuser apparatus.

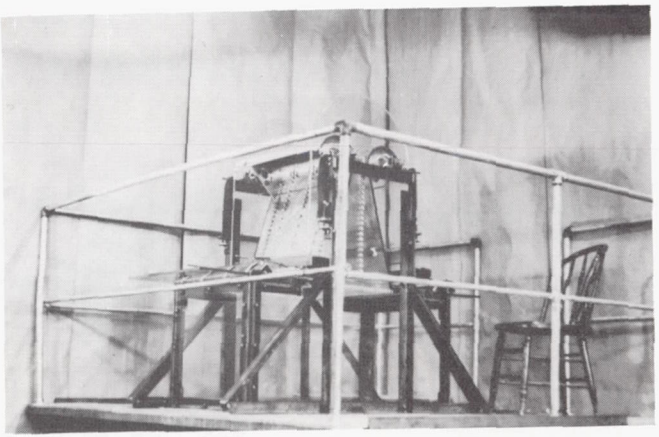

(b) Guard rail in place.

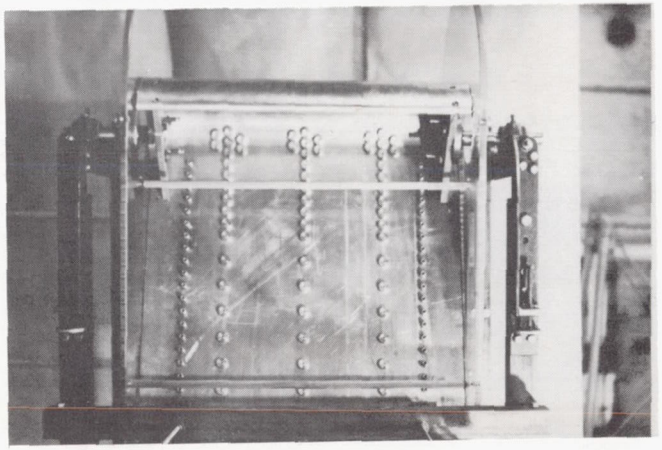

L-58-1352

(c) Back view of apparatus.

Figure 30.- Views and details of air-apparatus unit.

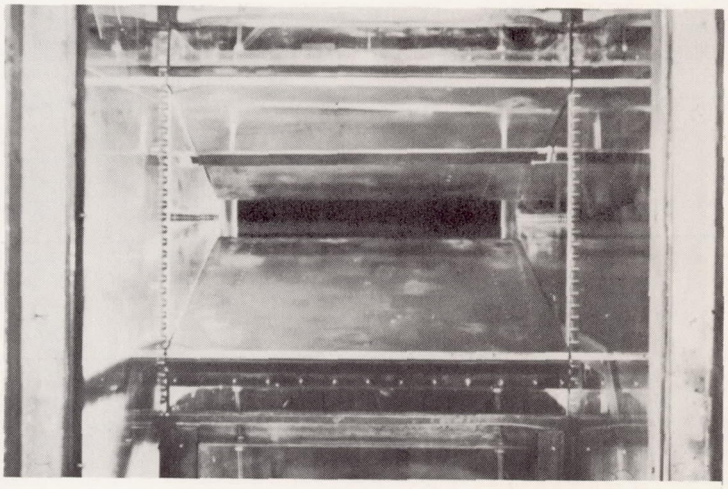

(d) Interior of diffuser.

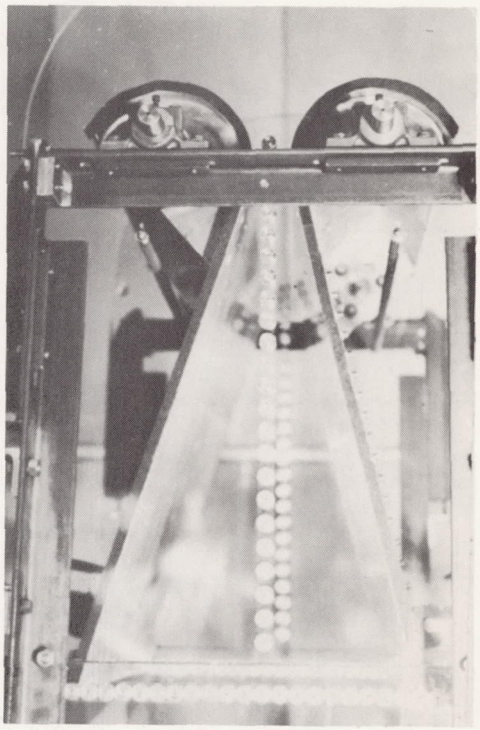

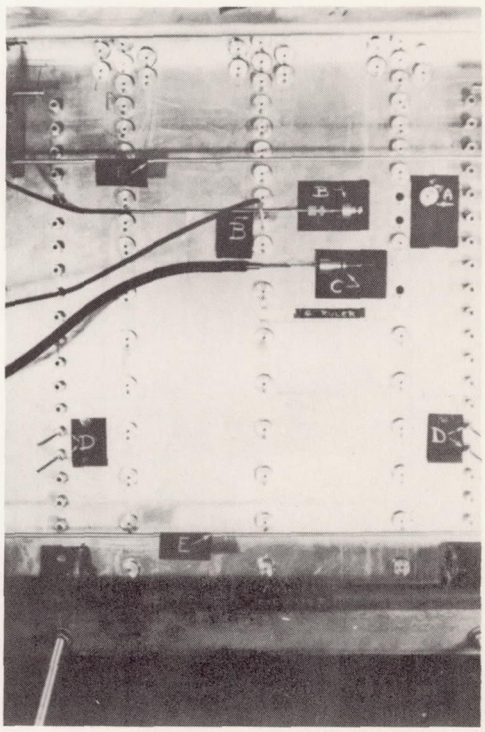

L-58-1351

(e) Side view of apparatus.

(f) Plate detail.

Figure 30.- Concluded.

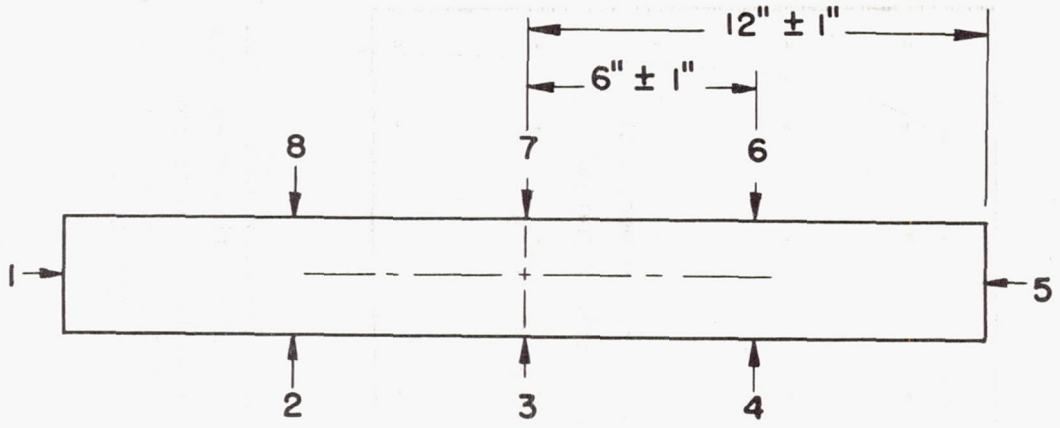

(a) Throat cross section.

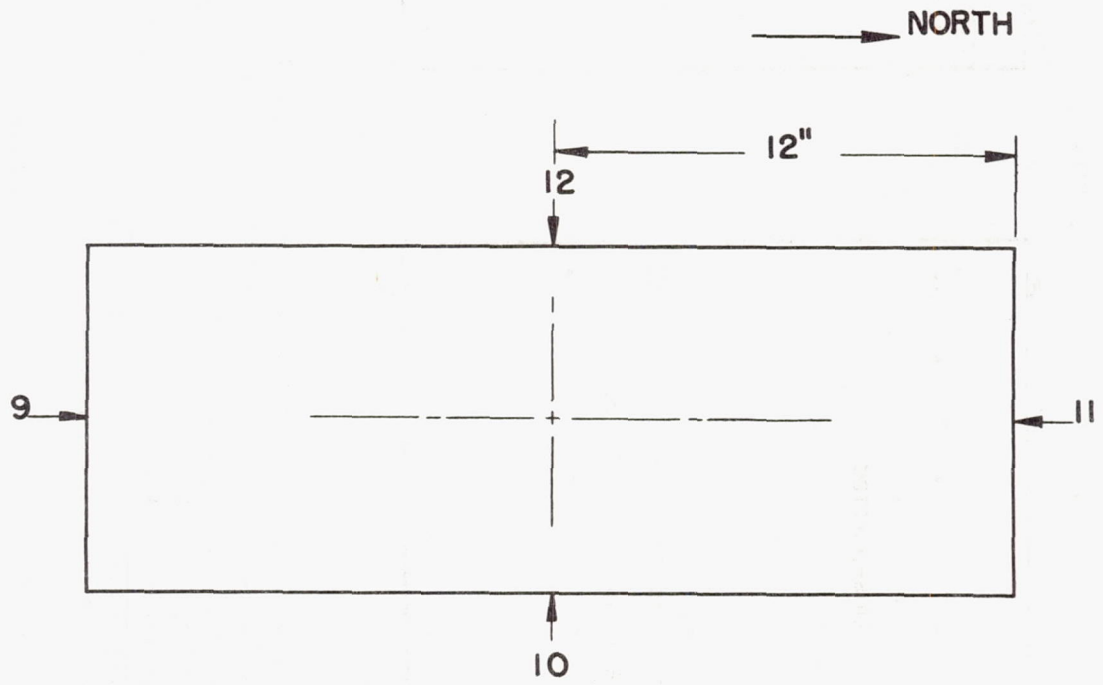

(b) Outlet cross section (as seen looking into diffuser from ahead of entrance).

Figure 31.- Location of static-pressure orifices for air diffuser.

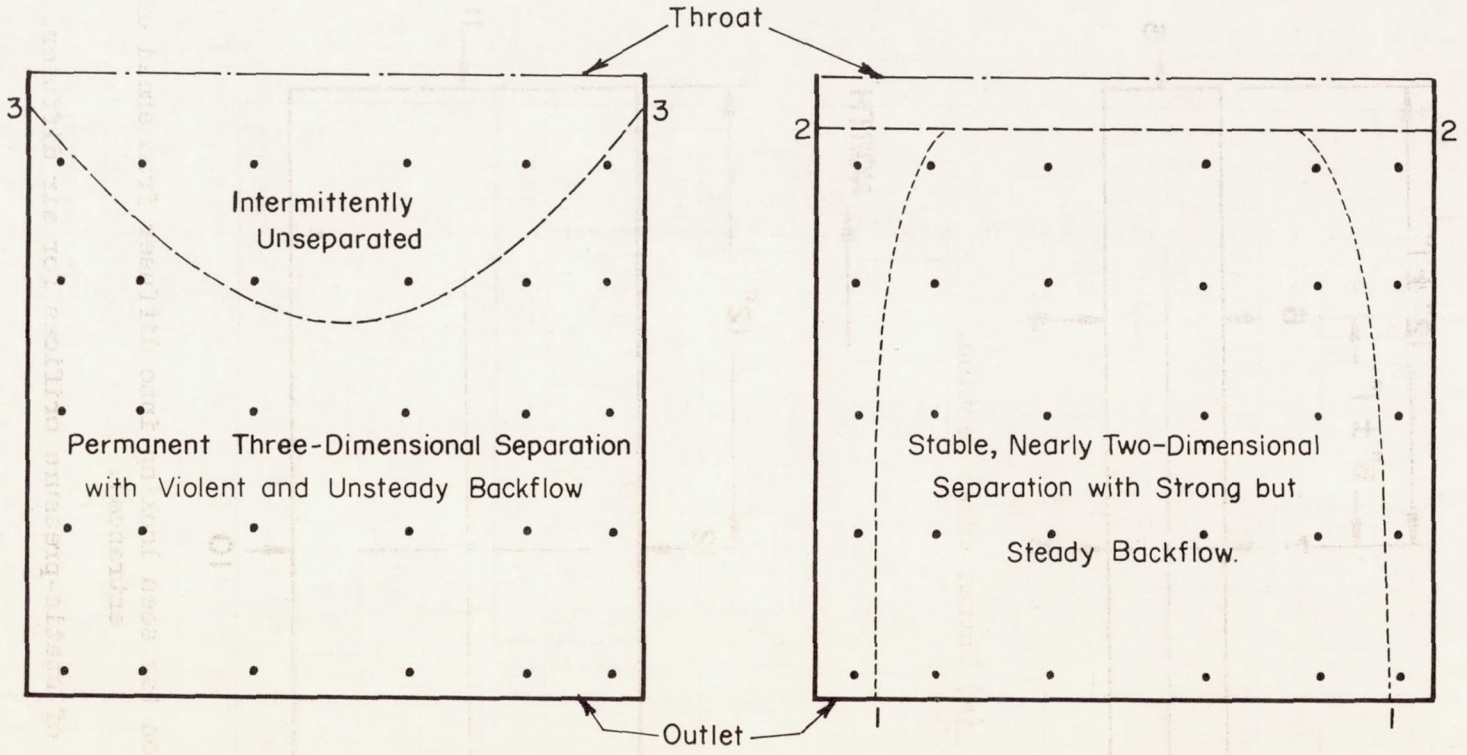

(a) Wide angles and high flow rates. Large R_W and suspected high turbulence; unsteady throat manometers. With two-dimensional separations, types 1-1 and 2-2, opposite wall was unseparated. With three-dimensional separation, type 3-3, opposite wall often was affected intermittently.

(b) Widest angles and low flow rates. Small R_W and relatively low turbulence; very steady throat manometers. With two-dimensional separations, types 1-1 and 2-2, opposite wall was unseparated.

Figure 32.- Types of fully established separation in air diffuser. Dots indicate locations of tufts.

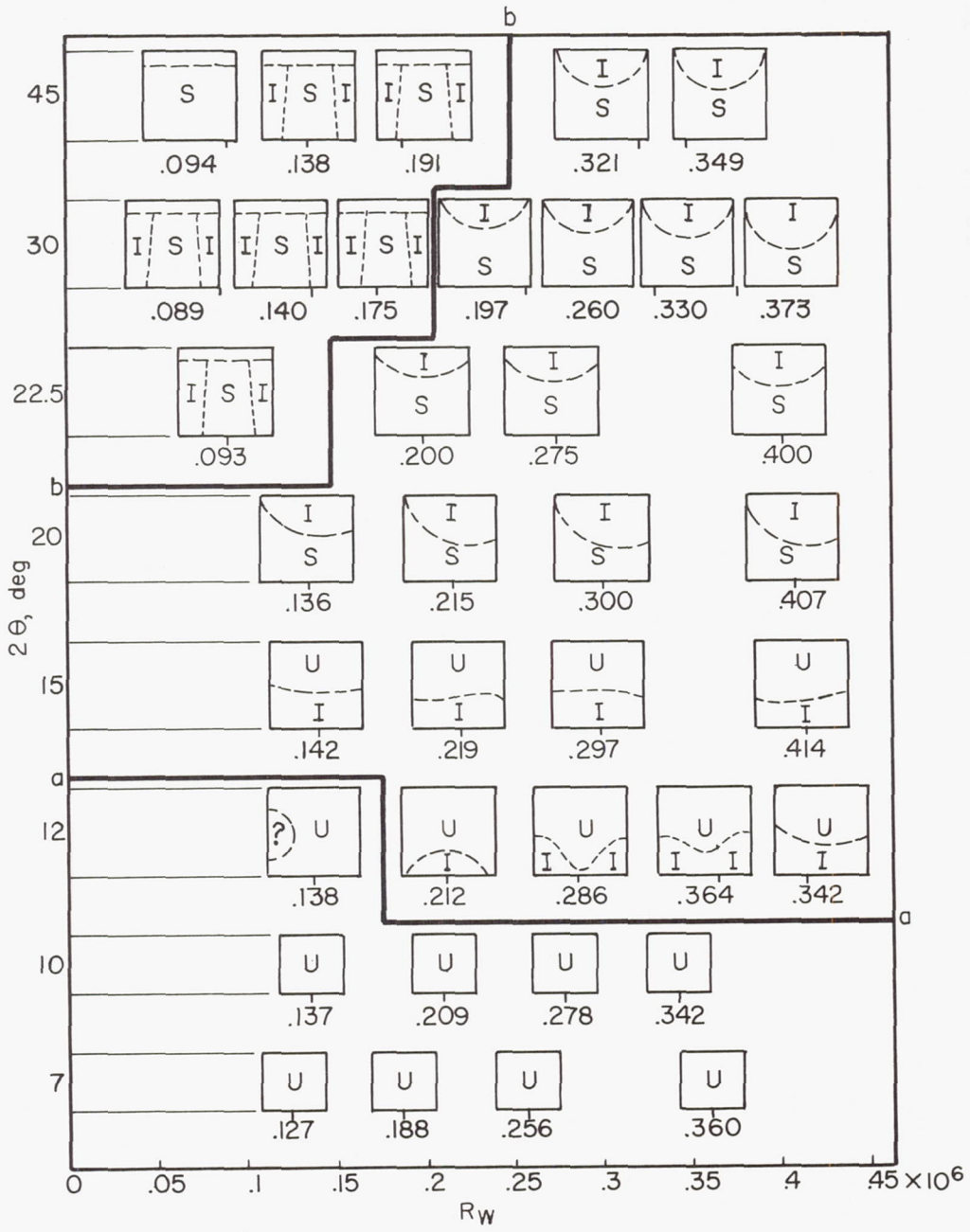

Figure 33.- Occurrence of separation in air diffuser with $L/W_1 = 8$. Squares represent diverging wall on which stable separation occurs or worse separated wall when separation is intermittent. S, separated; U, unseparated; I, intermittently separated; values under squares are $R_W \times 10^{-6}$.

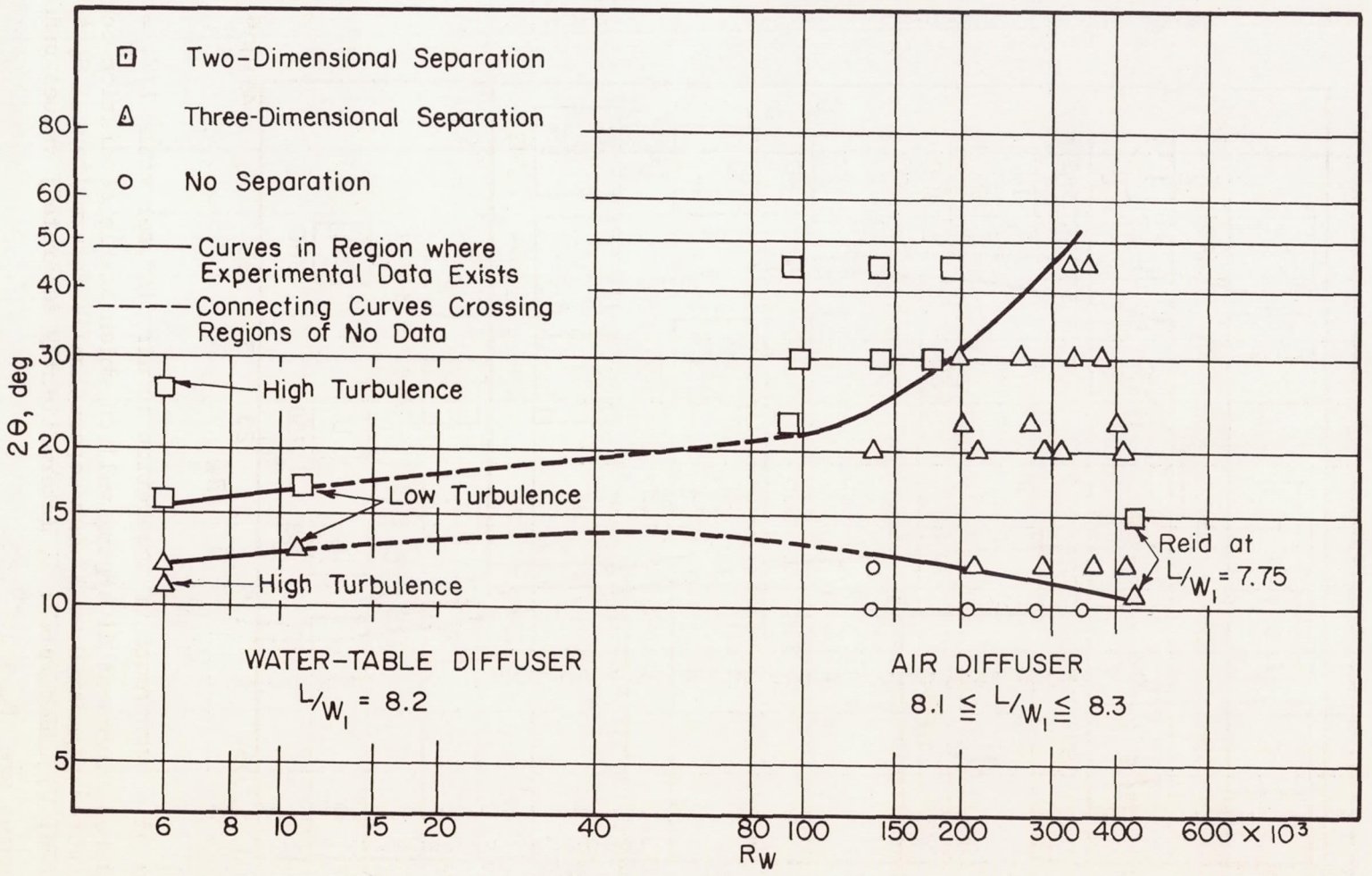

Figure 34.- Comparison of water-table-diffuser data, air-diffuser data, and data of Reid (ref. 7).

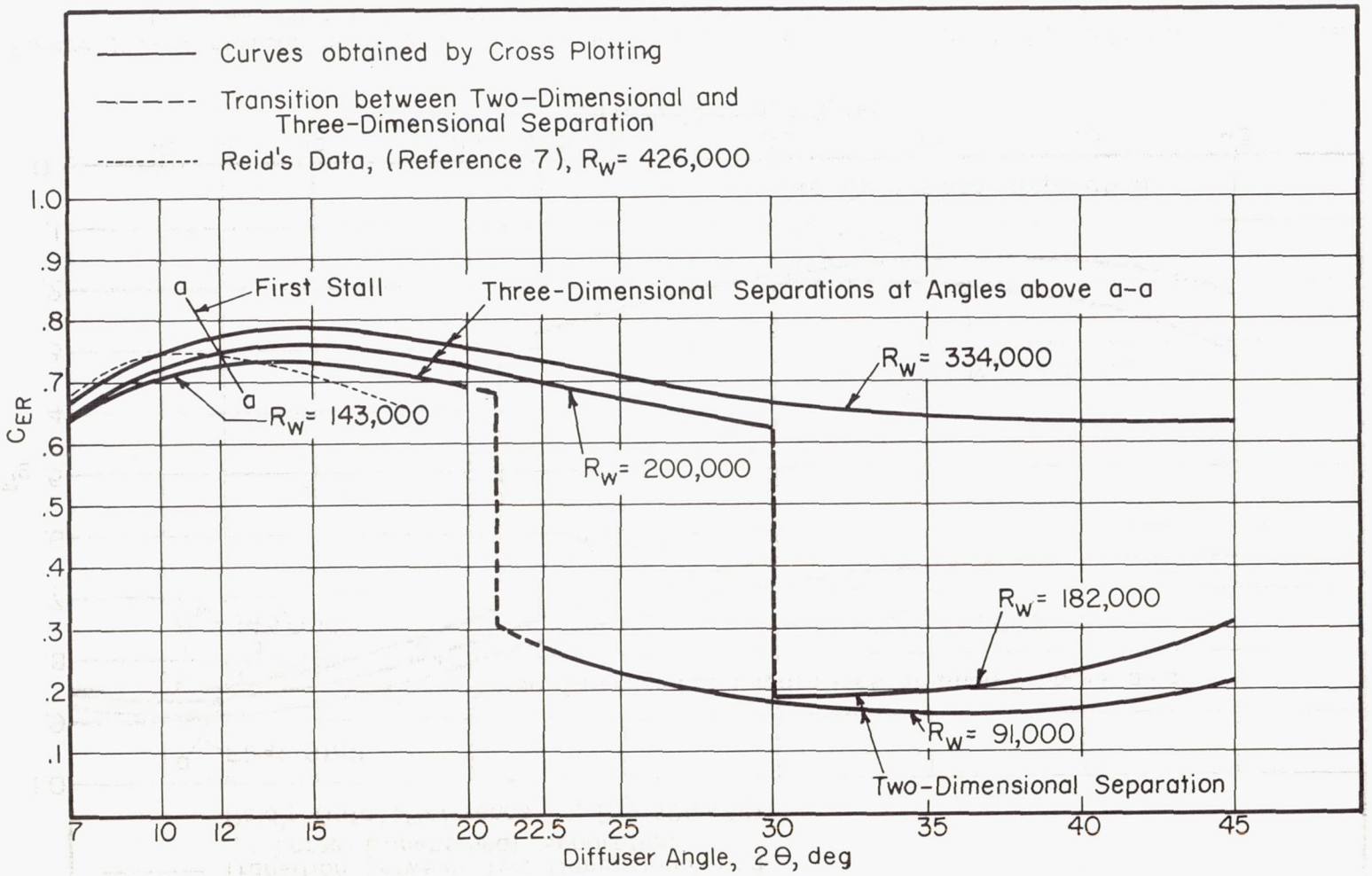

Figure 35.- Variation of recovery with air-diffuser angle and throat Reynolds number. It is believed that turbulence intensity increased directly with Reynolds number.

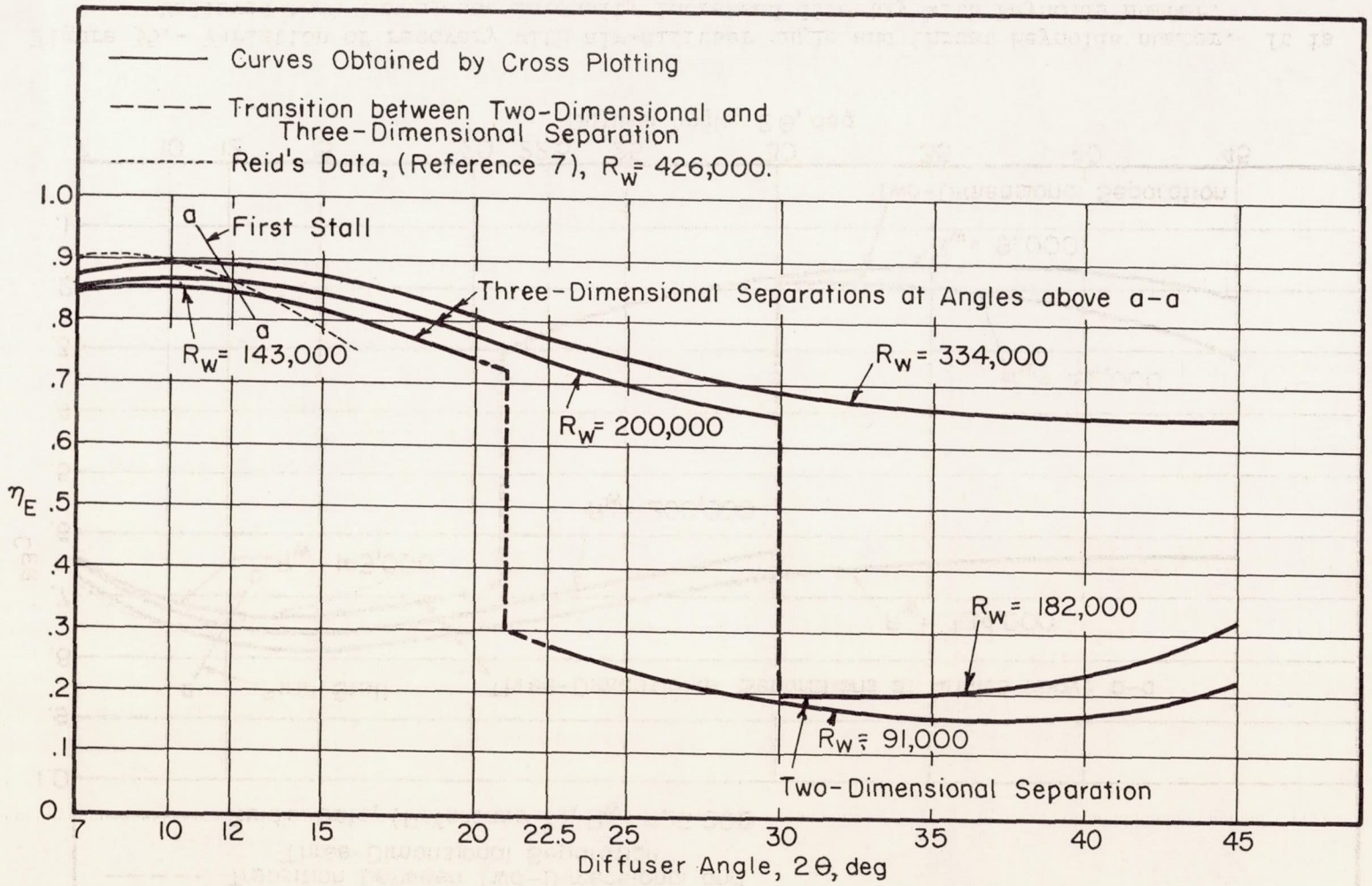

Figure 36.- Variation of efficiency with air-diffuser angle and throat Reynolds number. It is believed that turbulence intensity increased directly with Reynolds number.

NACA - Langley Field, Va.